The Role of Land-Atmosphere-Ocean Interactions in Rainfall Variability over West Africa

by

Cuiling Gong

Submitted to the Department of Civil and Environmental
Engineering
in partial fulfillment of the requirements for the degree of

Master of Science in Civil and Environmental Engineering

at the

MASSACHUSETTS INSTITUTE OF TECHNOLOGY

February 1996

Author . . . .
Department of Civil and Environmental Engineering
January 15, 1996

Certified by . . . .
Elfatih A. B. Eltahir
Assistant Professor
Thesis Supervisor

Accepted by . . . .
Joseph M. Sussman
Chairman, Departmental Committee on Graduate Students

The Role of Land-Atmosphere-Ocean Interactions in Rainfall Variability over West Africa

by

Cuiling Gong

Abstract

The severe persistent drought in West Africa during the last three decades has attracted the attention of hydrologists and meteorologists all around the world. The sources of moisture for rainfall, the impact of land-atmosphere-ocean interactions on rainfall, and the role of land conditions in the dynamics of rainfall in West Africa are the focus of this study.

The sources of moisture for rainfall in West Africa are identified first. A model of precipitation recycling is developed and applied to West Africa to obtain quantitative estimates of the moisture contributed by local evaporation as well as by advection from the surrounding regions. We estimated the recycling ratio for the entire region by specifying three sub-regions where evaporation is treated as the source of moisture: West Africa, Central Africa and the Tropical Atlantic Ocean. We find that evaporation from the Tropical Atlantic Ocean, West Africa, and Central Africa contribute about 23, 27 and 17 percent of rainfall in West Africa, respectively. Moisture fluxes from the Tropical Atlantic are almost in phase with rainfall in West Africa. However, we find that moisture supply from Central Africa is strongly regulated and limited by the westerly flow associated with the monsoon circulation. Atmospheric moisture provides the source for rainfall and controls its maximum amount; however, the large scale circulations that are associated with rainfall control where the moisture fluxes come from.

A theory for land-atmosphere-ocean interactions and West African rainfall is proposed and applied to anomalously dry and wet years. The land-atmosphere-ocean interactions determine the gradient of entropy between the ocean and the land, which, in turn, controls the development of monsoon circulations and hence affects West African rainfall. According to the theory, a large gradient of boundary layer entropy (BLE) corresponds to a strong monsoon circulation and a flat distribution of BLE corresponds to a weak or vanishing monsoon circulation. Observations on entropy, wind, rainfall, and the sea surface temperature (SST) in 1958, 1960, 1992, 1994 are consistent with the proposed theory: wet conditions occurred in 1958 and 1994, as did a large gradient of BLE; dry conditions and small gradient of BLE are observed

in 1960 and 1992. Variations in the gradient of BLE could result either from a low SST when the land is under 'normal' conditions, or from high entropy over land when the SST is 'normal', or from a low SST and high entropy occurring over land at the same time.

We studied the role of land surface conditions in rainfall variability over West Africa. In particular, we investigated the impact of land conditions on BLE during 1994 and 1992 rainy seasons. From the moist static energy budget analysis, we identified the main contributing factor to the unusually high entropy over land: energy loss through radiative cooling from the boundary layer was small in 1994. Rainfall in the early rainy season of 1994 raised the humidity levels and reduced the temperature in the boundary layer, and hence may have been responsible for the reduction in radiative cooling and energy loss through the top of the boundary layer. A statistical analysis suggests that rainfall has a significant descending trend after the 1940s, which can not be attributed to the SST conditions These statistical results suggest that processes other than SST (possibly deforestation or desertification) play important role in the rainfall variability over West Africa.

Thesis Supervisor: Elfatih A. B. Eltahir
Title: Assistant Professor

Acknowledgments

Contents

List of Figures

9

10

List of Tables

Chapter 1

Introduction

1.1   Objective

West Africa experienced extensive, severe and persistent drought during the last three decades. In the most severe years, 1972 and 1973, annual total rainfall were only 50% of the long-term mean. Farmer and Wigley (1985) analyzed the climatic trends for tropical Africa and concluded that the recent rainfall decline in West Africa is unprecedented in duration, intensity, spatial character, or seasonal expression. Nicholson's (1993) analysis, as shown in Figure 1-1, show that significant rainfall decline is observed over all the sub-regions that constitute West Africa. Even in the humid region of the Guinea Coast, rainfall decline is significant. But the Sahel and Soudan regions experienced the most severe rainfall deficits.

The rainfall deficit has strong impact on the water balance of the hydrological system in West Africa. From 1967 to 1972-3 the discharge of the Senegal river and Niger river declined by 50 and 70% respectively, and lake Chad was reduced in area by 65%. The level of the water table also fell and the annual floods on the inland deltas of the Niger and Senegal Rivers virtually disappeared.

Since the continent of Africa makes up a sizable portion of the global land surface, the dramatic climate change is a significant environmental problem. Understanding the natural variability of rainfall over West Africa is the objective of this study.
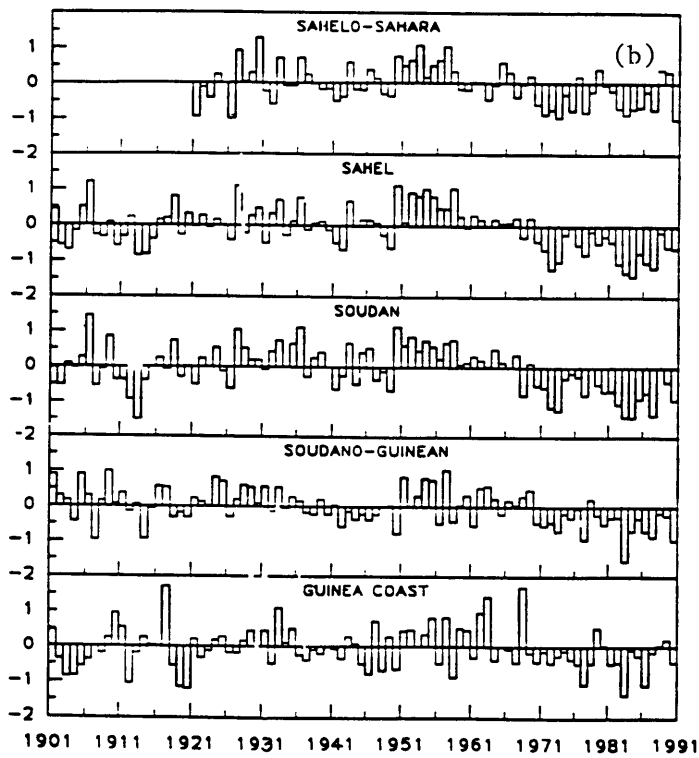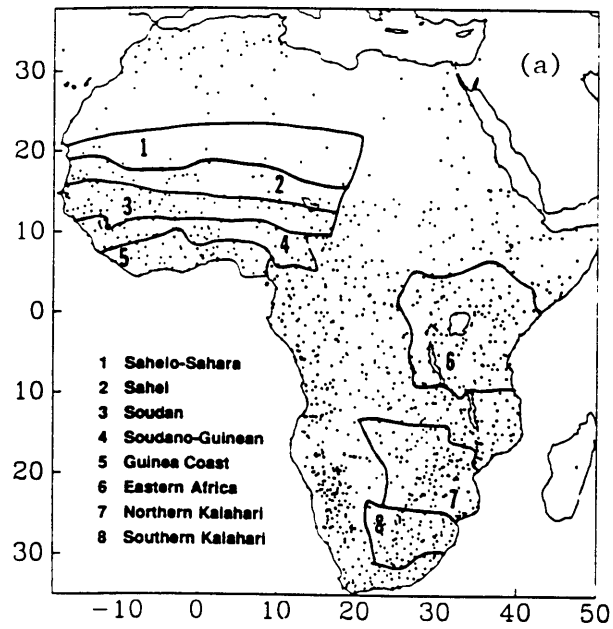
Figure 1-1: (a) Maps of rainfall stations and geographical regions   (b) Rainfall fluctuations in West Africa 1901 to 1990 (from Nicholson, 1993)

14

1.2 A Brief Review of Early Studies

Extensive studies have been done on the drought mechanisms over West Africa. But there is no generally accepted explanation yet. These studies mainly focus on the following areas: ocean-atmosphere interactions,land-atmosphere interactions, atmospheric circulation changes.

1. Ocean-Atmosphere Interactions

Many studies examine the relationship between the Sahel rainfall and the sea-surface temperature (SST). One of the first studies was that of Lamb(1978). Folland et al. (1986) identified an Atlantic SST anomaly pattern for Sahel dry years. Semazzi et al. (1988), and Hsiung and Newell (1983) show that Sahel rainfall variability may be the result of the global change in the patterns of the SST. A numerical study carried out by Palmer (1986) suggests that the Pacific Ocean, and Indian Ocean SSTs also have influence on the Sahel rainfall. Ropelewski and Halpert (1987) related rainfall to the Southern Oscillation/El Nino (ENSO) and found that statistical associations between rainfall and ENSO are very strong in East Africa and Southern Africa but no relationship is evident in Sahel. We will give a more detailed review of this area in Chapter 3.

2. Land-Atmosphere Interactions

Since human activities, such as desertification, deforestation, and overgrazing, alter the natural landscape dramatically, many researchers have studied the interactions between the land and the atmosphere. Charney (1975) first modeled albedo and rainfall changes as a result of removal of vegetation in the border of the desert. The impacts of soil moisture on rainfall are explored by Walker and Rowntree (1977), Sud and Fennessy (1984), and Powell and Blondin (1990). Prospero and Nees (1977, 1986) studied the relationship of dust production and Sahel rainfall and showed that the dust concentration strongly correlates with Sahel rainfall: the concentration of dust increases dramatically during years of Sahel drought. Carlson and Benjamin (1980), ben Mohamed and Frangi (1983, 1986) and Helgren and Prospero (1987) carried out similar studies.

3. Atmospheric Circulation Changes

Kraus (1977), Greenhut (1977) and Beer (1977) interpreted the changes in Sahel rainfall as a function of the position of the Intertropical Convergence Zone (ITCZ). Many investigations have shown that drought years in the sub-Saharan region are characterized by a weaker Tropical easterly jet (200 mb), a stronger mid-tropospheric (700 mb) African easterly jet, enhanced Hadley-type overturnings, enhanced horizontal temperature gradients, and the virtual disappearance of the 850 mb trough over West Africa, Tanaka et al. (1975), Kanamitsu and Krishnamurti (1978), Newell and Kidson (1979, 1984), and Dennett et al. (1985).

In a recent paper, Eltahir and Gong (1996) studied the relationship between the boundary layer entropy and the development of monsoon circulations in West Africa. They found that monsoon circulation is stronger when the gradient of the boundary layer entropy between the ocean and the land in West Africa is larger.

1.3 Outline

Chapter One introduces the objective of the study and gives a brief review of the early work. It also provides some background related to this research. Chapter Two deals with the sources of moisture in West Africa. Chapter Three presents the theory of Land-Atmosphere-Ocean interactions and its application in 1958 and 1960. Chapter Four presents the results of application of the theory to the 1994 rainy season and describes the role of the land conditions in West African rainfall. Finally, Chapter Five summarizes the findings, conclusions, and possible future research directions.

1.4 Background

We will provide some background about the climate in West Africa, monsoon circulations, and the definition of entropy in this section.

1.4.1 Climate in West Africa

The main characteristics of the climate in West Africa are the clearly defined wet and dry seasons. The dry season covers the months from October to May of the next year, and the rainy season covers the months of June, July, August and September. Most of the precipitation in West Africa is received in the rainy season. The isohyets are aligned in the east-west direction and the decrease in the total annual rainfall from the equatorial zone (more than 4000 mm) down to the Sahara (less than 25 mm) reveals the fundamental contrast between the dry northern masses of air, and masses of air of a southern origin. The latter become saturated with humidity over the Atlantic and deviate to the north-east after crossing the equator and submerge the whole of West Africa, which is traditionally called monsoons.

As mentioned before, there are two distinct features which appear in the West Africa drought. First, rainfall deficit spreads most of the regions of West Africa in the past three decades. Even in the humid Guinea coast, rainfall deficit is experienced. But significant rainfall deficit is observed in the Sahel and Soudan regions. Second, rainfall decrease is more evident in August and September as reported by Farmer and Wigley (1985). There is less persistent decrease in rainfall in June and July. Since rainfall in August and September is mainly produced by the monsoon circulation, it is reasonable to link rainfall deficit in West Africa to the dynamics of monsoon circulations.

1.4.2 Definition of Entropy

The original definition of entropy comes from the second law of thermodynamics, which implies that energy can only change from a higher level of availability to a lower level of availability, i.e, energy can only change from a more ordered form to a less ordered form. In mathematical form, it can be expressed as:

$$d\phi \geq \frac{dq}{T} \tag{1.1}$$

where $d\phi$ is the increase in entropy accompanying the addition heat dq to a unit mass of gas at temperature T.

For a reversible processes,

$$d\phi = \frac{dq}{T} = \frac{1}{T}[C_p dT - \alpha dp] = C_p[\frac{dT}{T} - k\frac{dp}{p}] = C_p\frac{d\theta}{\theta} \qquad (1.2)$$

where θ is the potential temperature that a parcel of air would have starting with temperature T and pressure P if it were subjected to an adiabatic compression or expansion to a final pressure of 100 kP_a.

Integrating the above equation, we get the explicit relation between entropy and potential temperature:

$$\phi = C_p ln\theta + const. \qquad (1.3)$$

Physically, entropy is a measure of disorder or chaos within a system. Without adding or subtracting energy from a system, an increase in entropy means a decrease in available energy and evolution toward a state of greater disorder. Entropy is a state variable and always increase with time. Entropy of the atmosphere in the boundary layer is a measure of the temperature and moisture content of the atmosphere. High temperature and high moisture content in the atmosphere correspond to high entropy values. The absorption of solar radiation and the release of latent heat are the largest sources of entropy in the atmosphere. Among the nonradiative processes, the water phase transitions dominate the entropy generation.

1.4.3   Monsoon Circulations

Monsoon circulations are characterized by a seasonal reversal of wind circulations, and widespread precipitation. The word 'monsoon' is derived from the Arabic word meaning a 'season'. The typical areas for the monsoon are the southern and southeastern parts of the Asian continent where the monsoonal shift in circulation is very pronounced and considerably assisted by the local distribution of continent and ocean. In winter, the northern portion of Asia and the adjacent high latitude are very cold.

With the coming of spring and increased continental warming over the continent, over the southern parts of india and Indo-China the strength of insolation creates a marked heat low, which draws in the cool and drier air on its northern flank and moist Indian Ocean air from the south. As a result, thunderstorms and squalls are triggered. Over the Tibetan Plateau a high altitude and shallow heat low is overlain by an upper anticyclone, which reinforces the easterly flow along the plateau's southern flank. A surface southwesterly flow begins to introduce moist unstable air, pushing the 'burst' of the monsoon from the southeast across India, and from the southwest across southern China.

The broad characteristics of monsoons are:

1. Intense rainfall, deep moist convection over land and near coastal regions of the summer subtropics where ocean lies near and across the equator.

2. A strong , convergent, cyclone in the vicinity of the intense rainfall and a strong divergent anticyclone aloft.

3. Strong cross-equatorial low-level flow equatorward of the intense rainfall region; low-level westerlies between the rainfall region and the equator; a strong easterly jet aloft equatorward of the upper-level anticyclone.

4. Occurrence for a few months around midsummer.

Monsoon circulation in West Africa is weak compared with the Asian summer monsoon, but it has significant impact on rainfall in West Africa. Two mechanisms, related to the monsoon circulation, are very important for the formation of rainfall. One is the moisture supply. Wind blows from the ocean and brings moisture to the land region. The other is associated with the vertical motion in the atmosphere. Monsoon circulation provides an uplift mechanism which brings the moist air to the upper levels of the atmosphere where water vapor is condensed into liquid water. A schematic diagram of the monsoon circulation is shown in Figure 1-2.
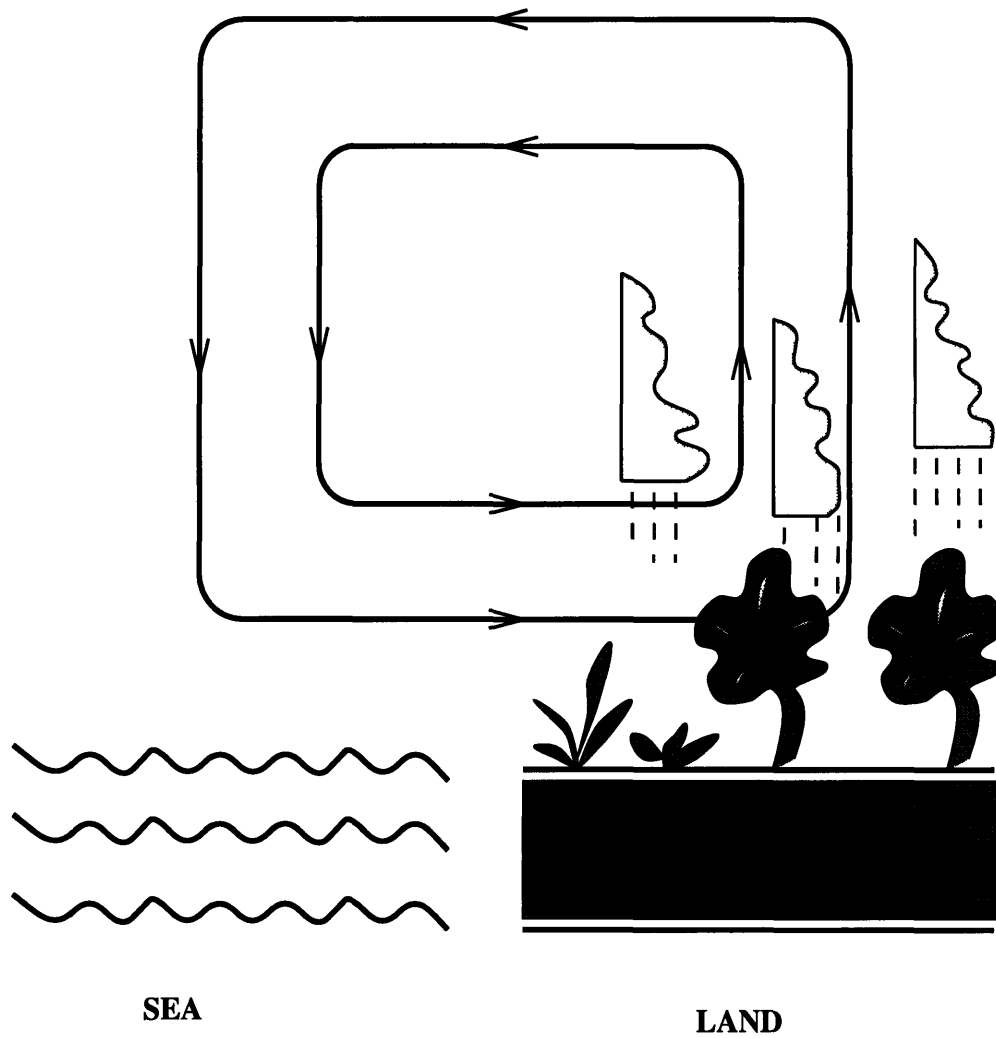
Figure 1-2: Sketch of development of monsoon circulation

Chapter 2

Sources of Moisture for Rainfall in West Africa

Rainfall over any land region is contributed by two sources: 1)water vapor that is advected into the region from the surrounding areas, and 2) water vapor that is supplied by evaporation from the same region. The objective in this chapter is to identify the sources of moisture for rainfall in West Africa and to obtain quantitative estimates of the moisture contributions by evaporation from the region and advection from the surrounding regions. A model of precipitation recycling is developed and used to estimate these contributions. The precipitation recycling ratio is defined as the contribution of evaporation in a specified region to precipitation in the same region or the surrounding areas. The importance of studying precipitation recycling is that the recycling estimates would enable us to define the regional hydrological cycle.

This chapter is organized as follows. The early work related to this study is summarized first. Section 2.2 describes the precipitation recycling model. The data is described in section 2.3. Section 2.4 presents results of the study. Section 2.5 summarizes findings and discussion.

2.1 Early Work

The issue of sources of moisture has been explored for a long time. One of the early studies was that of Benton et al.(1950) who pointed out that both the vertical motions in the atmosphere and horizontal motions that carry water vapor across the continents from oceans are important in order to produce significant precipitation. The same study estimated the sources of precipitation over the Mississippi basin and concluded that 90 percent of moisture was contributed by advection from outside the basin.

Budyko (1974) developed a simple one-dimensional model to estimate the moisture recycling in a territory. In his model, the water content of the atmosphere varies in accordance with the difference between the loss of water as precipitation and the gain from evaporation along a streamline. Budyko's model provides a lumped estimate of recycling along a single streamline. The calculations of the water balance components for the European territory of USSR showed that only 11 percent of the precipitation is formed from the local evaporation. He concluded that even on the most extensive continents, where the relative role of local evaporation is the greatest, the main portion of precipitation is formed from water vapor of external origin, not local.

Lettau et al. (1979) used the method of climatonomy to model coherently both the atmospheric and land phases of the water cycle. The model estimates the recycled part of the regional evaporation that varies from 15 percent to 32 percent in the region between 50 and 75 degrees west in the Amazon basin. Salati et al.(1979) and Brezgunov (1991) analyzed the recycling processes by measuring the distribution of stable Oxygen isotope's concentration in precipitation. Salati et al. (1979) did a qualitative analysis of the recycling process in the Amazon basin, but they did not provide any quantitative estimate of recycling. A large amount of moisture that is added to the air mass modifies the isotopic composition of precipitation. Therefore, the concentration of isotopes in precipitation can be used to estimate the relative contribution of water vapor advection to local precipitation. Although the isotopic

analysis can give qualitative information about the origins of precipitation, it is hard to give a quantitative estimation of recycling ratios based on isotopic analysis.

Russell et al. (1981) introduced a finite-difference scheme, called the "slope scheme", to solve a tracer transport equation. Incorporating Russell's slope scheme, Koster et al. (1986) investigated the origin of water precipitating in different geographic regions using version II of the NASA/GISS GCM. Water evaporating from various source regions is "tagged" and then followed as a tracer. They concluded that in Sahel region, the contributions of water vapor in summer from the tropical Atlantic and Africa/Asia are 60 percent and 30 percent respectively.

Lamb (1983) studied West African water vapor variations during the rainy seasons by analyzing the observations in very deficient and near-average rainy seasons. He concluded that Subsaharan drought does not associate with the northward supply of unusually dry surface air to West Africa from the tropical Atlantic. Westerly and southwesterly directions of the advective water vapor flux within the low-level onshore flow are more predominant.

Brubaker et al. (1993) modified Budyko's model to estimate the recycling ratio for regions that do not lie parallel to a streamline. The land regions studied include Eurasia, North America, South America and Africa. They found that the contribution of regional evaporation to regional precipitation varies substantially with location and seasons. The recycling ratio in West Africa estimated from their model varies from 10 percent to 48 percent in different months. Similar to Budyko's model, their model is still a lumped model which does not show the spatial variation of the recycling ratio.

Savenije (1995) suggested to use the salinity of the rainfall to estimate the rate of moisture recycling. It is assumed that the amount of salt of marine origin is uniformly distributed in the moisture content of the atmosphere. He concluded that the recycling of moisture in the Sahel is responsible for more than 90 percent of the rainfall . As we will discuss later, the reason for such a high recycling ratio is that only meridional advection is considered; the zonal advection of moisture was ignored in this model.

Eltahir and Bras (1994) developed a recycling model that accounts for both spatial

and seasonal variabilities of precipitation recycling. Eltahir (1993) applied that model to the Amazon basin and estimated that about 25 percent of rainfall is contributed by the local evaporation. The model of Eltahir (1993) estimates the contribution of moisture evaporated in any source region to precipitation in the same region. Although we use a model similar to that of Eltahir (1993), we extend that model and estimate the contribution of moisture evaporated in any source region to precipitation not only in the same region but also in the surrounding areas.

2.2   The Recycling Model

This recycling model is based on mass balance. First, the area under consideration as a source of moisture is defined. Second, regions, in which evaporated moisture may potentially precipitate, are specified as shown in Figure 2-1(a). Figure 2-1(b) and 2-1(c) show two types of control volumes in the atmosphere: one is above the source region; the other is above the surrounding areas. The dimension of the control volume depends on the resolution of the observation data. For this application, the horizontal dimensions are 2.5 by 2.5 degrees in zonal and meridional directions, and the vertical extent is from the land surface to 100mb height. Since above 100 mb height, water vapor content is very low, water vapor exchange at the top of the control volume is negligible. Applying the law of mass conservation to the control volumes results in the following equations:

for control volumes that are inside the source region (type A),

$$\frac{\partial N_i}{\partial t} = I_i + E_i - O_i - P_i \qquad (2.1)$$

$$\frac{\partial N_o}{\partial t} = I_o - O_o - P_o \qquad (2.2)$$

for control volumes that are outside the source region (type B),

$$\frac{\partial N_i}{\partial t} = I_i - O_i - P_i \qquad (2.3)$$

24
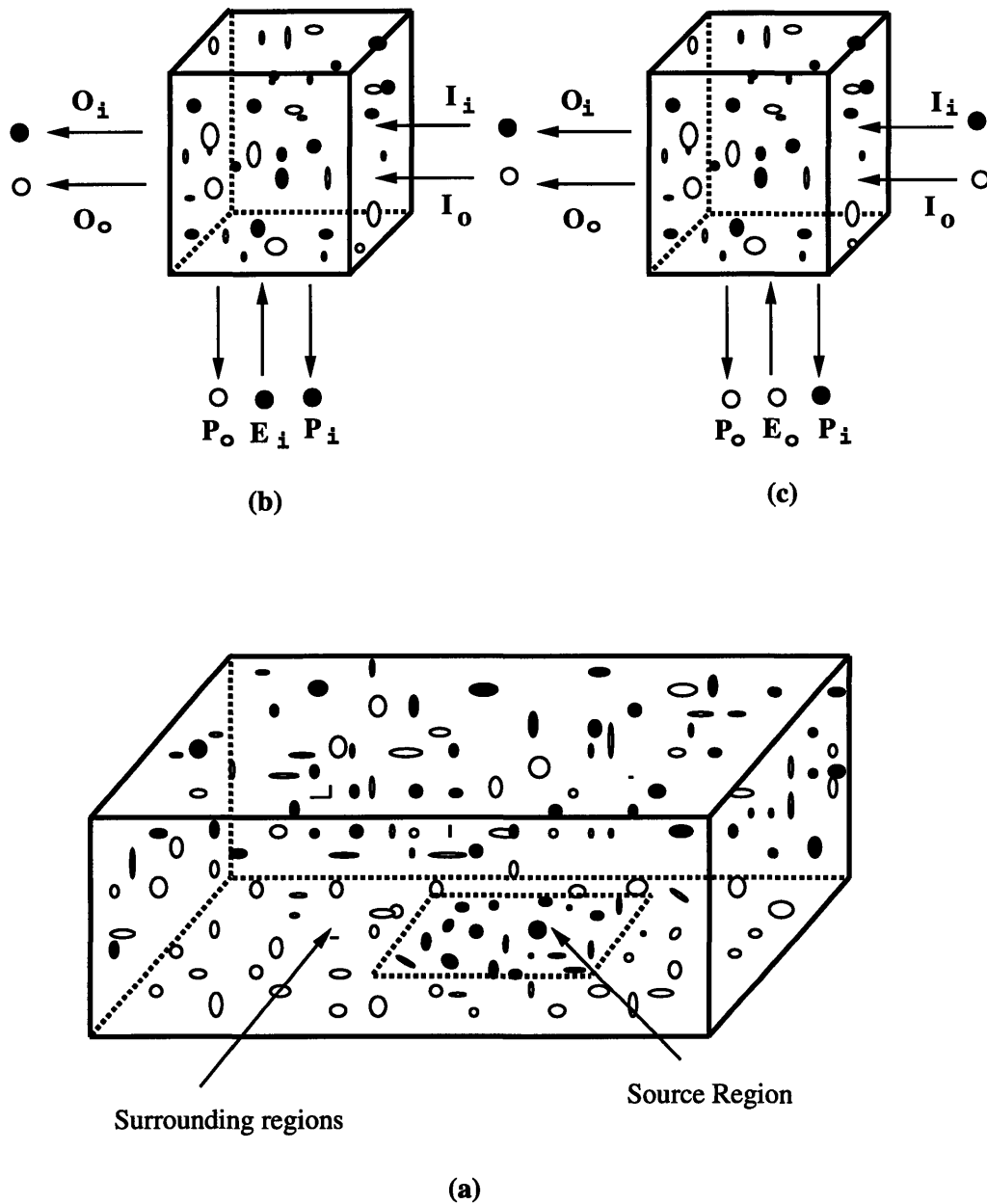
Figure 2-1: (a) definition of source and surrounding regions   (b) Control volume in the source region   (c) Control volume in a surrounding region   (note that water vapor molecules evaporated from the source region and surrounding regions are represented by solid and open circles respectively)

$$\frac{\partial N_o}{\partial t} = I_o + E_o - O_o - P_o \qquad (2.4)$$

where E is evaporation; N is the storage of water vapor molecules in the control volume; I and O are the Inflow and Outflow of moisture; subscripts i and o represent the origins of the water vapor molecules: i denotes water vapor molecules that evaporate inside the source region and o denotes water vapor molecules that evaporate outside the source region. Note that the inflow and outflow include both zonal and meridional fluxes; P is precipitation.

Two assumptions are involved in the model: 1) the atmospheric water vapor is well mixed within the planetary boundary layer ($\approx 1km$), in other words water vapor molecules that evaporate from the surface and those advected into the control volume are well mixed; 2) the rate of change of storage of water vapor within a control volume is negligible compared to the fluxes into the control volume at the monthly time scale. The first assumption is supported by observations of Crum and Stull (1987) for the mid-latitudes and observations of Harris et al. (1988) for the Amazon basin. To support the second assumption, Eltahir (1993) computed the monthly flux of water vapor and the rate of change in storage of water vapor at a single location in the Amazon basin at the monthly time scale and found that the rate of change in storage of water vapor is quite small compared to the water vapor fluxes. Budyko (1974) pointed out that the molecules of water vapor of local and external origin are completely mixed in the atmosphere due to turbulent mixing.

Based on the first assumption, we suggest that

$$\rho = \frac{P_i}{P_i + P_o} = \frac{O_i}{O_i + O_o} = \frac{N_i}{N_i + N_o} \qquad (2.5)$$

where ρ is the precipitation recycling ratio.

Applying the second assumption to the mass conservation equations 2.1 to 2.4, we get the following equations:

for control volumes of type A,

$$I_i + E_i = O_i + P_i = \rho(O_i + O_o) + \rho(P_i + P_o) \qquad (2.6)$$

26

$$I_o = O_o + P_o = (1 - \rho)(O_i + O_o) + (1 - \rho)(P_i + P_o) \tag{2.7}$$

for control volumes of type B,

$$I_i = O_i + P_i = \rho(O_i + O_o) + \rho(P_i + P_o) \tag{2.8}$$

$$I_o + E_o = O_o + P_o = (1 - \rho)(O_i + O_o) + (1 - \rho)(P_i + P_o) \tag{2.9}$$

Dividing equation 2.6 by equation 2.7 and rearranging the equation, we get a simplified expression of recycling ratio for type A control volumes:

$$\rho = \frac{I_i + E_i}{I_i + E_i + I_o} \tag{2.10}$$

which is the ratio of the sum of the part of inflow with origin in the source region and evaporation to the sum of the total inflow and evaporation. Similarly, for type B control volumes, the recycling ratio is defined by

$$\rho = \frac{I_i}{I_i + E_o + I_o} \tag{2.11}$$

In this case, naturally local evaporation does not appear in the numerator. Note that these definitions of recycling ratio impose no restrictions on the distributions of evaporation and precipitation; therefore, the spatial variability of the recycled precipitation can be calculated. The procedures for applying the model are summarized in the following:

1. Divide the whole area into small cells corresponding to the resolution of the data. Estimate water vapor fluxes and evaporation in each grid. The grid system is shown in Figure 2-2. Note that the grid for ρ is located at half of the distance between the grid points.

2. The recycling ratios are estimated by iteration. First an initial value is guessed and assigned to each grid point. Then outflow is partitioned into O_i and O_o using equation 2.5. Note that the grids are connected with each other; therefore, the outflow in grid (i, j) is equal to the inflow in grid (i+1, j) in the zonal direction.

27

Similarly, the meridional outflow has the same characteristics. I_i and I_o can be estimated directly from O_i and O_o in the surrounding grids and a new estimate of ρ can be obtained using equation 2.10 or 2.11.

3. Compare the new estimate of ρ with the previous one. If the difference is small enough, the new estimate is taken as the final result; otherwise, the iteration is repeated until convergence is reached.

The advantage of the model is that the recycling ratio in one grid point takes into account information in the surrounding grids. Note that the outflows in the surrounding grids are partitioned by the recycling ratios in those grids and inflows in one grid point are equal to outflows in the surrounding grids; therefore, the recycling ratio in one grid point is related to the recycling ratios in all grid points in the area.

The areal average of recycling ratio for a particular month can be estimated by using precipitation as a weighting factor.

$$\rho_a = \frac{\Sigma P(i,j)\rho(i,j)}{P_t} \tag{2.12}$$

where P_t is the total precipitation in the area, $P(i,j)$ is the precipitation in grid (i,j), and $\rho(i,j)$ is the recycling ratio in the same grid.

The yearly or seasonal average of recycling ratio at any grid point (i,j) can be obtained using the following equation:

$$\rho_y(i,j) = \frac{\Sigma P(i,j,k)\rho(i,j,k)}{P_t(i,j)} \tag{2.13}$$

where $P_t(i,j)$ is the yearly precipitation in grid (i,j), $P(i,j,k)$ is the monthly precipitation in grid (i,j), and $\rho(i,j,k)$ is the monthly recycling ratio in the same grid.

2.3   Data

A subset of the European Center for Medium-range Weather Forecasts (ECMWF) global data is used to estimate water vapor fluxes and evaporation. The data are
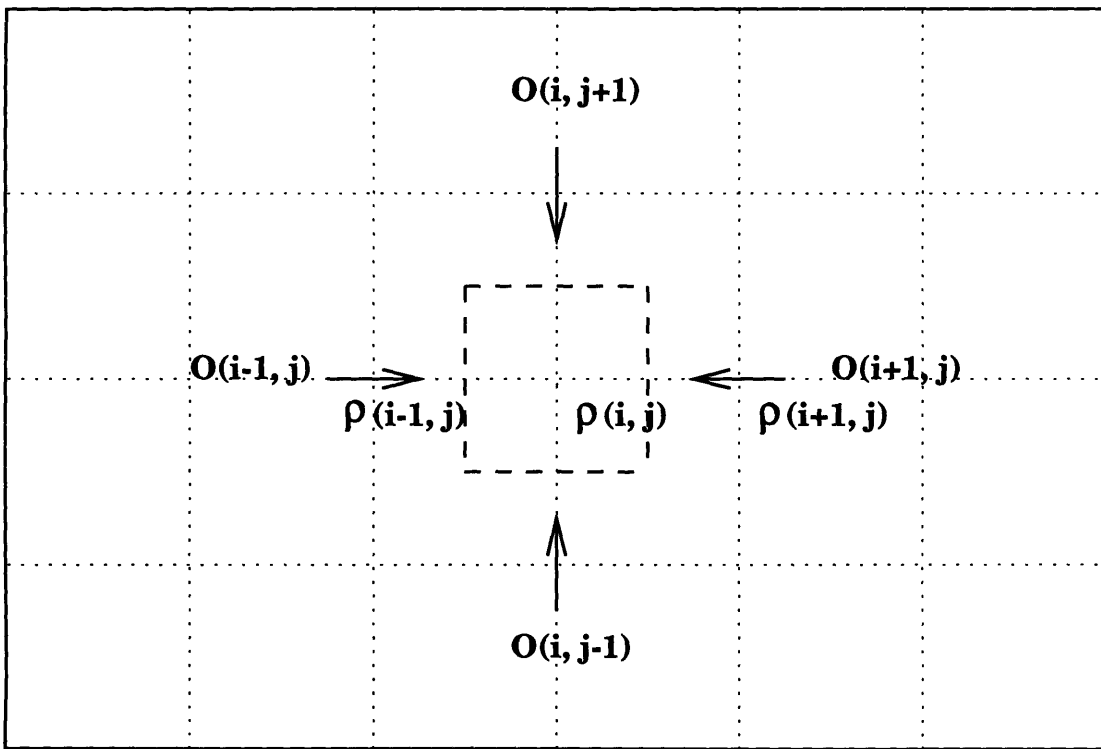
Figure 2-2: The grid system for the estimation of recycling ratios

produced by the data assimilation system, which takes observations from the surface meteorological stations, upper-air measurements and satellite data as input. The dataset includes temperature, relative humidity, wind, and latent heat flux. The data on wind, temperature, and humidity have spatial resolution of 2.5 by 2.5 degrees in zonal and meridional directions and 15 pressure levels in the vertical direction. There are two forecasts daily. The data on latent heat flux have a resolution of 1.125 by 1.125 degrees in zonal and meridional directions. There are two forecasts daily between 1985 and 1990 and four forecasts after 1990. The temporal coverage of the data is from January 1985 to the current year.

The domain of the current study area is between 10S and 30N and from 20W to 50E. Three regions, in which the precipitation recycling is to be estimated, are specified: West Africa is defined as the region between 5N and 15N and from 10W to 15E; Central Africa, between 5N and 15N and from 15E to 40E; and the Tropical Atlantic Ocean, between 5S and 5N and from 10W to 15E. Figure 2-3 shows the location of these regions. Note that the number of grid points are the same in these regions. Data from January 1992 to December 1994 are selected for the analysis since they contain more input from satellite data and hence are more reliable than those in previous years.

The monthly evaporation is estimated from latent heat fluxes:

$$E(i,j) = \frac{L(i,j)}{\lambda} \tag{2.14}$$

where λ is the latent heat coefficient ($= 2.5e6J/Kg$) and $L(i,j)$ is the latent heat flux.

The monthly atmospheric water vapor flux is computed from the data on wind, temperature, and humidity in the upper atmosphere and on the land surface. The fluxes in zonal and meridional directions are computed using the following equations:

$$F_1 = \frac{\epsilon L_1}{g} \sum_{i=1}^{n} (Rh)_i e_s(T_i) U_i d(lnP_i) \tag{2.15}$$
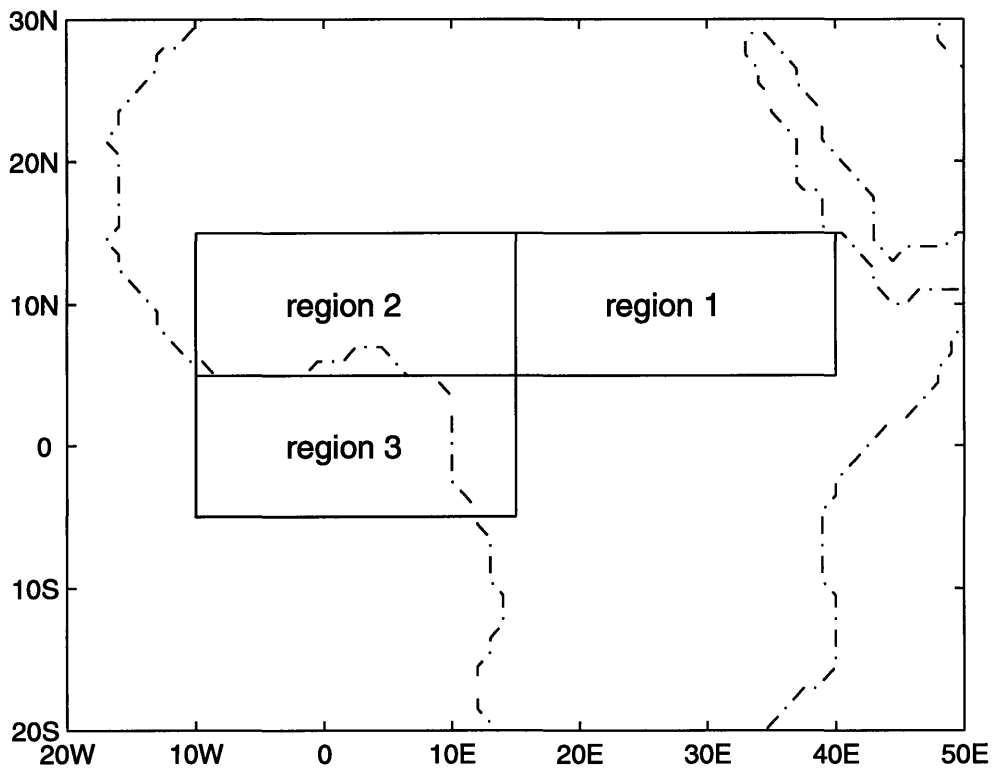
Figure 2-3: The domain of the study area and three specified regions

$$F_2 = \frac{\epsilon L_2}{g} \sum_{i=1}^{n} (Rh)_i e_s(T_i) V_i d(lnP_i) \tag{2.16}$$

where ϵ is the ratio of molecular weight of water vapor to that of dry air; U, V are the zonal and meridional wind velocities; T is temperature; P is pressure; e_s is the saturation vapor pressure; R_h is the relative humidity; g is the gravitational acceleration; L_1 and L_2 are the distances in zonal and meridional directions; the subscript n represents the pressure levels which range from 1000mb to 100mb. Note that hydrostatic distribution of pressure is assumed in the above equations. The fluxes and evaporation at the monthly time scale are estimated by adding the daily values within each month.

The precipitation data are used as weighting factors in the estimation of the regional recycling ratio. The precipitation data for West Africa are taken from the Shea Climatological Atlas 1950-1979 (Shea, 1986) dataset. This dataset has a spatial resolution of 2.5 by 2.5 degrees in zonal and meridional directions.

There are two datasets that are available and contain all the information we need for estimating the moisture fluxes. These are Geophysical Fluid Dynamics Laboratory (GFDL) data and ECMWF global data. The GFDL dataset has resolution of 2.5 by 5.0 degrees in zonal and meridional directions and 11 pressure levels in vertical direction. The time coverage of the dataset is from 1958 to 1989. The data are in monthly average. To compare the two datasets, we compute the climatology of water vapor fluxes.

Table 2.1 shows the ten years (1980 - 1989) average of net fluxes coming into West Africa in each month estimated from the GFDL dataset. Since in most months the net fluxes are negative, this implies that West Africa acts like a net source of moisture and supplies water vapor to the surrounding areas. Climatologically, West Africa can not supply water vapor to other regions since there is no net convergence of surface water flow into the region. Therefore, the GFDL dataset is not very accurate in the estimation of water vapor fluxes in West Africa. Table 2.2 shows the three year (1992-1994) average of net fluxes coming into regions 2 and 3 estimated from the

ECMWF dataset. We can see that in the land region (region 2) the net water vapor fluxes are positive, and in the ocean region (region 3) the net water vapor fluxes are negative. These results are more consistent with the typical hydrological conditions over lands and oceans, since the ocean usually supplies moisture to land. Therefore, the ECMWF dataset is chosen for the recycling analysis.

2.4 Results of Study

2.4.1 Precipitation recycling ratio

Recycling ratios are computed only for the rainy season from June to October since there is very little rainfall in the dry season. The estimates of evaporation and fluxes presented are expressed in monthly averages for a period of three years. According to the report of ECMWF describing this dataset, the coverage by observations from West Africa is quite low, which may cause some errors in the estimation of the recycling ratio. However, as the satellite measurements become more available, the accuracy and coverage of the observations in West Africa will improve greatly. The recycling estimation will be more accurate accordingly.

The evaporation is estimated using equation 2.14 and the results for June, July, August, and September are shown in Figure 2-4. The location of the 50 mm contour line is an indicator of the extent of rainfall in West Africa since the soil moisture and evaporation will increase as rainfall increases. In June there is less rainfall in West Africa since the rainy season just starts. Figure 2-4(a) shows that the 50 mm contour line is around 12N in West Africa and evaporation is very low north of 12N. Evaporation increases significantly in West Africa from July to September because of the increase of rainfall in those months. The northward movement of the 50 mm contour line in July can be seen in Figure 2-4(b). In August, this contour line penetrates further north and reaches 20N as seen in Figure 2-4(c). But the same contour line starts to retreat to the south in September as shown in Figure 2-4(d).

Moisture Fluxes in the zonal and meridional directions are calculated using equa-

Table 2.1: Climatology Net Water Vapor Fluxes Estimated from GFDL (Km^3)

month	monthly fluxes
January	-6.9
February	-139.8
March	-137.4
April	3.1
May	0.0
June	139.4
July	-98.2
August	10.3
September	79.7
October	17.2
November	-168.4
December	-34.0
total	-335

Table 2.2: Climatology Net Water Vapor Fluxes Estimated from ECMWF (Km^3)

month	region 2	region 3
January	-229.3	-14.4
February	-134.3	46.6
March	15.1	230
April	40.4	221.3
May	105.2	-68.52
June	111.4	-218.8
July	186.6	-213.6
August	357.1	-281.0
September	374.7	-233.2
October	169.5	-182.6
November	-152.6	-92.8
December	-279.4	-88.5
total	564.5	-895.5

tion 2.15 and 2.16. The vector form of fluxes in June, July, August, and September is plotted in Figure 2-5. The figure shows that the water vapor fluxes in the zonal direction are much larger than those in other directions in all the months. Moisture fluxes coming from the Tropical Atlantic Ocean increase from June to August as shown in Figures 2-5(b) and 2-5(c) because of the development of monsoon circulation, which brings moisture from the ocean to the land over West Africa. In September, the monsoon circulation becomes weak and the moisture fluxes in the zonal direction is again dominant as shown in Figure 2-5(d).

The climatology of precipitation in June, July, August and September is plotted in Figure 2-6. This figure shows clearly that rainfall in the region increases from June to August. In June, rainfall starts to build up as shown in Figure 2-6(a). In July and August, rainfall increases further and reaches about 200 mm and 250 mm as shown in Figure 2-6(b) and 2-6(c). Rainfall starts to decrease in September as shown in Figure 2-6(d). The climatology of precipitation is used as weighting factors in estimating the areal and seasonal average of the recycling ratios.

The monthly precipitation recycling ratios are calculated based on the estimates of evaporation and water vapor fluxes in those four months. In order to identify the sources of moisture, we specify three source regions as described in section 2.3. Figure 2-7 shows the recycling ratio distributions in the entire study area with the source region specified as Central Africa. Figures 2-7(a), (b), (c), and (d) show the results in June, July, August and September respectively. These figures show that the evaporation in Central Africa contributes to precipitation in both Central and West Africa in all the four months. The recycling ratios increase from June to August and start to decrease in September, which is consistent with the evaporation observations. Figure 2-8 shows the recycling ratio distribution with the source region specified as West Africa. This figure shows that the evaporation in this region contributes more to the local precipitation but has little contribution to the precipitation in Central Africa and the Tropical Atlantic. Similarly Figure 2-9 shows the recycling ratio with the source region specified as the Tropical Atlantic Ocean. Clearly, the evaporation in the Tropical Atlantic Ocean has important contributions to precipitation in West

35

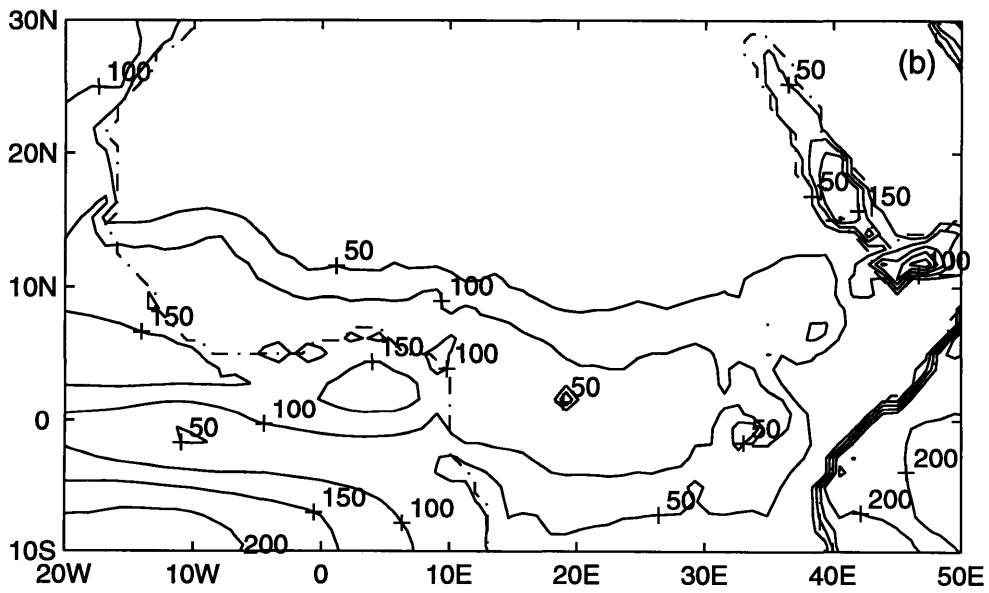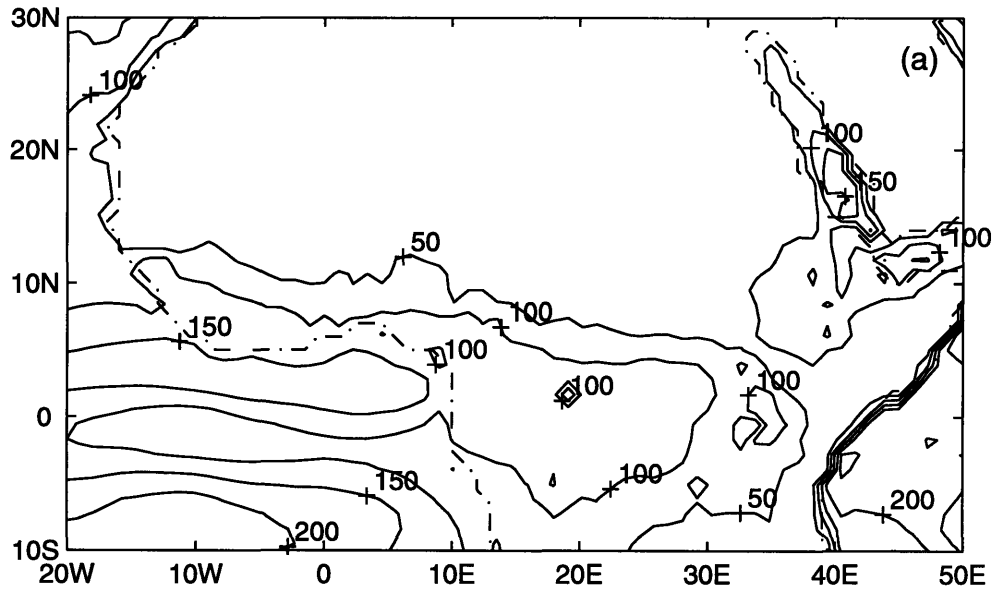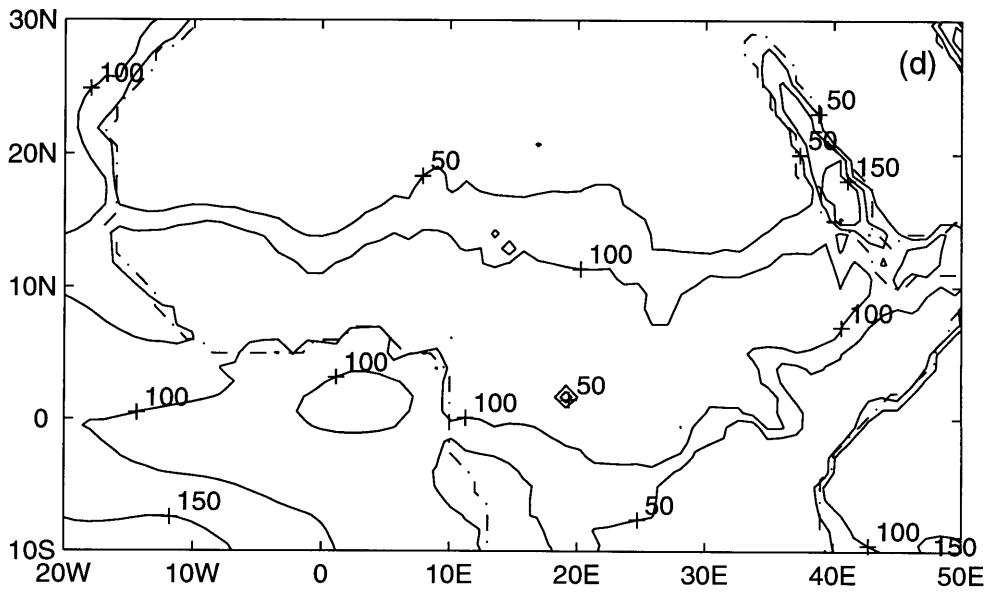Figure 2-4: Monthly evaporation in West Africa in mm for (a) June (b) July (c) August and (d) September
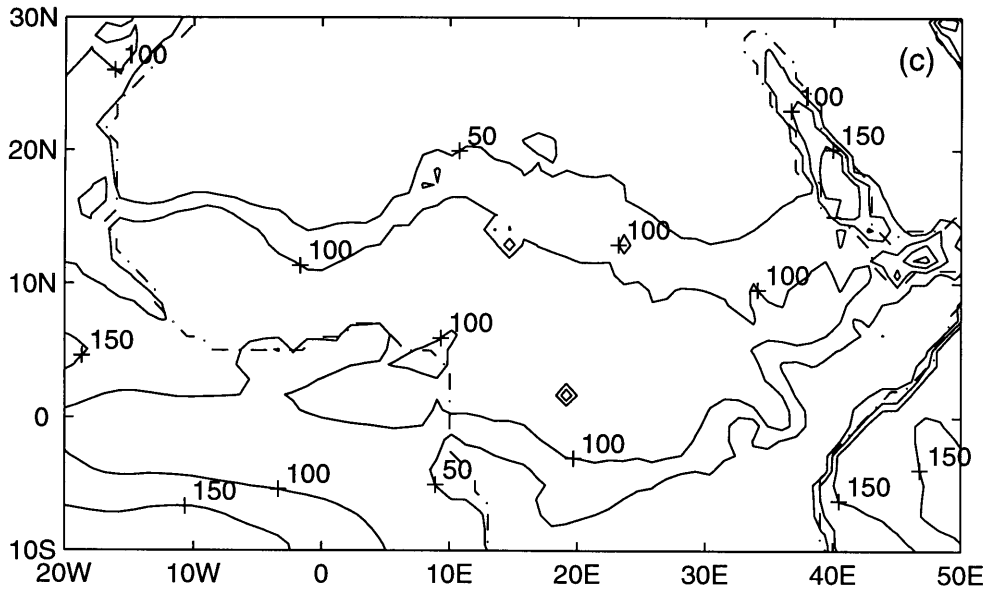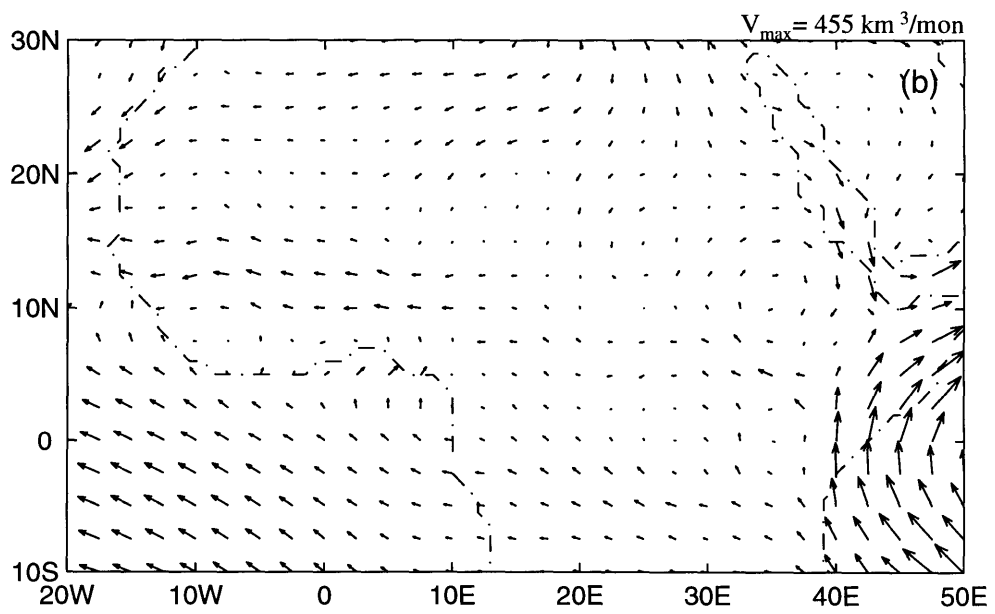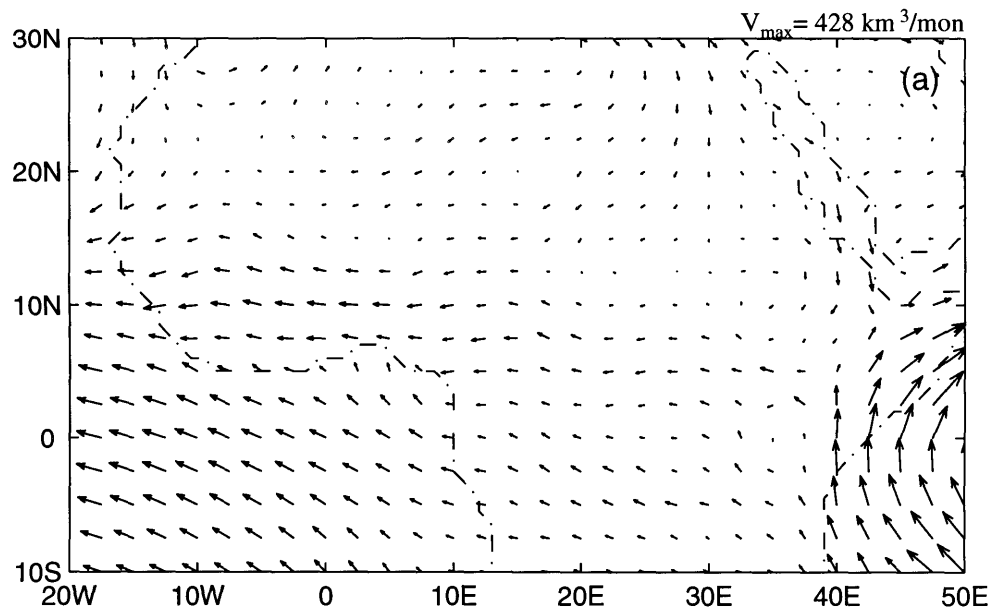
Figure 2-4: Continued

Figure 2-5: Distribution of water vapor fluxes in West Africa in Km^3 for (a) June (b) July (c) August and (d) September
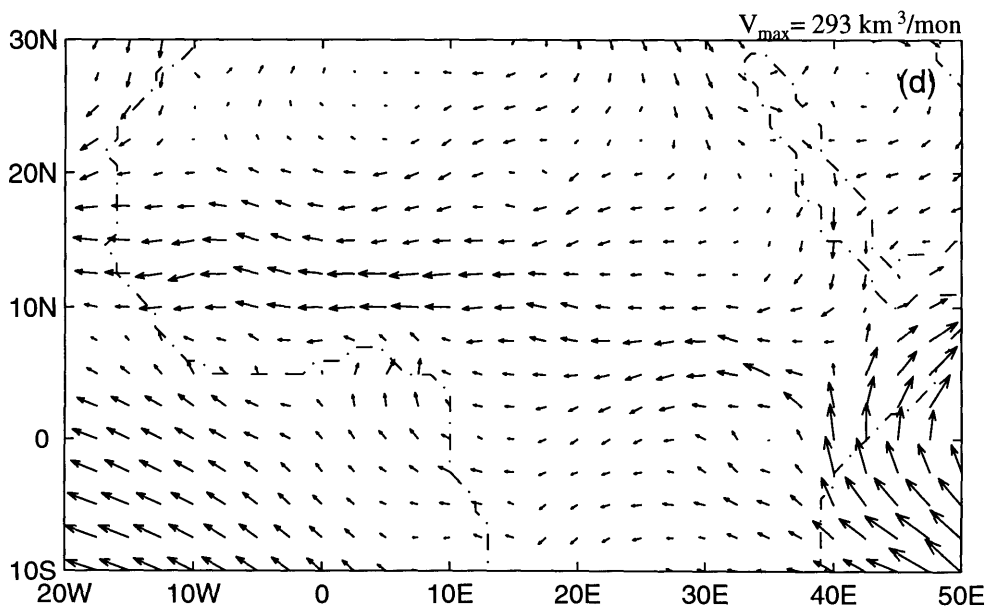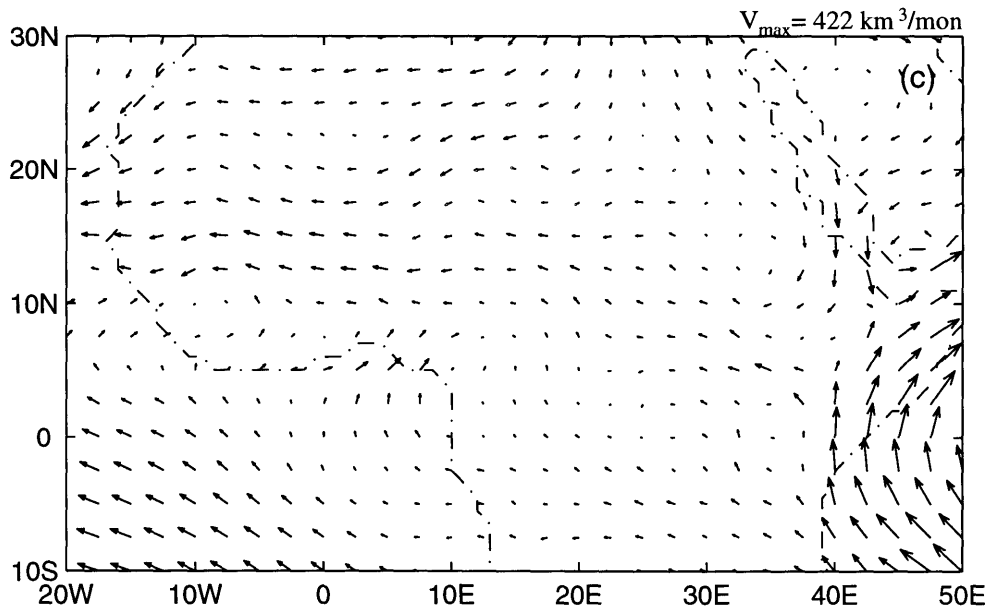
Figure 2-5: Continued
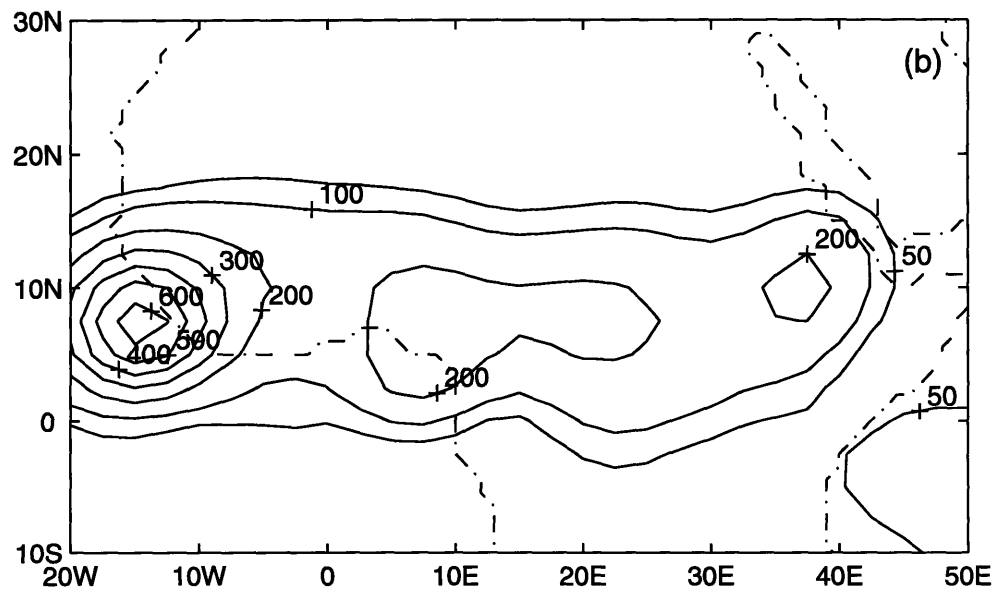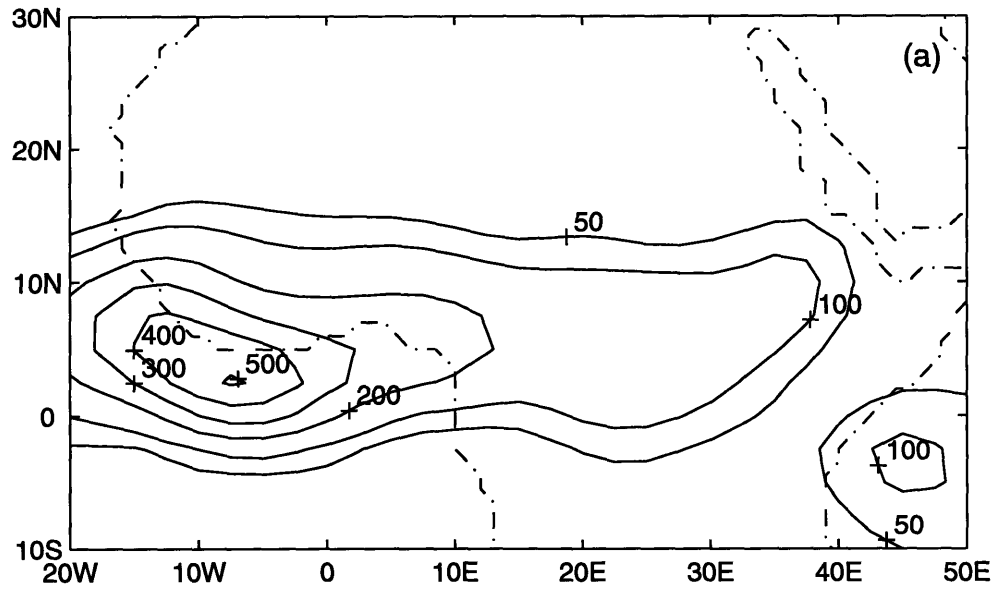
Figure 2-6: Climatology precipitation in West Africa in mm for (a) June (b) July (c) August and (d) September
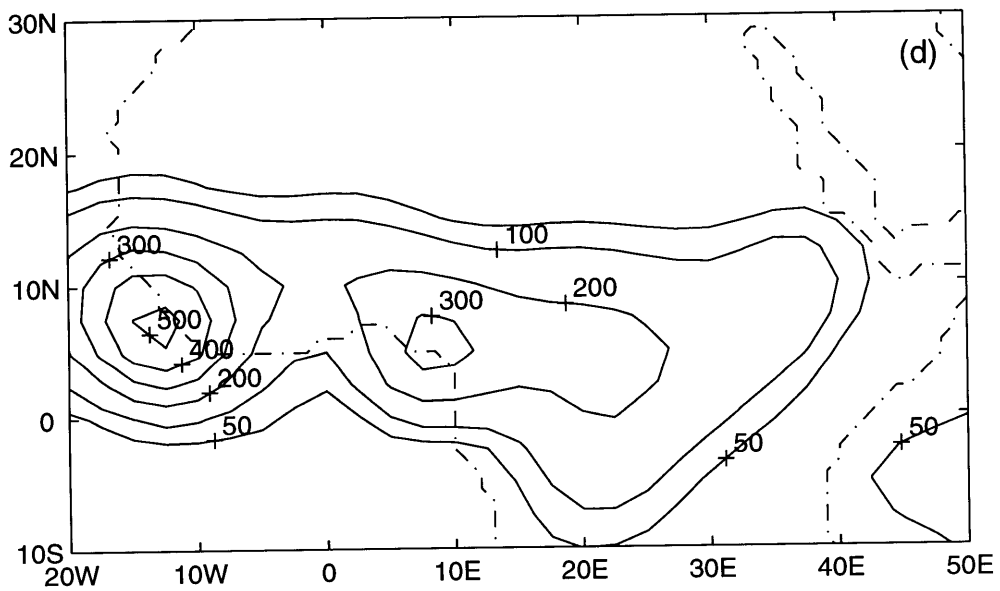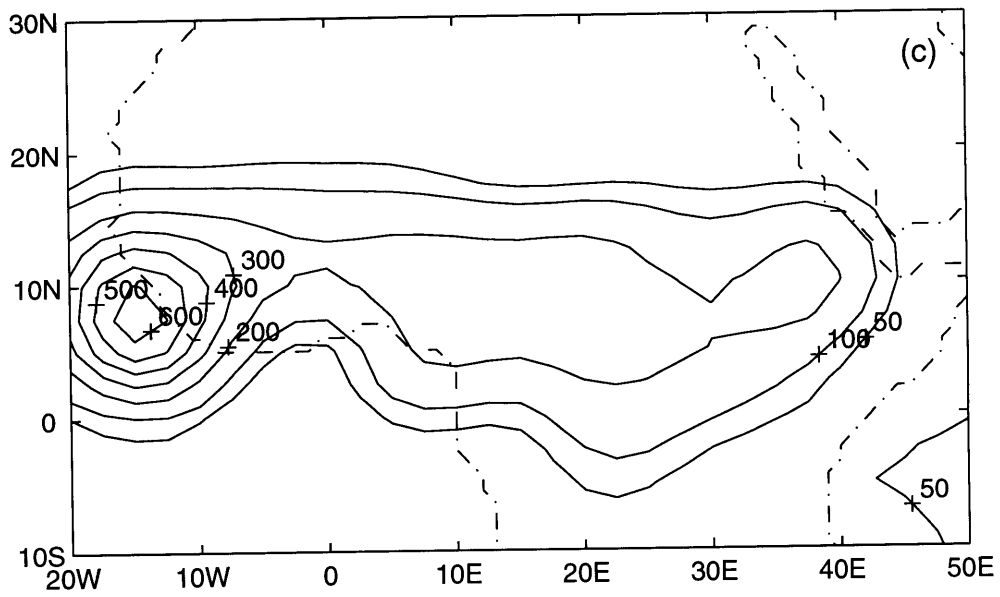
Figure 2-6: Continued

Africa. The contribution of evaporation increases from June to August as shown in Figure 2-9(a), (b) and (c) and starts to decrease in September as shown in Figure 2-9(d).

To investigate the recycling process further, we estimated the areal average of monthly recycling ratio in the three source regions using equation 2.12. There are nine cases to be considered: the recycling ratio in region 1, 2, and 3 in cases of the source region being region 1, 2 and 3 respectively. Figure 2-10 shows the summary of the results for the nine cases. In each case, recycling ratios in five months (June to October) are estimated. For example, in case (a), the recycling ratio represents the contribution of evaporation in region 1 to precipitation in region 1. The estimates of the recycling ratio in June, July, August, September and October are 25%, 27%, 40%, 40% and 40% respectively. In cases (b) and (c), the recycling ratio represents the contribution of evaporation in region 1 to precipitation in regions 2 and 3. Similarly, we can interpret the other six cases.

The areal average precipitation recycling ratios averaged throughout the rainy season are estimated using an equation similar to equation 2.13. The total yearly precipitation is replaced by the total precipitation throughout the rainy season. The results are presented in Table 2.3. The first row in Table 2.3 indicates that evaporation in Central Africa contributes 35 percent of rainfall in Central Africa, 17 percent of rainfall in West Africa and 7 percent of rainfall in Tropical Atlantic Ocean in the rainy season. The other two rows can be interpreted similarly. The areal average recycling ratio in West Africa during the rainy season is 23 percent when the source region is specified as the Tropical Atlantic Ocean, which is larger than the 17 percent contributed by Central Africa. This result is consistent with the decrease of moisture supply from the east during the rainy season, and increase of moisture supply from the south during the same period.

Since most of the rainfall is received during the rainy season, June to October, as shown in Figure 2-14(a), the recycling ratio for the rainy season can be used as an approximate measure of the yearly recycling ratio. The spatial distribution of the recycling ratio in the rainy season with the source region specified as West Africa is
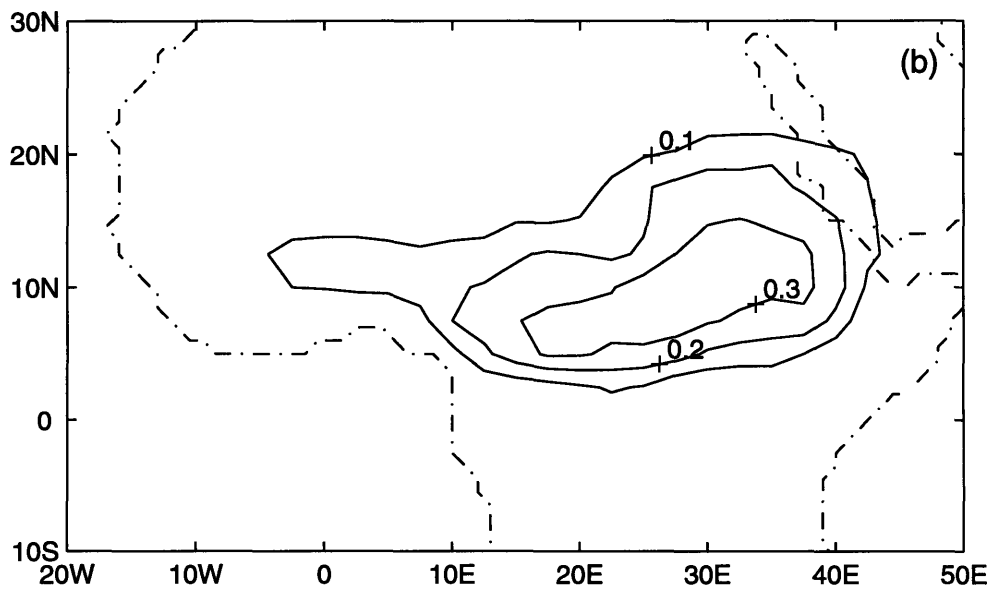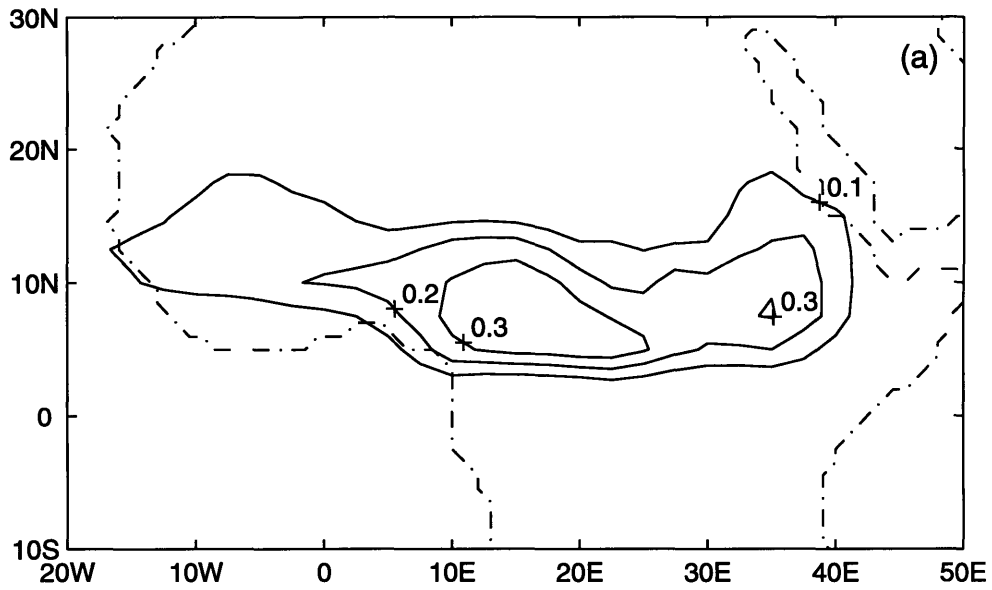
Figure 2-7: Spatial distribution of the precipitation recycling ratio with the source region specified as region 1 for (a) June (b) July (c) August and (d) September
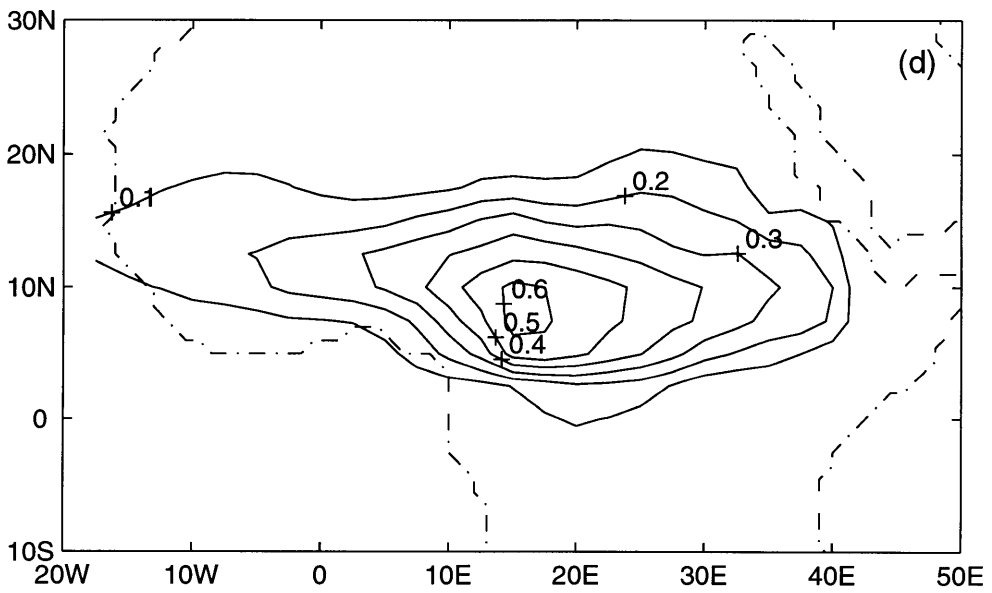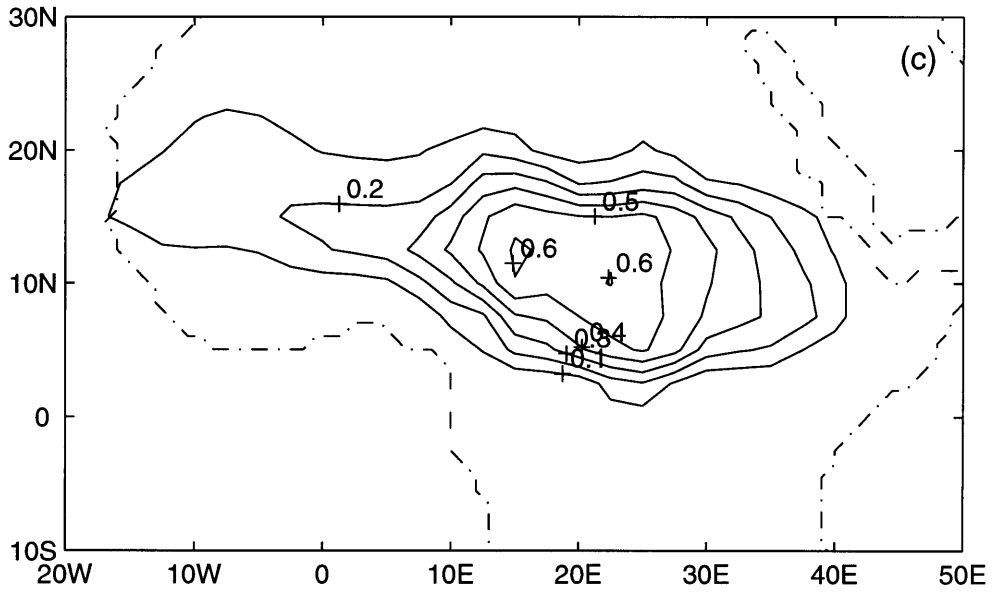
Figure 2-7: Continued
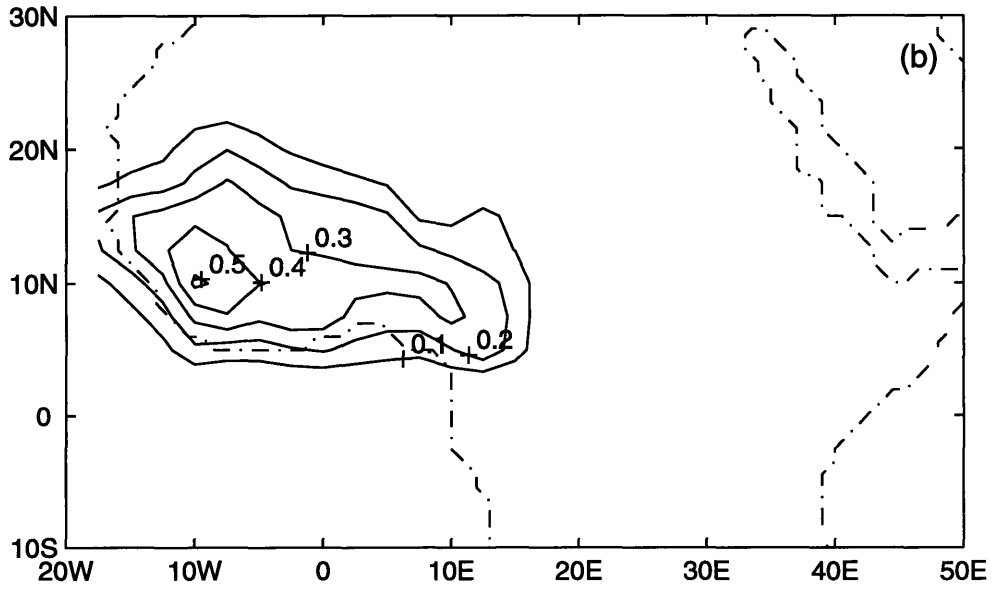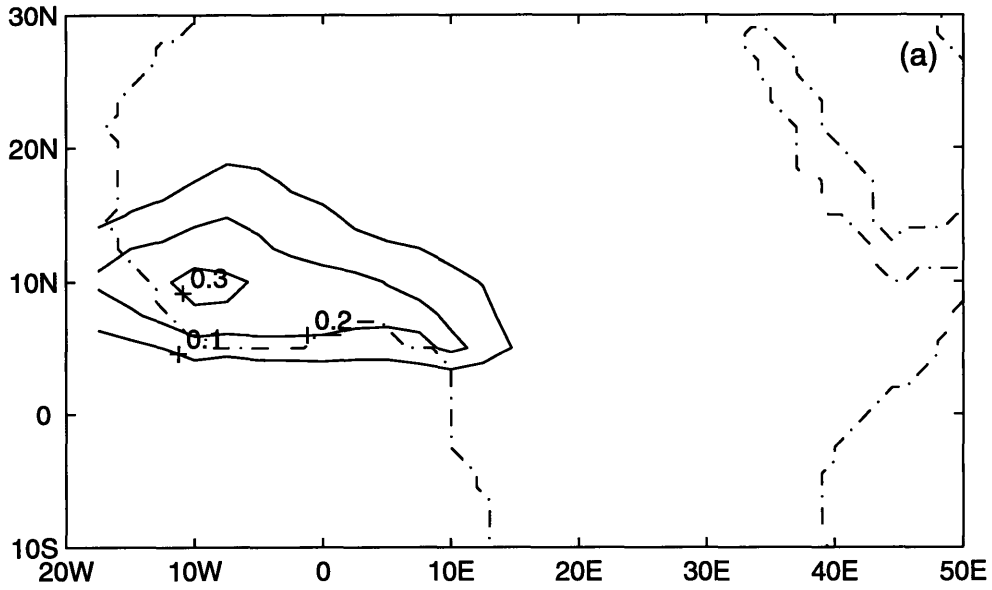
Figure 2-8: Spatial distribution of the precipitation recycling ratio with the source region specified as region 2 for (a) June (b) July (c) August and (d) September
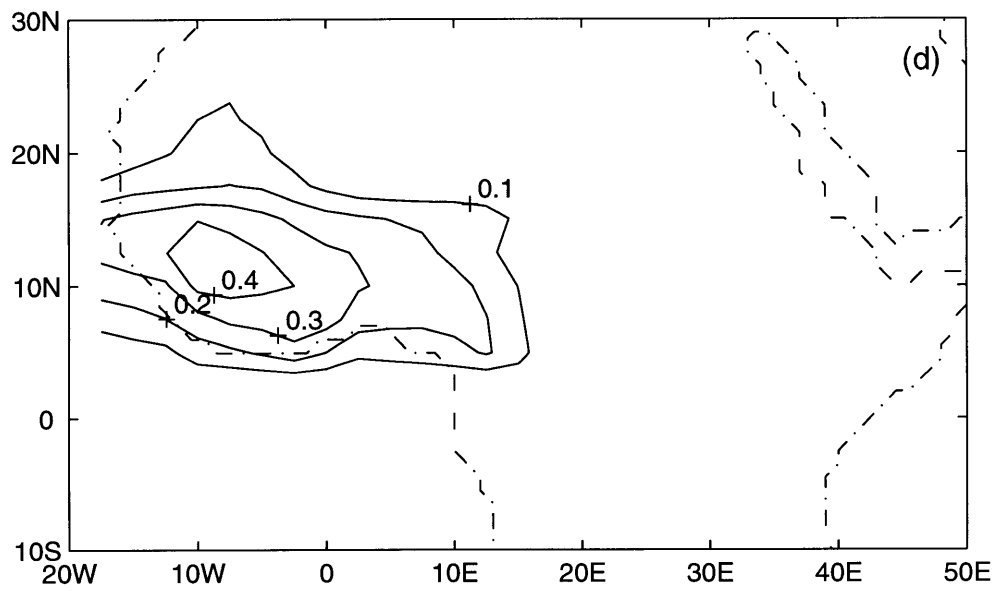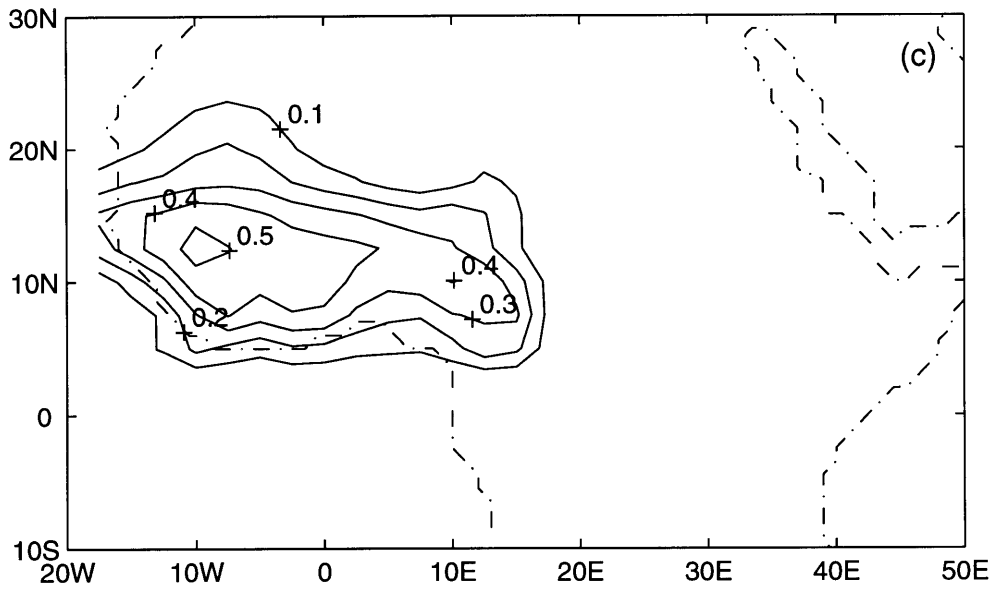
Figure 2-8: Continued
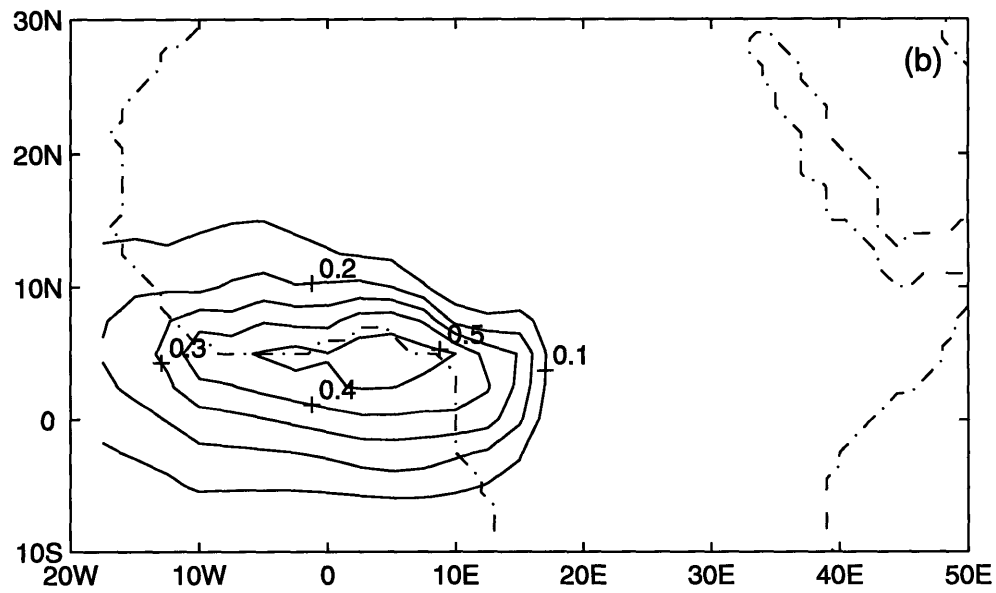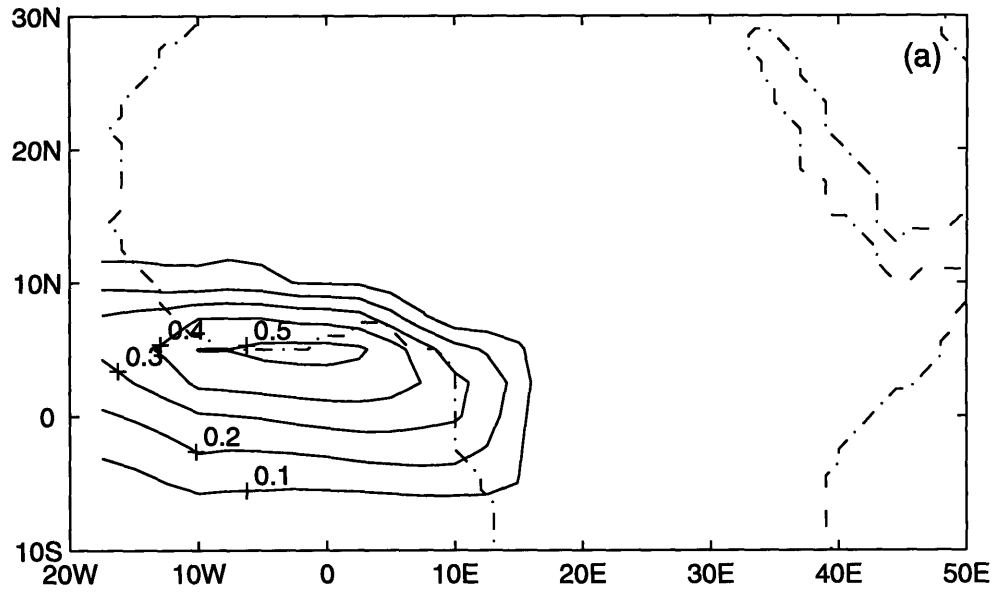
Figure 2-9: Spatial distribution of the precipitation recycling ratio with the source region specified as region 3 for (a) June (b) July (c) August and (d) September
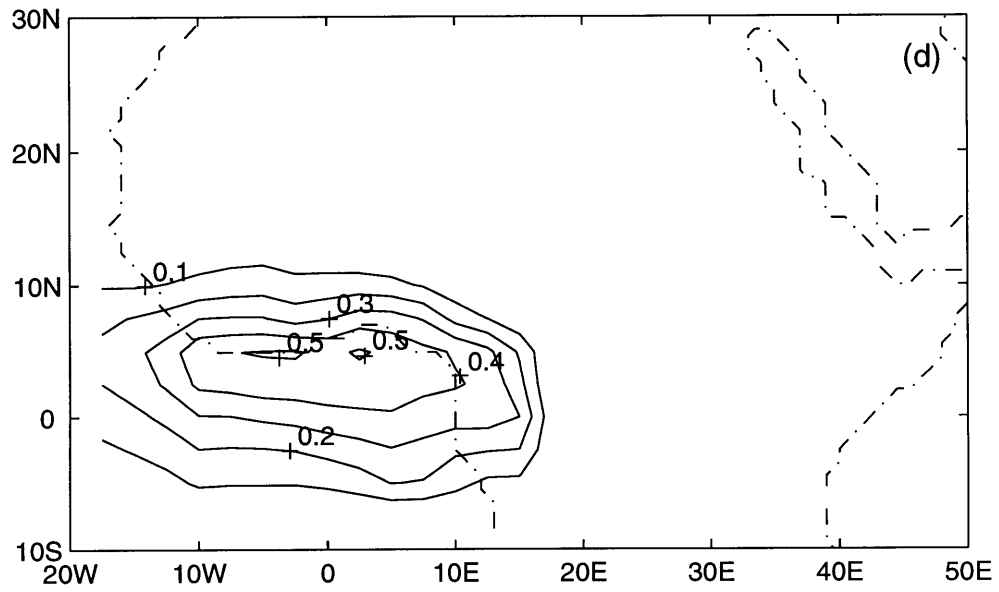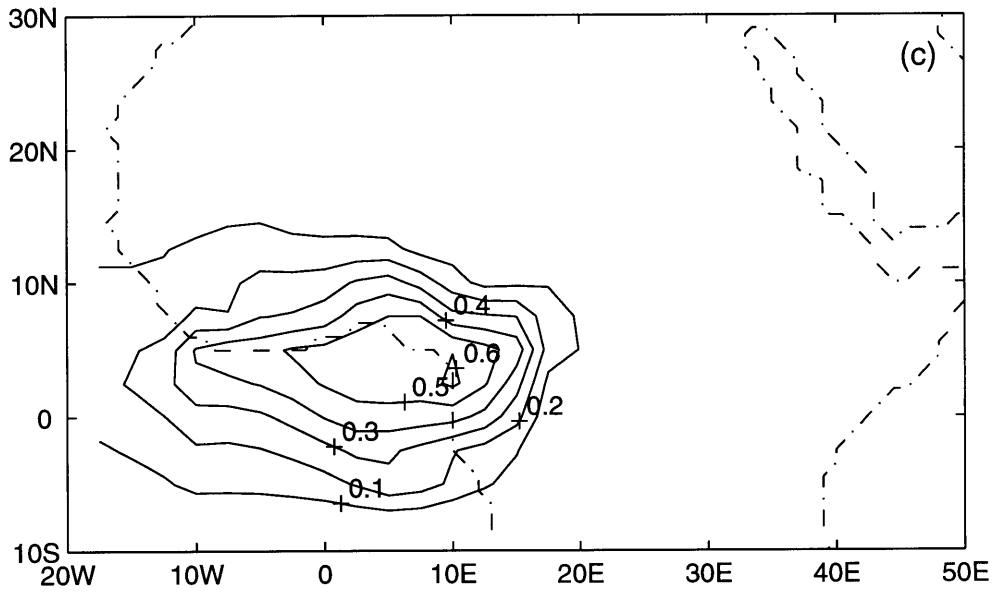
Figure 2-9: Continued
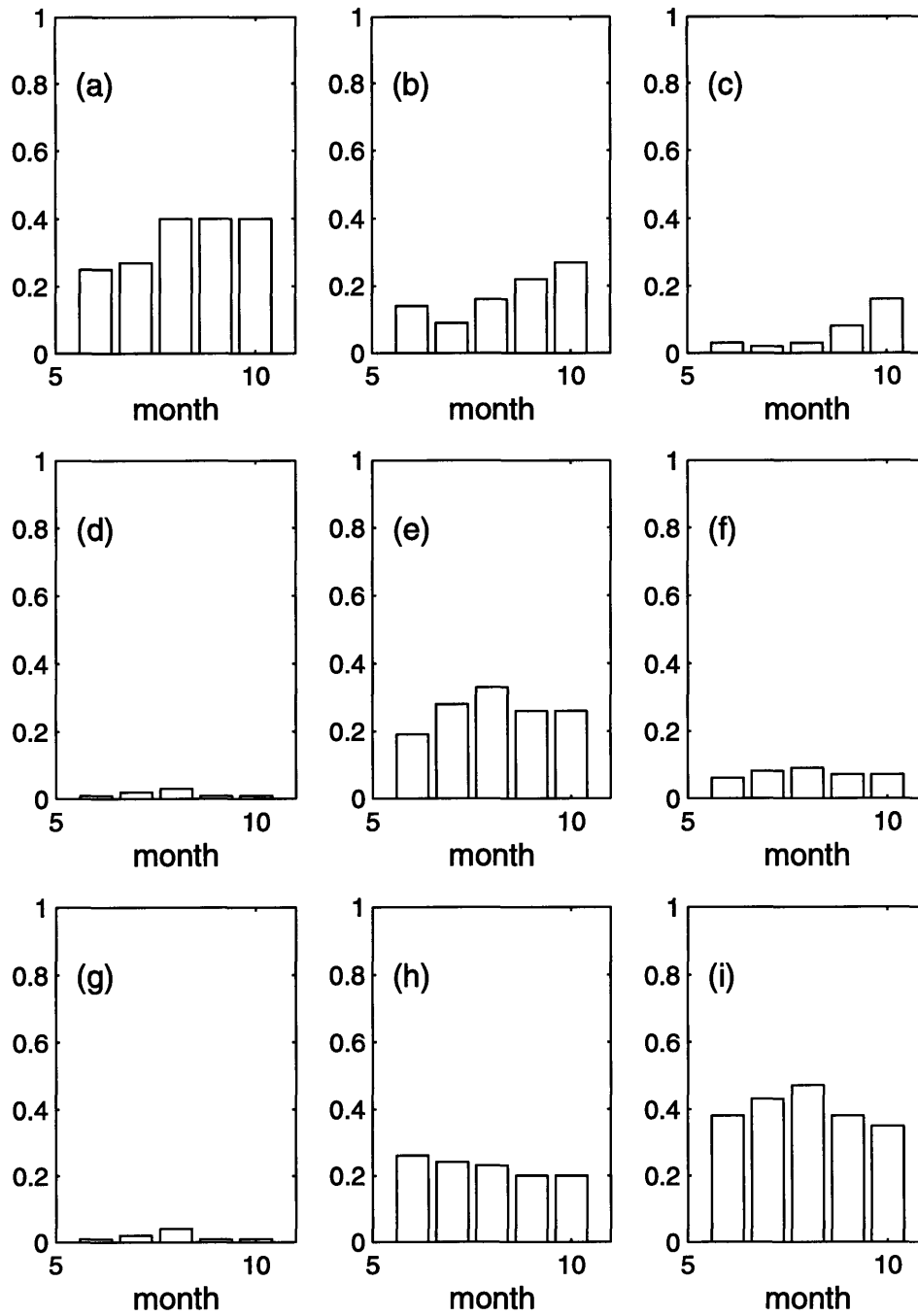
Figure 2-10: Areal monthly average of the precipitation recycling ratio in (a) region 1 (b) region 2 (c) region 3, all with the source region specified as region 1; and (d) region 1 (e) region 2 (f) region 3, all with the source region specified as region 2; and (g) region 1 (h) region 2 and (i) region 3, all with the source region specified as region 3.

Table 2.3: Areal Precipitation Recycling Ratios in the Rainy Season

	Central Africa	West Africa	Atlantic Ocean
Central Africa	0.35	0.17	0.07
West Africa	0.02	0.27	0.07
Atlantic Ocean	0.02	0.23	0.39

plotted in Figure 2-11. The figure shows that the recycling ratio in the rainy season in West Africa varies from 10 percent to 40 percent.

2.4.2 Scaling Study

A further analysis is performed to study the variation of the recycling ratio estimated for different sizes of the source region. In general, the recycling ratio increases if the source region is larger. As an extreme, if the source region is the total area of the earth, then the recycling ratio will be 100%. The objective of this analysis is to test how the recycling ratio scales as the area of the source region changes. The recycling ratio depends on the scale and the hydroclimatological conditions of the region, for example, the recycling ratio for the same area in West Africa and in the Amazon basin will be different. On the other hand, for the same region the recycling ratio would depend on the scale of the area considered. Hence in order to compare recycling ratios in different regions we need to study the recycling process at the same scale. In this study, the relation between the areal average of the recycling ratio and the area of the source region in West Africa is investigated.

The entire area of West Africa is divided into small square cells of equal sizes and with the length of each side equivalent to the specified scale. The smallest scale we can use for this analysis is the resolution of the ECMWF data ($\sim 250km$), and the largest scale is the entire area. Each cell is treated as a single well-mixed box so that I_i is equal to zero. Equation 2.10 becomes

$$\rho = \frac{E}{E + I} \tag{2.17}$$
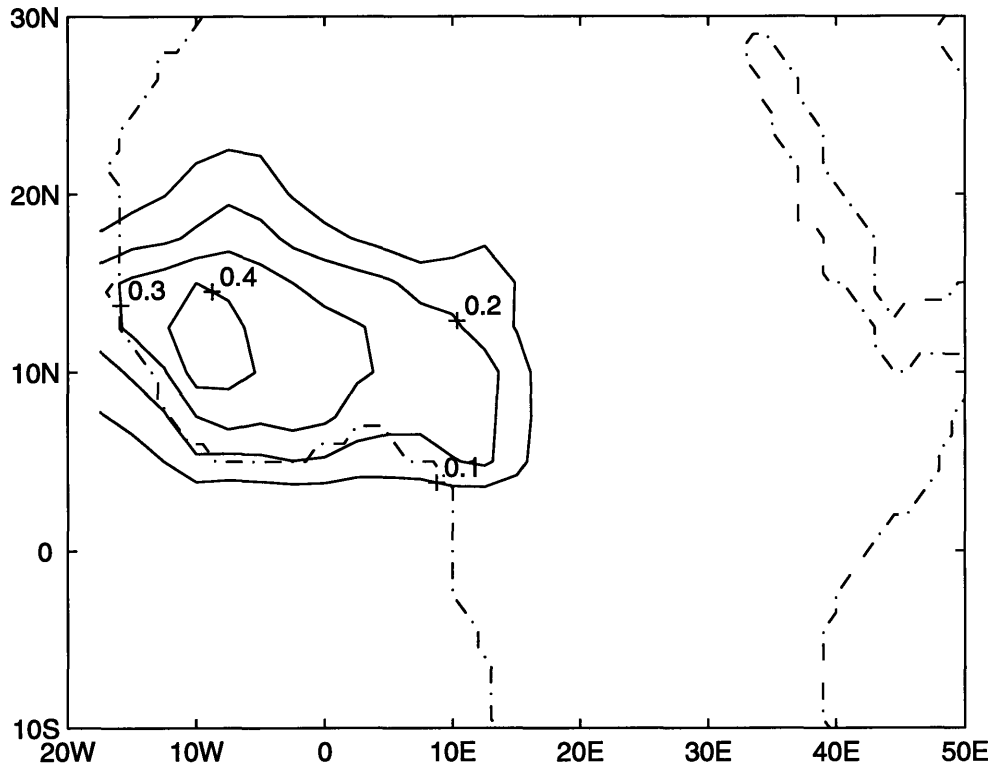
Figure 2-11: Distribution of the precipitation recycling ratio in the rainy season with the source region specified as region 2

The recycling ratio is estimated in each cell and then averaged over all the cells with the same scale. Data used for this scale analysis are based on the evaporation and flux data in August 1992. The result of the scaling study is shown in Figure 2-12. The slope of the line reflects the regional hydrologic properties. For this particular study, the relation between the recycling ratio and area of the source region can be described by

$$\rho = 0.0053X^{0.57}; \quad R^2 = 0.96 \tag{2.18}$$

where X is the length scale of the square cells. Compared to the Amazon basin, where the relation between the annual recycling ratio and area of the source region is described by $\rho = 0.0056X^{0.5}$ (Eltahir, 1993), the recycling ratio is higher in West Africa in August when the scale of the cells are the same. The higher the recycling ratio, the more the local evaporation contributes to rainfall in the source area. Thus rainfall in West Africa in August has more contributions from local evaporation than annual rainfall in the Amazon Basin.

2.4.3   Fluxes Across the Boundaries of West Africa

The fluxes across the southern, northern, and eastern boundaries of West Africa are also studied. The objective is to study the temporal variations of these fluxes. The monthly fluxes across the three boundaries from January 1992 to December 1994 are plotted in Figure 2-13(a), (b) and (c) respectively. It is seen that the fluxes across the southern and eastern boundaries are much larger than those across the northern boundary. Comparing the precipitation shown in Figure 2-14 and the fluxes variations, we can see that the incoming fluxes from the southern boundary of the region have very similar shape as the precipitation curve, while fluxes from the eastern and northern boundaries are not in phase with the precipitation. The atmospheric dynamics behind these observations are discussed in the next section.
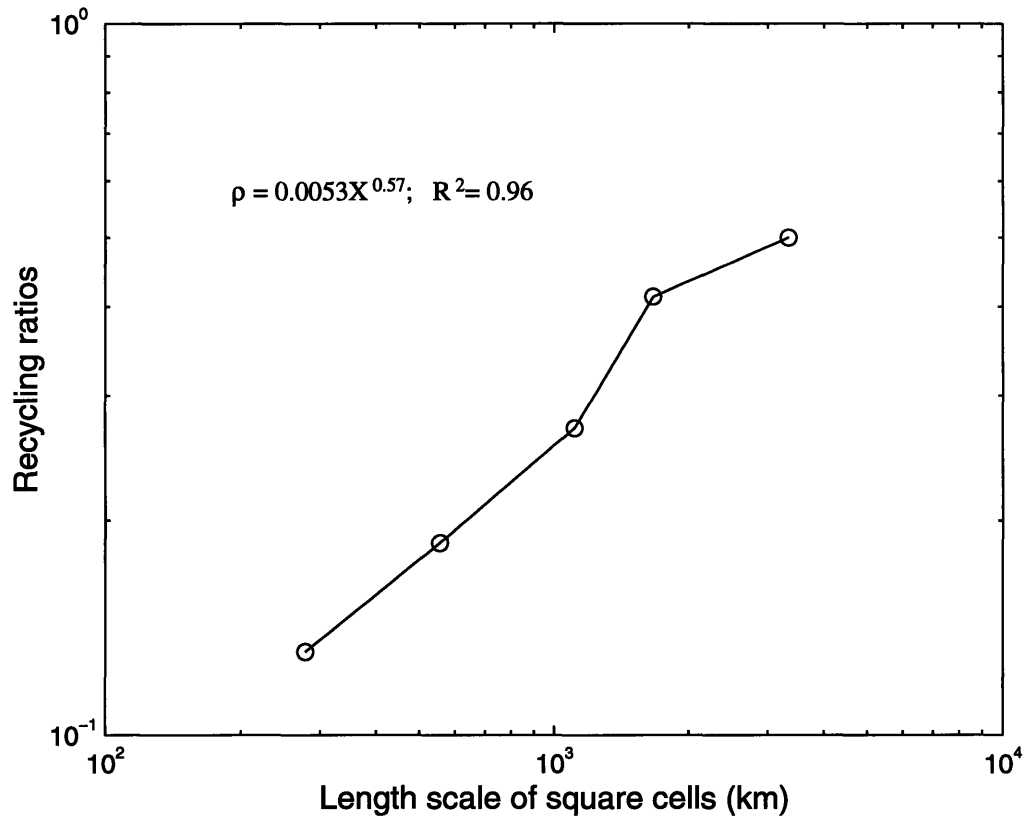
Figure 2-12: Relation between the precipitation recycling ratio and the size of the region
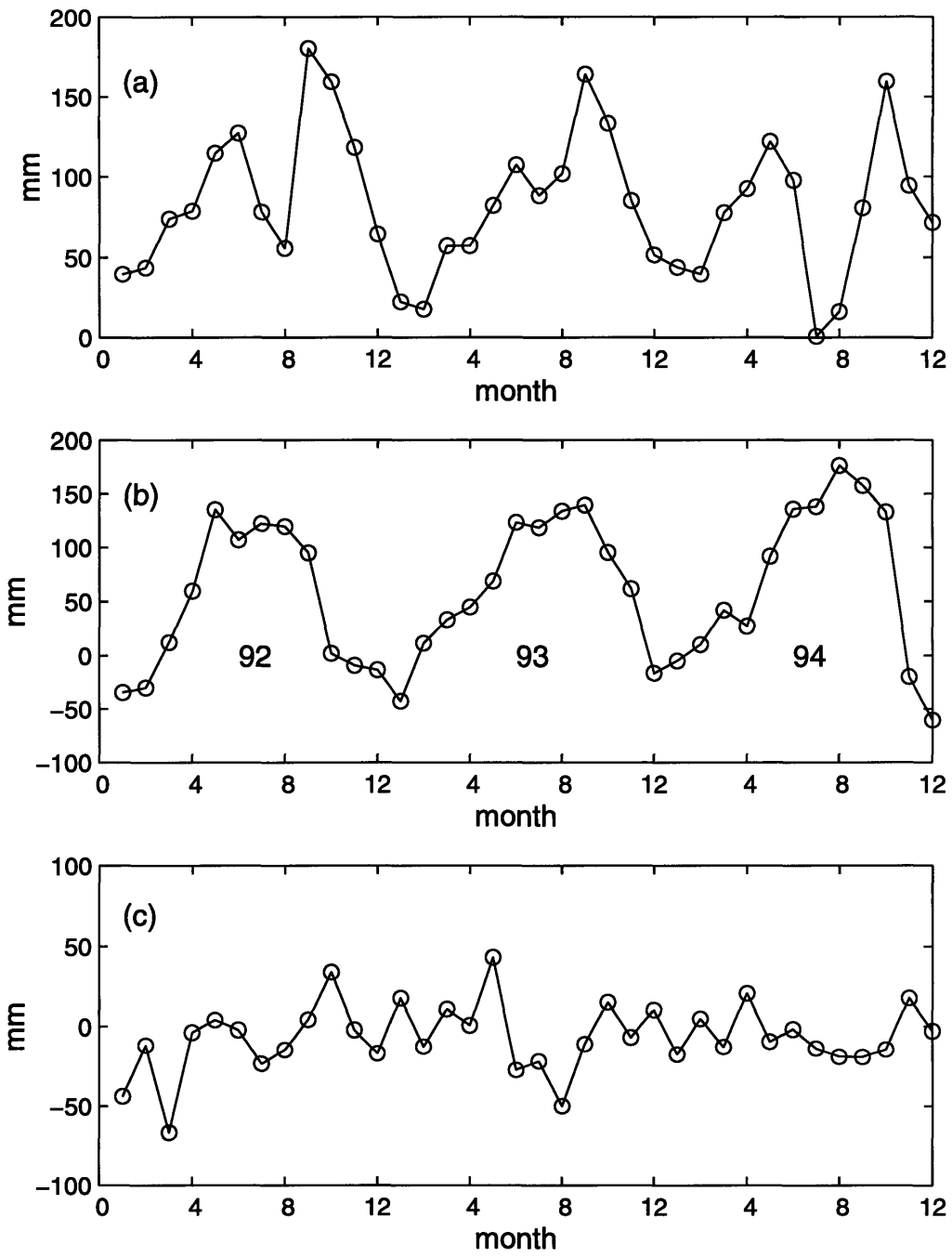
Figure 2-13: Water vapor fluxes coming from (a) eastern (b) southern (c) northern boundaries of West Africa
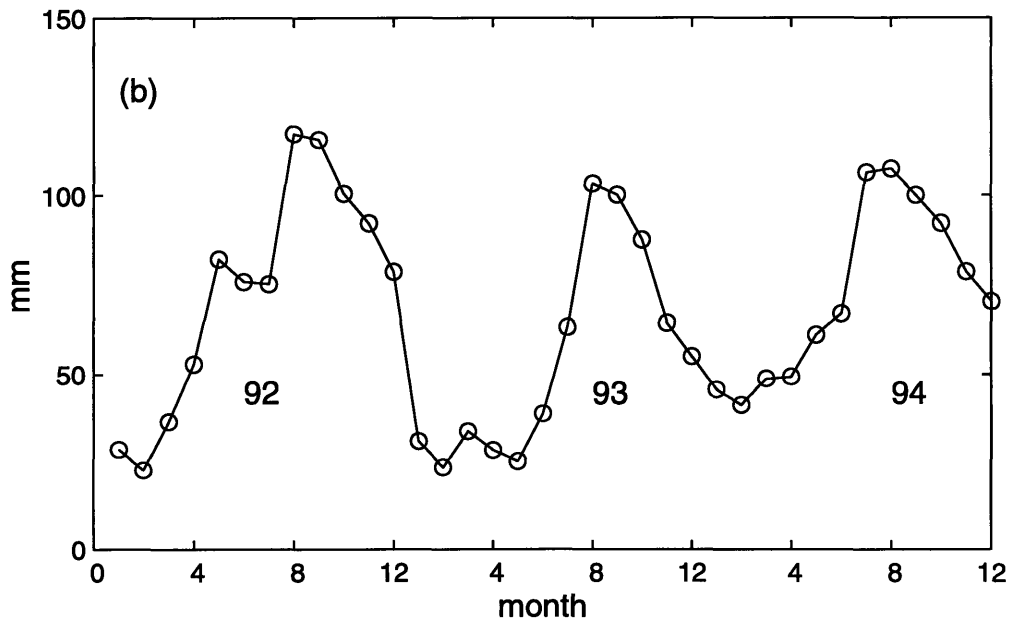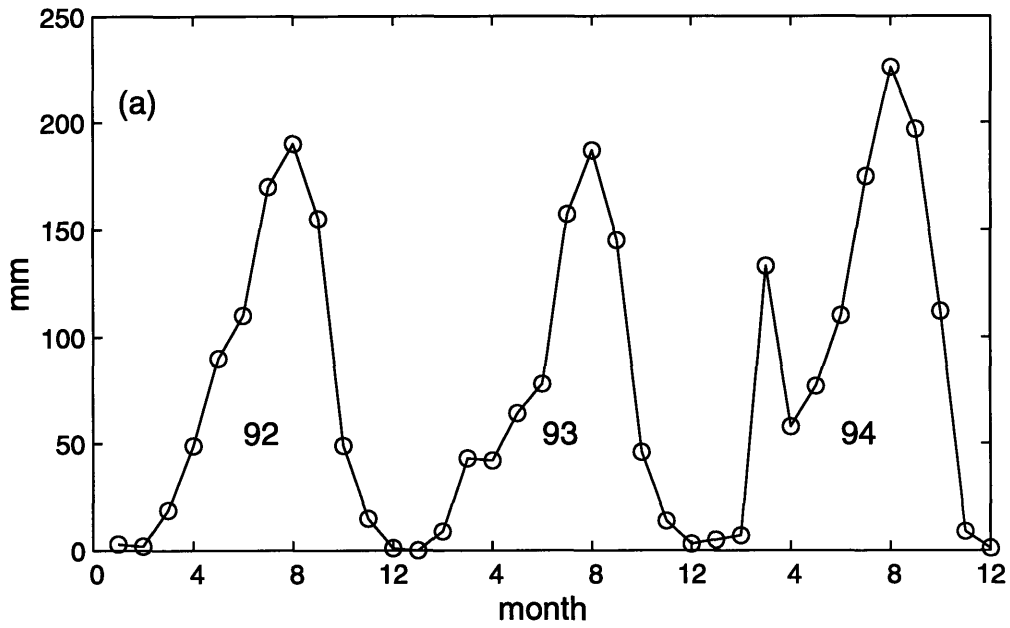
Figure 2-14: The time series of (a) monthly precipitation   (b) monthly evaporation
from 1992 to 1994

2.5 Discussion and Findings

The precipitation in West Africa is mainly contributed by local evaporation and evaporation in the areas to the east and to the south of the region. These three components contribute about 70 percent of the total precipitation in West Africa. Evaporation from the two African land regions, combined, contributes more rainfall to West Africa than the Tropical Atlantic Ocean, 44 percent in comparison to 23 percent. However, the Tropical Atlantic Ocean contributes nearly as much rainfall as local evaporation in West Africa.

The local evaporation in West Africa contributes about 30 percent of the precipitation, which indicates a significant potential for interactions between the local surface hydrology and climate. Based on the scaling studies, we find that contribution of the local evaporation to rainfall in West Africa and the Amazon basin changes by different magnitude as the area increases by the same amount. Although the magnitude of this difference is not large, the contribution of local evaporation increases faster in West Africa as the area increases.

Rainfall has direct impact on the magnitude of evaporation. Figure 2-14(b) shows that evaporation is closely associated with rainfall, see Figure 2-14(a). Moisture supply and rainfall in West Africa relate to each other closely. As shown in Figure 2-11, moisture flux and rainfall in West Africa exhibit similar seasonal variation. On one hand, atmospheric moisture provides the source for rainfall and controls the maximum amount of rainfall. During the dry season, moisture supply to West Africa is very low as shown in Figure 2-13; rainfall shown in Figure 2-14(a) is low too. On the other hand, rainfall is associated with atmospheric circulations, which control where the moisture fluxes come from. Rainfall regulates the moisture supply from the Atlantic Ocean and Central Africa. In the early months of the rainy season, significant moisture is supplied to West Africa from the east, and the convective rainfall heats the upper troposphere, which could induce large scale meridional circulation when other conditions are desirable. Once the large scale monsoon circulation develops around August, the cross-equatorial southerly flow induces strong westerlies which shut off

the easterlies partially or even totally depending upon the strength of the monsoon. As a result, moisture supply from Central Africa decreases significantly in monsoon months: August and September. Figure 2-13 shows this feature clearly during 1994. In the same period, the moisture supply from the Tropical Atlantic Ocean increases significantly, which is almost in phase with the rainfall.

The variation of moisture supply is reflected in the areal average of recycling ratios. Figure 2-10(b) shows the contribution of the moisture evaporated in Central Africa to rainfall in West Africa. It is shown that recycling ratio drops during the monsoon months because of the decrease of moisture supply to West Africa from the east. Evaporation in West Africa increases as monsoon develops, therefore the local recycling ratio increases as shown in Figure 2-10(e). Moisture supply from the Tropical Atlantic Ocean increases in the monsoon months, but since the local evaporation increases during the same period, the recycling ratio for the moisture advected from the ocean remains the same or slightly decreases.

Vertical motion is a necessary ingredient to produce significant rainfall. The moisture supply in West Africa does not vary very much from 1992 to 1994, but there is much more rainfall in 1994 than in 1992 and 1993. We argue that the strong monsoon circulation in 1994, which provides an uplift mechanism, is responsible for the large amount of rainfall. Monsoon circulation and West African rainfall will be further studied in next chapter.

Chapter 3

Land-Atmosphere-Ocean Interactions and Rainfall Variability over West Africa

3.1 Introduction

In this chapter, we will develop and apply the dynamical theory of zonally-symmetrical thermally-direct circulation to the West African region. A specific relation is proposed between the distribution of the moist entropy in the boundary layer and the development of monsoon circulation. We will focus on the period prior to the onset of the current drought episode and study the processes that are important in regulating the natural variability in rainfall and circulation over West Africa.

Many studies have been done to investigate the mechanisms of rainfall variability over West Africa. Most of the studies can be classified into two categories. One of the two categories emphasizes the impacts of interactions between the land and the atmosphere on the regional climate. The other category focuses on the role of ocean-atmosphere interactions in the variability of rainfall in West Africa.

Studies in the first category investigate the impacts of the changes in the land surface processes involving surface albedo, soil moisture, and vegetation coverage, on

the dynamics of regional rainfall. The early work on the land-atmosphere interaction in West Africa was carried out by Charney (1975). He proposed the hypothesis that the change of vegetation coverage at the desert border affects the location of the Inter-Tropical Convergence Zone (ITCZ), which is directly related to Sahel rainfall. But Charney's mechanism did not take into account the effect of soil moisture and evaporation. Walker and Rowntree (1977) studied the effect of soil moisture and evaporation on rainfall in West Africa and they found that wet soil moisture conditions will result in a relatively wet year in West Africa. Other researchers also studied the role of land surface processes in regional climate: Yeh at al. (1984), Sud and Fennessy (1984), Sub and Molod (1988), Cunnington and Rowntree (1986), Kitoh et al. (1988), Powell and Blondin (1990), and Rodriguez-Iturbe et al. (1991). The results of these studies suggest that the land surface condition plays an important role in the variability of West African rainfall.

Studies in the the second category concentrate on the role of the ocean in the dynamics of atmosphere over West Africa. The correlation between the Sahel rainfall and the SST in the Tropical Atlantic is studied by Lamb (1978) and Lamb and Peppler (1992). They find that warm (cold) SST anomalies in the Atlantic Ocean correspond to dry (wet) years in Sahel. Folland at al. (1986) studied the relation between Sahel rainfall and SSTs over the oceans and found that the global SST correlates with the Sahel rainfall. Lough (1986) applies principle component analysis to the SST in the Tropical Atlantic and correlates the dominant patterns with rainfall in the Sahel region. Owen and Ward (1989) suggest that Sahel rainfall can be predicted by using the SST observations. All these studies are consistent in suggesting that the Tropical Atlantic, in particular the SST, plays a significant role in rainfall variability over West Africa.

Here we propose that rainfall variability in West Africa is regulated by the large scale ocean-land-atmosphere interactions. The dynamics of wet and dry years over West Africa are not just governed by the land-atmosphere interactions, or the ocean-atmosphere interactions alone. They are governed by the ocean-land-atmosphere interactions simultaneously. The meridional gradient of moist entropy in the boundary

layer between the ocean and the land reflects these interactions.

We will review some early work in developing the dynamical theory of zonally symmetric circulationins and describe the proposed theory of ocean-atmosphere-land interactions in section 3.2. The analysis of observations of wind, temperature, humidity and rainfall are given in Section 3.3. Finally, Section 3.6 summarizes the findings and discussion.

3.2 Dynamical Theory of Monsoon Circulation

3.2.1 Early Work

Lindzen and Hou (1988) and Hou (1993) studied the Hadley circulation for zonally averaged heating centered off the equator. They find that the shift of tropical heating toward the summer pole, on time scales longer than a few weeks, leads to a more intense cross-equatorial 'winter' Hadley circulation and enhanced upper-level tropical easterlies.

Plumb and Hou (1992) studied the response of a dry zonally symmetric atmosphere to a thermal forcing that is localized in the subtropics. On the basis of inviscid steady-state theory, they find that the atmosphere adopts a steady-state of thermal equilibrium with no meridional flow if the forcing is below a threshold. With supercritical forcing, the thermal equilibrium state breaks down and a strong meridional circulation develops. The criterion for the thermal equilibrium state derived from the angular momentum conservation and heat balance equations is given by

$$-\frac{1}{2}\frac{gD}{T_o}\frac{1}{\cos\varphi}\frac{\partial}{\partial\varphi}[\frac{\cos^3\varphi}{\sin\varphi}\frac{\partial T_e'}{\partial\varphi}] < 2\Omega^2 a^2 \sin\varphi\cos^2\varphi \qquad (3.1)$$

where Ω and a are the earth's rotation rate and radius, φ is the latitude, T_o is the reference background temperature, D is the height of the upper boundary of the atmosphere, $T_e' = \frac{1}{D}\int_0^D T_e dz$ and T_e is an equilibrium temperature.

Equation 3.1 can be satisfied if the forcing is weak and the thermal equilibrium solution is obtained. For a sufficiently strong forcing, the above condition is violated, the

60

response of the atmosphere must take the form of an angular momentum-conserving solution in the region of the forcing, and an inviscid meridional circulation develops.

Zheng and Plumb (1995) derived a regularity condition for the thermal equilibrium solution later on in terms of moist variables:

$$2\Omega^2 a^2 \sin\varphi\cos^2\varphi + \frac{1}{2}\frac{1}{\cos\varphi}\frac{\partial}{\partial\varphi}[\frac{\cos^3\varphi}{\sin\varphi}\frac{\partial s^*}{\partial\varphi}(T_s - T_t)] > 0 \qquad (3.2)$$

where s^* is the saturation entropy, T_s and T_t are temperatures at the surface and upper atmosphere.

Emanuel et al.(1994) proposed a theory for large scale steady circulations in a convecting atmosphere at statistical equilibrium. They link the large scale circulations to the distribution of the subcloud layer entropy in space and time by assuming that the convective neutrality condition holds in moist atmospheres. They apply their theory to the tropics and develop a criterion similar to that of Plumb and Hou (1992):

$$1 + \frac{1}{f}\nabla\frac{1}{f}(T_o - T_T)\nabla s_b \geq 0 \qquad (3.3)$$

where f is the Coriolis force, T_o and T_T are the temperatures of the surface and tropopause, respectively, and s_b is the actual subcloud-layer entropy. When the condition given in equation 3.3 is satisfied, the radiative-convective equilibrium state is sustained. When the criterion is violated, the thermally direct circulation develops.

Emanuel (1995) carried on this development further and derived an integral form of criterion for the thermal-equilibrium circulation, which is very useful for those regions that include the equator since equation 3.3 is not applicable near the equator. The derivation assumes that in radiative-convective equilibrium the atmosphere is nearly neutral to moist convection. The critical distribution of θ_{eb} is given by:

$$\theta_{eb} = \theta_{em}\exp[-\chi\frac{(\cos^2\varphi_m - \cos^2\varphi)^2}{\cos^2\varphi}] \qquad (3.4)$$

where

$$\chi = \frac{\Omega^2 a^2}{2C_p(T_s - T_t)} \qquad (3.5)$$

61

and φ_m is the latitude at which θ_e has its maximum value θ_{em}. The relation between the boundary layer entropy and the equivalent potential temperature θ_{eb} is given in the first chapter.

3.2.2 Theory of Land-Atmosphere-Ocean Interactions

Our theory is built on the results of earlier studies on the dynamics of zonally-symmetrical thermally-direct atmospheric circulation. As proposed by Eltahir and Gong (1996), the observations on rainfall, temperature and humidity suggest that climate in West Africa can be approximately by a zonally symmetrical description. Rainfall variability in West Africa is the result of large scale land-atmosphere-ocean interactions. We assume that the vertical distribution of saturation entropy is uniform and hence the subtropical thermal forcing is uniquely related to the meridional distribution of boundary layer entropy.

For a zonally symmetrical circulation, the thermal wind relation is described by

$$\frac{\partial u}{\partial p} = \frac{1}{f}\frac{\partial \alpha}{\partial y} \tag{3.6}$$

where u is the zonal wind, p is pressure, f is Coriolis parameter, α is specific volume, and y is the distance in the meridional direction. The Maxwell's relations (Emanuel, 1994) imply that

$$\left(\frac{\partial \alpha}{\partial y}\right)_p = \left(\frac{\partial \alpha}{\partial s^*}\right)_p \frac{\partial s^*}{\partial y} = \left(\frac{\partial T}{\partial p}\right)_{s^*} \frac{\partial s^*}{\partial y} \tag{3.7}$$

where s^* is saturation entropy, $s^* = C_p ln(\theta_e^*)$, where C_p is specific heat capacity at constant pressure, and θ_e^* is the equivalent potential temperature of air if saturated at the same pressure and temperature. Assuming a moist adiabatic lapse rate and integrating the thermal wind equation from the surface (wind is assumed to be zero) to the tropopause, we get the following relation,

$$u_t = -\frac{1}{f}(T_0 - T_t)\frac{\partial s_b}{\partial y} \tag{3.8}$$

where u_t and T_t are wind and temperature at the tropopause, T_0 is surface temperature, and s_b is boundary layer entropy. The absolute vorticity at the tropopause is given by

$$\eta_t = f - \left(\frac{\partial u_t}{\partial y}\right) = f + \frac{\partial}{\partial y}\left(\frac{1}{f}(T_0 - T_t)\frac{\partial s_b}{\partial y}\right) \tag{3.9}$$

The above equation shows the relation between absolute vorticity at the tropopause and the meridional distribution of boundary layer entropy (Emanuel et al., 1994). Plumb and Hou (1992) show that the atmosphere adopts either the radiative-convective equilibrium regime or an angular momentum conserving regime. A radiative-convective equilibrium regime should exist if the absolute vorticity at the tropopause has the same sign as the Coriolis parameter f. This condition can be described by the following equation if the geostrophic balance is assumed,

$$1 + \frac{1}{f^2}\frac{\partial}{\partial y}\left((T_0 - T_t)\frac{\partial s_b}{\partial y}\right) - \frac{\beta}{f^3}(T_0 - T_t)\frac{\partial s_b}{\partial y} > 0 \tag{3.10}$$

where $\beta = \frac{\partial f}{\partial y}$. A similar equation can be derived assuming a gradient wind balance,

$$4\Omega^2 a^2 \sin\varphi\cos^3\varphi + \left(\frac{\partial}{\partial\varphi}\left[\frac{\cos^3\varphi}{\sin\varphi}\frac{\partial s_b}{\partial\varphi}(T_0 - T_t)\right]\right) > 0 \tag{3.11}$$

where φ is the latitude. An angular momentum conserving regime should dominate the dynamics of the atmosphere if the above conditions are not satisfied. The distribution of entropy in the atmospheric boundary layer determines which of the two regimes dominates the dynamics. The physical variables that control the above threshold behavior are the gradient and the second derivative of the meridional distribution of boundary layer entropy. Since absolute vorticity is proportional to the gradient of angular momentum, a zero absolute vorticity in the tropopause is an indicator of an angular momentum conserving regime. The latter describes the monsoon circulation.

The dynamical theory of monsoon circulation provides a general theoretical framework for understanding the natural variability in the dynamics of the atmospheric

circulation over West Africa. The theory predicts that a flat meridional distribution of boundary layer entropy is not associated with a strong monsoon circulation, and a relatively large gradient of entropy would favor a strong monsoon circulation. Since the gradient of the boundary layer entropy over West Africa is controlled by both ocean and land, the meridional distribution of boundary layer entropy is regulated by changes in either the SST or entropy over land. The dynamics of wet and dry years are not governed by the land-atmosphere or the ocean-atmosphere interactions alone but by the land-atmosphere-ocean interactions.

3.3 Analysis of Observations

3.3.1 Data

The data used in this study are extracted from the Geophysical Fluid Dynamics Laboratory (GFDL) atmospheric circulation data (Oort, 1994). This monthly dataset has a resolution of 2.5 degrees in the meridional direction, 5 degrees in the zonal direction, and 11 pressure levels in the vertical direction. The data covers the period 1958 to 1989. The analysis of rawinsondes records is based on the observations at 00Z for the first ten years. In the rest of years it is abased on more than one daily observation, which makes the full data record not homogeneous. The period 1958 to 1967 is selected for the analysis since observations are relatively homogeneous, and hence the natural variability in the dynamics of the atmospheric circulation over West Africa can be studied. The year 1958 is the wettest year during the ten years period according to the analysis of Nicholson (1994). The year 1960 is the driest year in the same period. Figure 3-1 shows the standardized rainfall departures in the ten years period.

3.3.2 Results of Analysis

1. Comparison of the wind fields

The observations of zonal wind at 5E averaged over August and September in
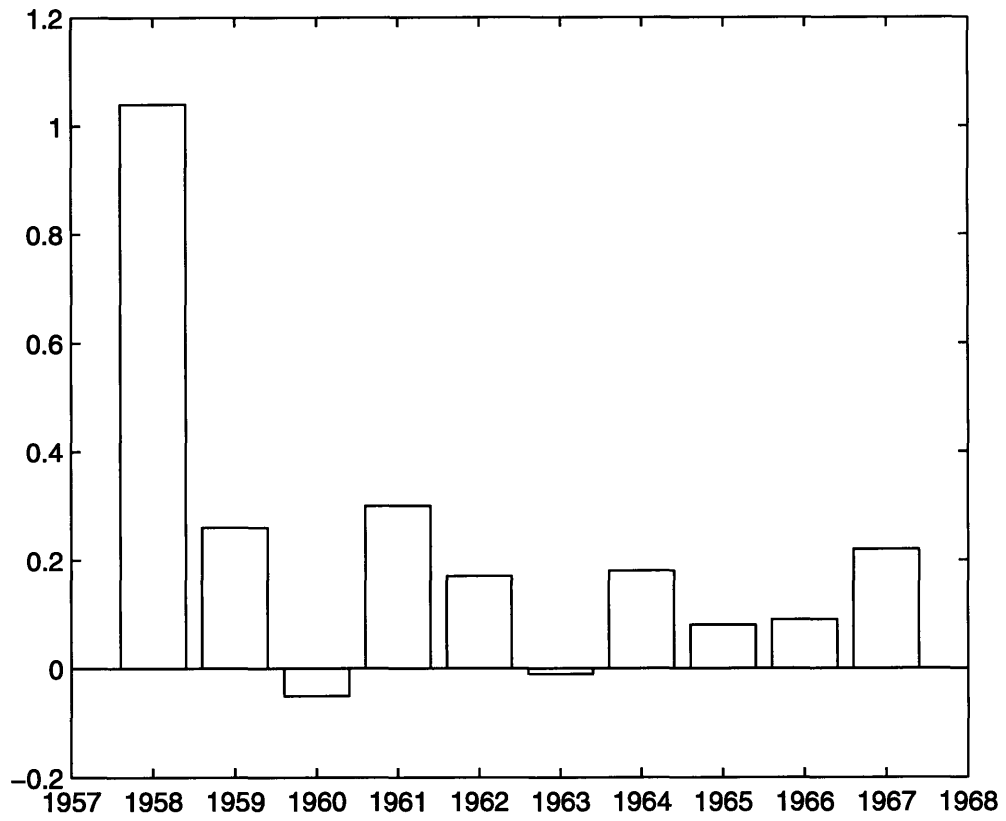
Figure 3-1: Rainfall departures from the mean (Nicholson, 1993)

1958 and 1960 are plotted in Figure 3-2(a) and Figure 3-2(b). The zonal wind at the upper atmosphere is much stronger in 1958 compared to that in the same period in 1960, indicating a stronger easterly jet in the upper atmosphere in 1958.

Similarly, the observations of meridional wind at the same location and time are plotted in Figure 3-3(a) and Figure 3-3(b). Stronger meridional circulations are observed in 1958: divergent flow in the upper atmosphere ($\sim$ 200mb) and convergent flow in the lower levels of the atmosphere ($\sim$ 700mb). The meridional circulation is relatively weak in 1960. The contrast of meridional circulations between 1958 and 1960 reflects the strength of the monsoon circulation in those two years: a strong monsoon circulation in 1958 and a weak monsoon circulation in 1960.

2. Comparison of the relative vorticity fields

The relative vorticity is calculated based on the wind distribution:

$$\zeta_r = \frac{\partial v}{\partial x} - \frac{\partial u}{\partial y} \tag{3.12}$$

where u is the zonal wind, v is the meridional wind, ζ_r is the relative vorticity.

Figure 3-4 shows the relative vorticity distributions at 2.5E averaged over August and September in 1958 and 1960. At the upper atmosphere ($\sim$ 200mb), the magnitude of the relative vorticity is much larger in 1958 compared to that in 1960 around 10S and 15N. Note that the observed relative vorticity in the upper atmosphere is negative in the northern hemisphere and positive in the southern hemisphere, while the planetary vorticity is positive in the northern hemisphere and negative in the southern hemisphere. Hence, the absolute vorticity, which is the sum of the planetary and relative vorticities, should approach zero at locations in the northern hemisphere when the magnitude of the relative vorticity is significant enough to cancel the planetary vorticity. Comparing Figure 3-4(a) to Figure 3-4(b), we can see that the absolute vorticity is more likely to achieve zero in the upper atmosphere in 1958, which corresponds to a well developed monsoon circulation in West Africa. The cancellation between the relative vorticity and planetary vorticity is more evident at 200mb.

66
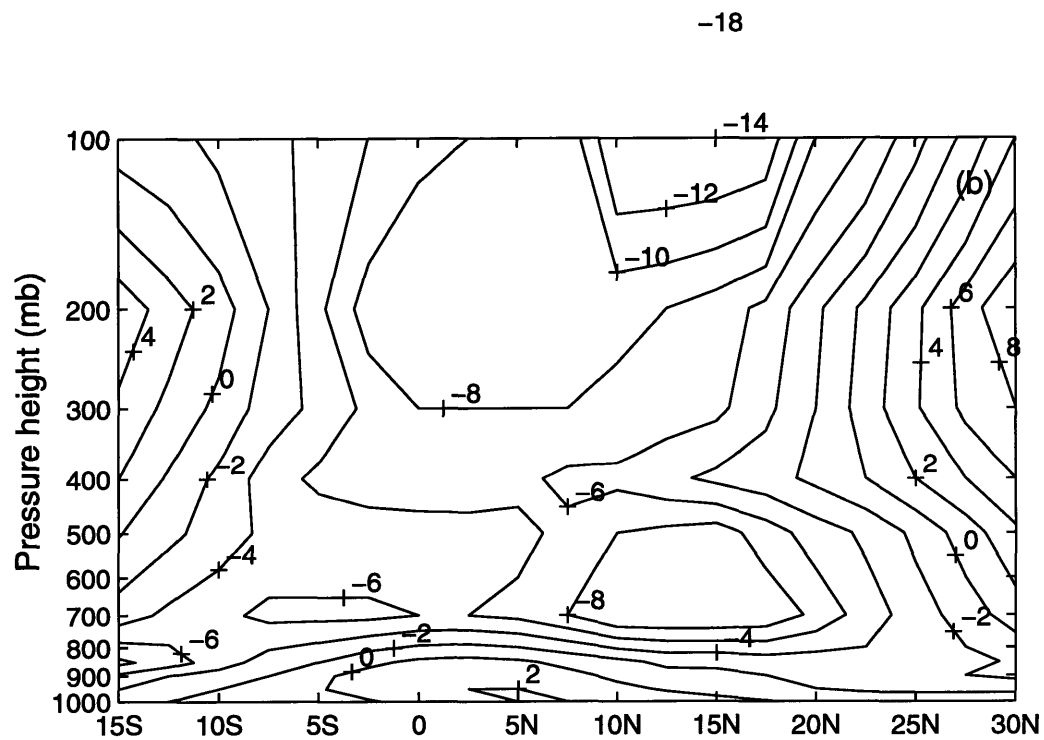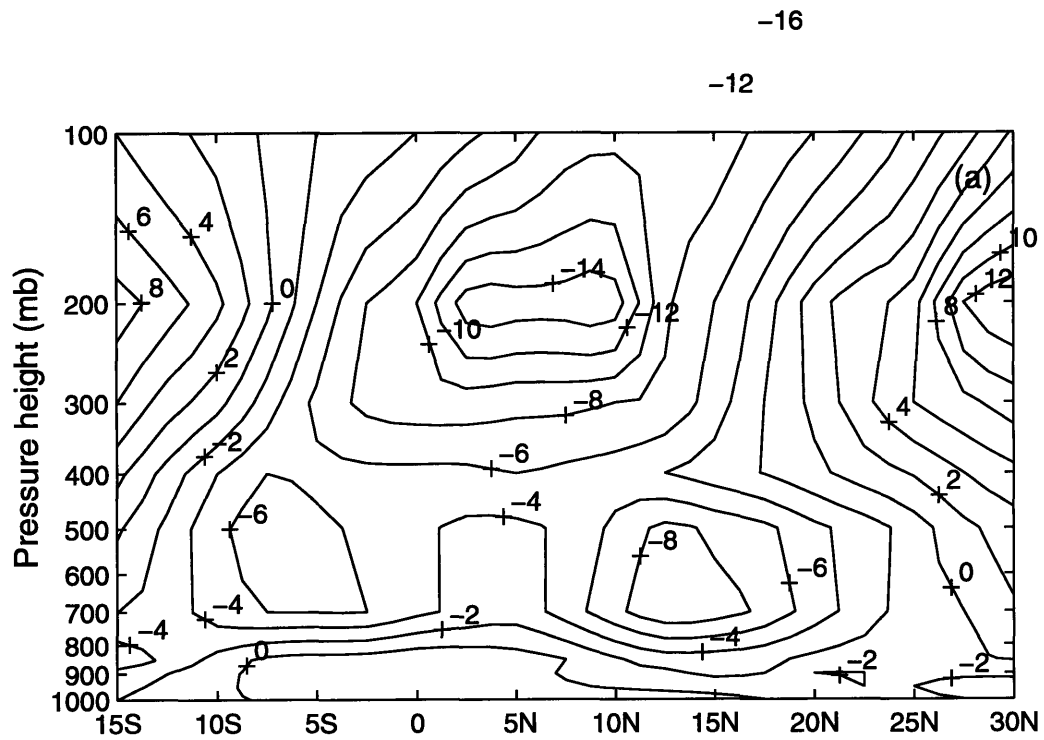
Figure 3-2: Zonal wind (m/s) at 5E averaged over August and September (a) 1958 (b) 1960
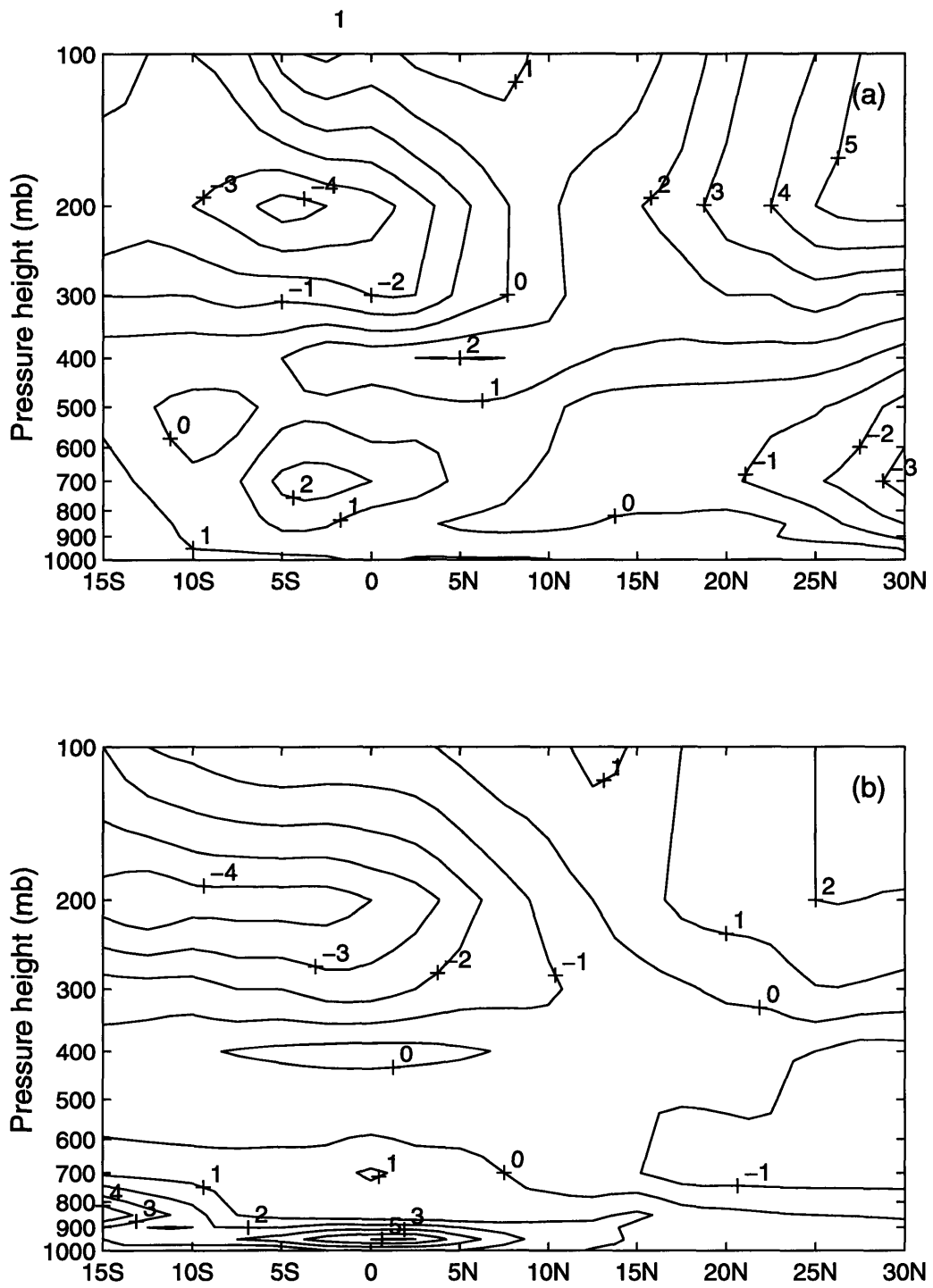
Figure 3-3: Meridional wind (m/s) at 5E averaged over August and September   (a) 1958   (b) 1960
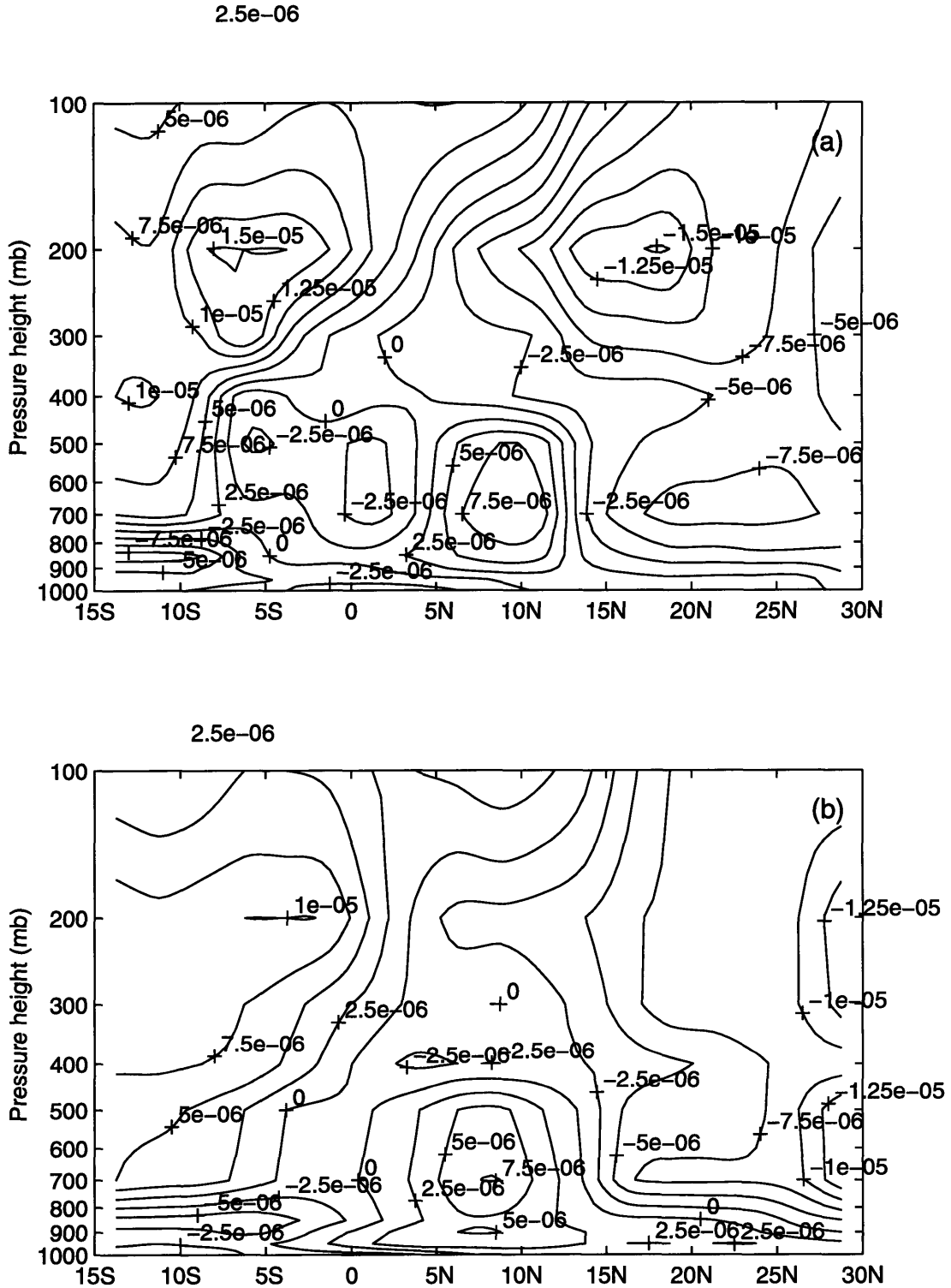
Figure 3-4: Relative vorticity (s^{-1}) at 2.5E averaged over August and September
(a) 1958   (b) 1960

3. Comparison of the relative, planetary, and absolute vorticities at 200mb

The planetary vorticity is calculated using the following equation:

$$f = 2\Omega \sin \phi \qquad (3.13)$$

where Ω is the angular rate of rotation of the earth and ϕ is the latitude. The absolute vorticity ζ_a is the summation of the relative vorticity ζ_r and the planetary vorticity f.

$$\zeta_a = \zeta_r + f \qquad (3.14)$$

Figure 3-5 shows the comparison of the relative, planetary, absolute vorticities at 200mb in 1958 and 1960. The solid line is the absolute vorticity, the dash line is the relative vorticity and the dash-dot line is the planetary vorticity. In 1958, the absolute vorticity is very close to zero in a large range of latitudes, while in 1960, the magnitude of the absolute vorticity is significantly different from zero in a large region. The relation between the absolute vorticity and the angular momentum is given by

$$\zeta_a = -\frac{1}{a^2 \cos \phi} \frac{\partial M}{\partial \phi} \qquad (3.15)$$

where ϕ is the latitude and M is the angular momentum. If ζ_a reaches zero, then the angular momentum M will be constant along the latitudes. Since the absolute vorticity is proportional to the gradient of angular momentum, the zero absolute vorticity implies that the angular momentum is conserved, which is an indicator of the development of a healthy monsoon circulation.

4. Comparison of the distributions of the boundary layer entropy

The boundary layer entropy is computed based on the observations of temperature and humidity in 1000mb and 925mb and averaged between 10W and 10E. First the potential temperature is estimated based on Bolton's (1980) formula:
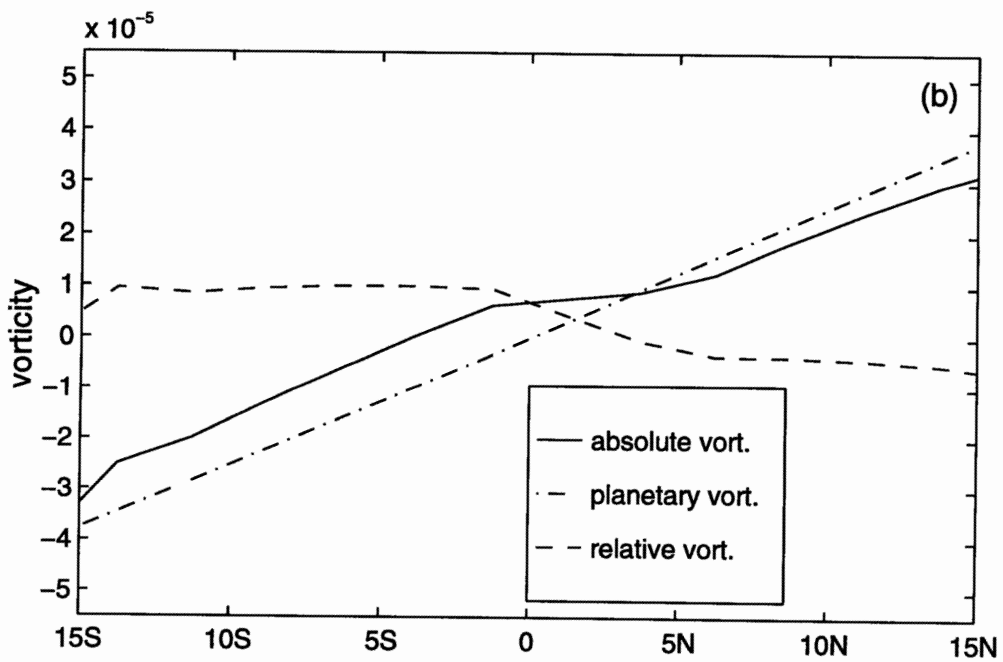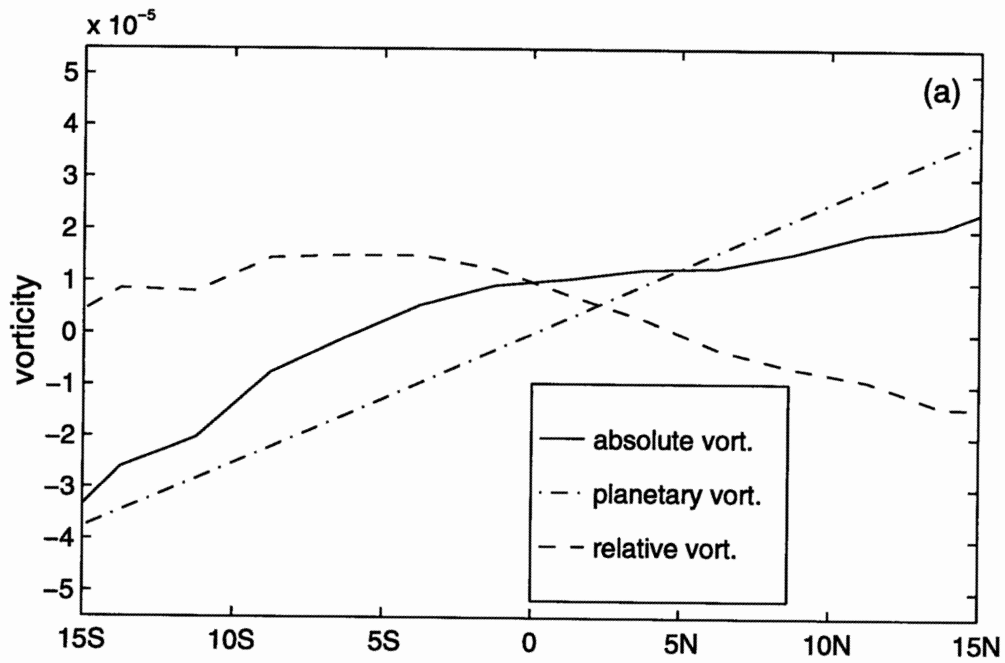
Figure 3-5: Relative vorticity (s^{-1}) at 2.5E and 200mb averaged over August and September   (a) 1958   (b) 1960

$$\theta_e = \theta exp[(\frac{3.376}{T_L} - 0.00254)10^3 q(1 + 0.81q)] \qquad (3.16)$$

where

$$\theta = T_k \left(\frac{1000mb}{p}\right)^{0.2854(1-0.28q)} \qquad (3.17)$$

and T_L is the absolute temperature at the lifting condensation level given by

$$T_L = 55 + \frac{1}{\frac{1}{T_k - 55} - \frac{log(R_h/100)}{2840}} \qquad (3.18)$$

T_k is temperature, R_h is the percentage of relative humidity, q is the mixing ratio in kg/kg, and p is the pressure. Once the potential temperature is obtained the boundary layer entropy can be estimated using equation 1.3.

Figure 3-6 shows the distributions of the boundary layer entropy between 15S and 30N in July 1958 and 1960. The gradient of the boundary layer entropy distribution between the land and ocean is much larger in July 1958 than that in July 1960. A stronger monsoon circulation is expected in 1958 according to the dynamical theory of monsoon circulation. Indeed, it is much wetter in 1958 than 1960.

The theory of land-atmosphere-ocean interactions over West Africa that has been described in the previous section assumes that the atmosphere in a moist-neutral state. Once the atmosphere reaches this state, the saturation moist entropy of the free atmosphere can be replaced by the actual moist entropy of the subcloud layer. Figure 3-7 shows the distributions of the entropy averaged in the boundary layer (1000 mb $\sim$ 900 mb), which is represented by the solid line, and the upper level atmosphere (850 mb $\sim$ 300mb) represented by the line with asterisks in July 1958 and 1960. It is evident that the difference of entropy between the boundary layer and the upper level atmosphere is very small in both 1958 and 1960.

The boundary layer entropy averaged over August and September in 1958 and 1960 is also plotted in Figure 3-8. The distribution of the boundary layer entropy in August and September is very similar to that in July.

5. Comparison of the observed and critical distribution of the boundary layer

Figure 3-6: Boundary layer entropy in July   (a) 1958   (b) 1960
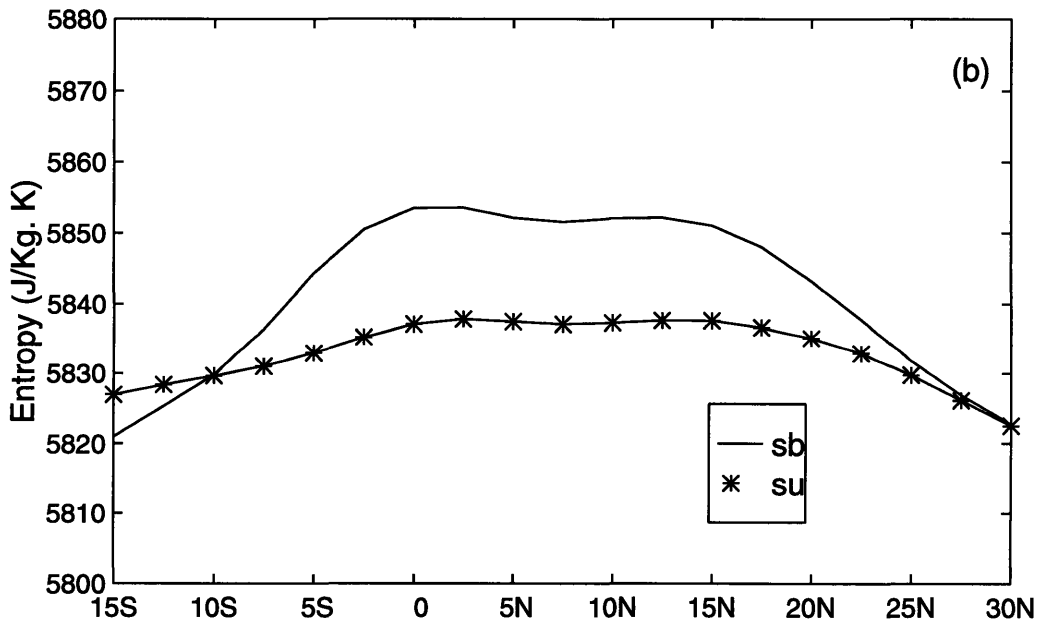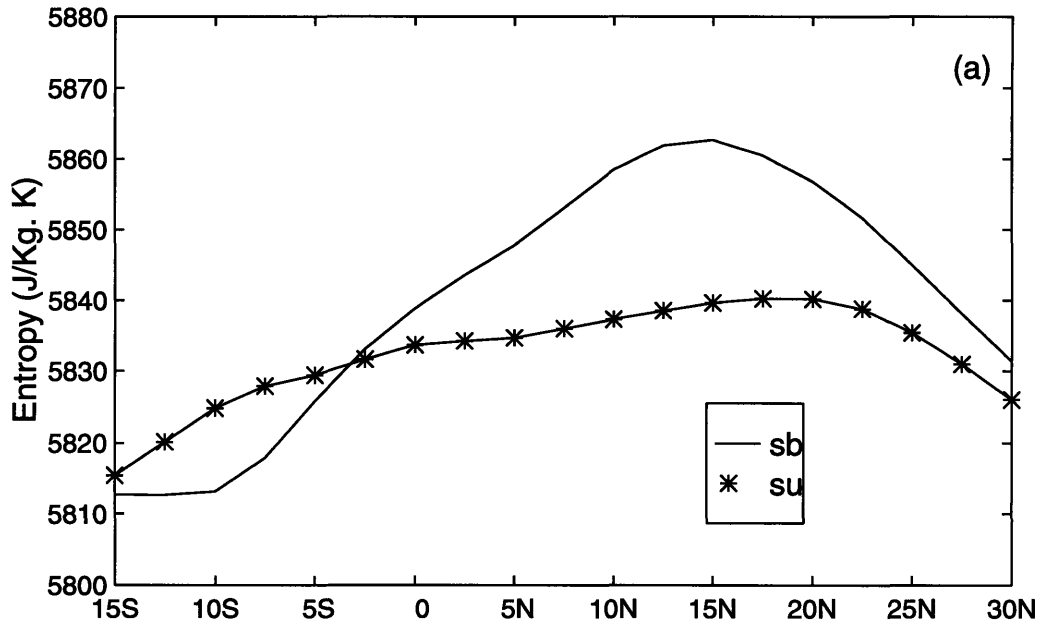
Figure 3-7: Comparison of entropy in the boundary layer and the upper level of atmosphere in July   (a) 1958   (b) 1960

74
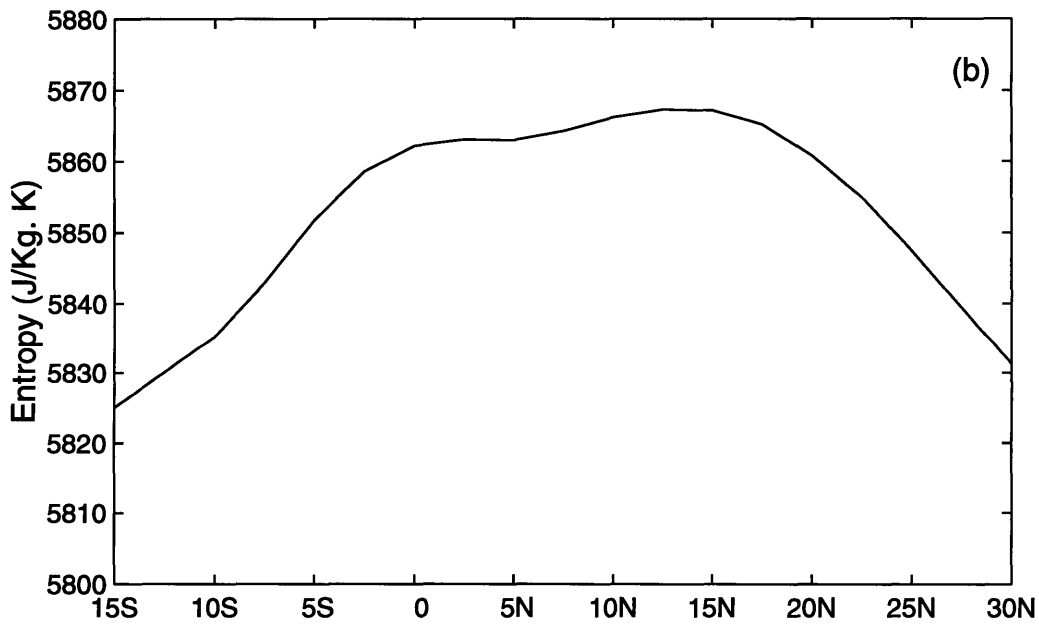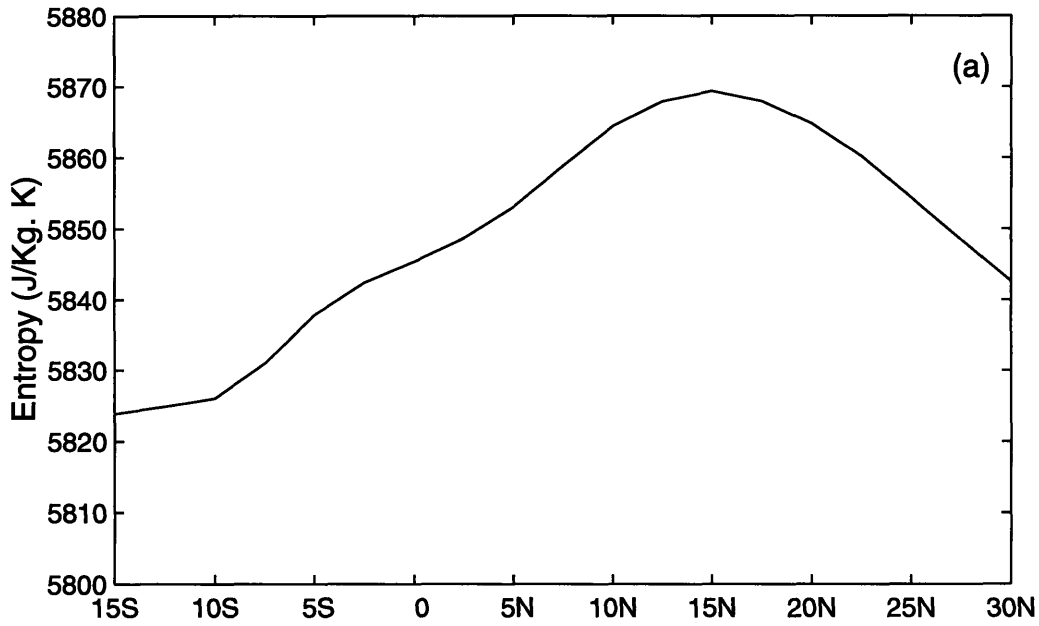
Figure 3-8: Boundary layer entropy averaged over August and September (a) 1958
(b) 1960

entropy

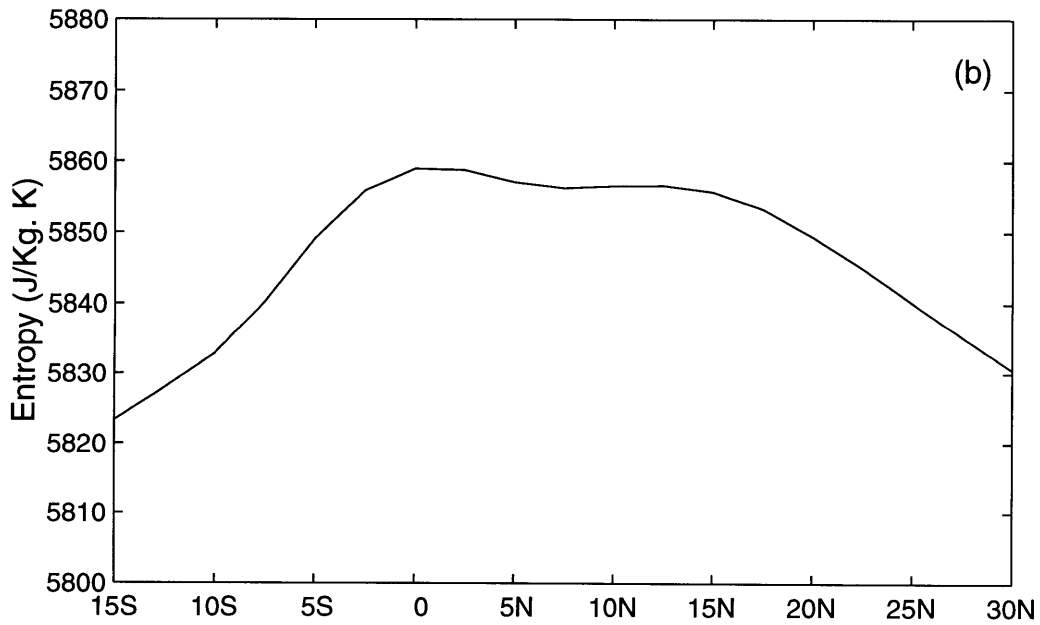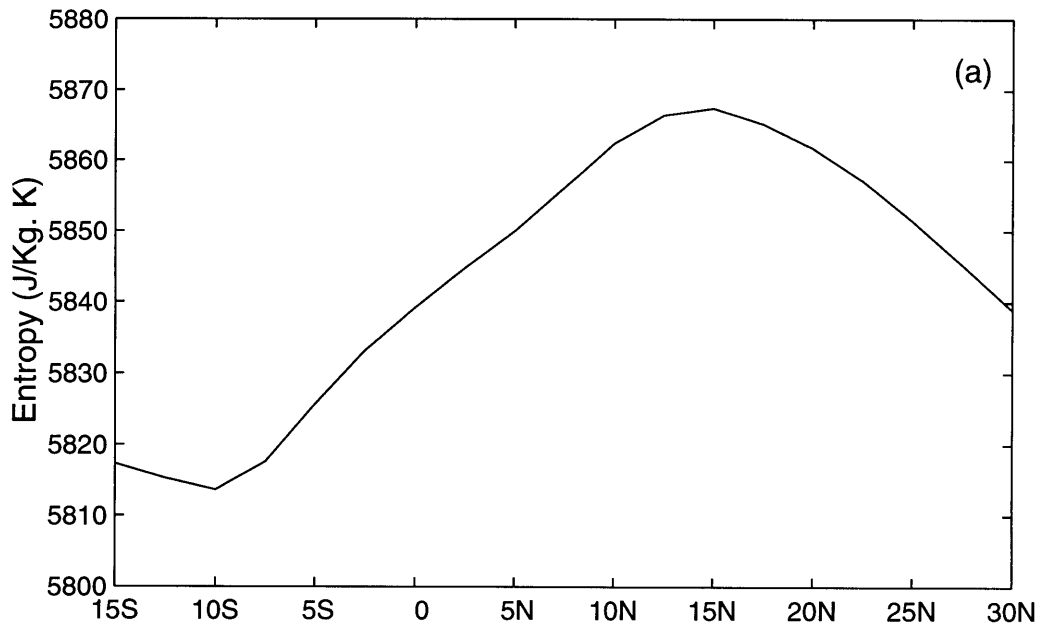Figure 3-9 shows the comparison of the observed entropy in July and Emanuel's critical entropy distribution between 0 and 30N (Emanuel, 1995). The solid line is the critical distribution and the dash line is the actual observed entropy distribution. The critical distribution of the boundary layer entropy is plotted based on the equation 3.4, where θ_{em} and φ_m are specified the same as the observed data. It is seen that the gradient of the entropy distribution between the ocean and land in July 1958 is much larger than the critical distribution; this confirms that a stronger monsoon circulation is likely to develop in August. In contrast, the gradient of the entropy distribution in July 1960 is less than the critical distribution, thus the monsoon circulation is not expected to develop in August 1960.

In summary, the observations in West Africa are consistent with the proposed relation between the dynamics of monsoon circulation and the gradient of the distribution of boundary layer entropy. In the wet year (1958), a relatively large meridional gradient of boundary layer entropy and a healthy monsoon circulation are observed. In the dry year (1960), a flat distribution of the boundary layer entropy and a weak monsoon circulation are observed.

In general the tropical atmosphere tends to have a uniform vertical distribution of moist entropy. Rainfall resulting from the moist convection heats the upper troposphere, which results in negative relative vorticity near the tropopause. In 1958, the magnitude of the negative vorticity reaches a level that may cancel the planetary vorticity over a large region. According to the dynamical theory of the monsoon circulation, zero absolute vorticity near the tropopause should lead to an angular momentum conserving regime, which indicates a healthy monsoon circulation. The latter provides a large scale forcing for rainfall. In the relatively dry year (1960), the adiabatic heating due to water vapor condensation in the upper atmosphere is not significant enough to induce a large negative relative vorticity near the tropopause that is sufficient to cancel the planetary vorticity. A radiative-convective equilibrium regime is likely to dominate the dynamics of the atmosphere in that year. Rainfall is mainly the result of the local convective storms.
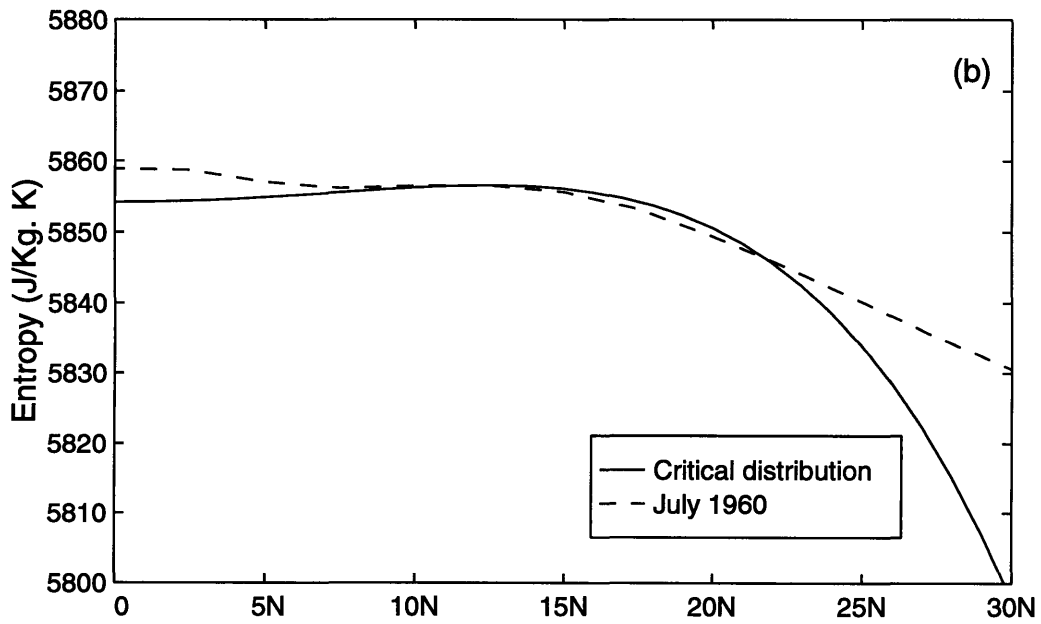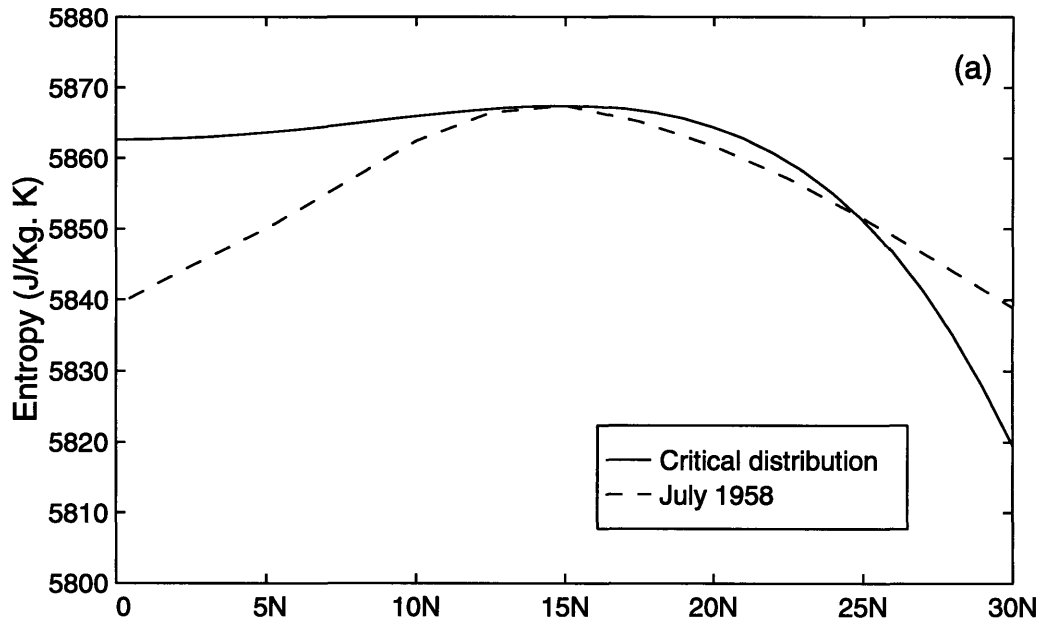
Figure 3-9: Comparison between the observed entropy distribution in July and the Emanuel's critical distribution (a) 1958 (b) 1960

The results of the analysis on wind are consistent with the results reported by Kidson (1977), which suggest that the decline of rainfall over the Sahel region is associated with weaker easterly jet. We suggest that the weakening of the easterly jet in relatively dry years is due to the flat distribution of the boundary layer entropy.

3.4 Comparison of Charney's Mechanism and the Mechanism of Monsoon Circulations

In 1975, Charney suggested that removal of vegetation at the desert border would increase surface albedo and cause an additional radiative cooling. Enhancement of sinking motion is the only process that can balance the additional radiative cooling. This sinking motion would push the Inter-Tropical Convergence Zone (ITCZ) southward and cause a decrease in rainfall. Charney's mechanism is illustrated in Figure 3-10(a). The main weakness of Charney's mechanism is in the fact that vegetation in the desert border grows in response to rain and follows closely the seasonal cycle of rainfall. The vegetation that exists by the end of the short rainy season may not survive more than few months into the long dry season. Recent satellite pictures of vegetation in Africa, such as those presented by Tucker et al.(1991), illustrate clearly the close relation between rainfall and vegetation in this region. Under these conditions, the vegetative cover lacks the memory that is needed to carry information between successive years and thus the Charney mechanism fails to explain the persistence of the continuing drought in West Africa.

The proposed description of the dynamics of monsoon circulation provides a better approach than Charney's mechanism to explain the natural variability of the rainfall in West Africa. Changes in either SSTs or land conditions could modify the distribution of boundary layer entropy. This distribution affects the monsoon circulation and West African rainfall. Figure 3-10(b) shows the weakened monsoon circulation due to either high SST or low boundary layer entropy over land. The removal of vegetation along the coast could weaken the monsoon circulation or even suppress

the circulation entirely.

3.5 The Role of the SST in the Dynamics of West African Monsoons

Many studies have been done in establishing the relation between the SST in the Tropical Atlantic and rainfall in West Africa. Lamb (1978) presents composites of the SST distribution in the Tropical Atlantic for wet and dry years in the Sahel region. Six wet years and seven dry years are chosen for the composite analysis. The distributions of SST anomalies in the region of SETA are averaged separately for the wet and dry years. Figure 3-11 shows that warm (cold) SST anomalies that are associated with dry (cold) years. Similar findings were reported by Lamb and Peppler (1992). Lough (1986) also finds that the second eiger-vectors of the SST anomalies correlate negatively with the Sahel rainfall for the period of 1948 to 1972. All these empirical observations show that Sahel rainfall is significantly correlated to the SST conditions in the SETA: a warm (cold) SST anomaly in that region is associated with dry (wet) conditions in the Sahel region.

The meridional distribution of boundary layer entropy south of the land-ocean border located around 5N is largely controlled by the SST over the South Eastern Tropical Atlantic (SETA). The inter-annual variability in the magnitude and distribution of the SST may influence the dynamics of West African Monsoons and rainfall variability over West Africa. The role of the SST in the dynamics of West African monsoons is summarized in Figure 3-12(a). The proposed theory provides a reasonable explanation to the dynamics behind the observed relation between the SST anomaly in the SETA and Sahel rainfall. According to the theory, the dynamics of monsoons are regulated by the meridional gradient of boundary layer entropy. The boundary layer entropy over the ocean is mainly controlled by the SST. As shown in Figure 3-12(a), A warm (cold) SST anomaly over SETA would lead to large (small) fluxes of moist entropy and hence small (large) gradient of boundary layer entropy.

79

NEW CIRCULATION   ORIGINAL CIRCULATION

SEA   LAND   DESERT

(a)

WEAK CIRCULATION   ORIGINAL CIRCULATION

SEA   LAND   DESERT

(b)
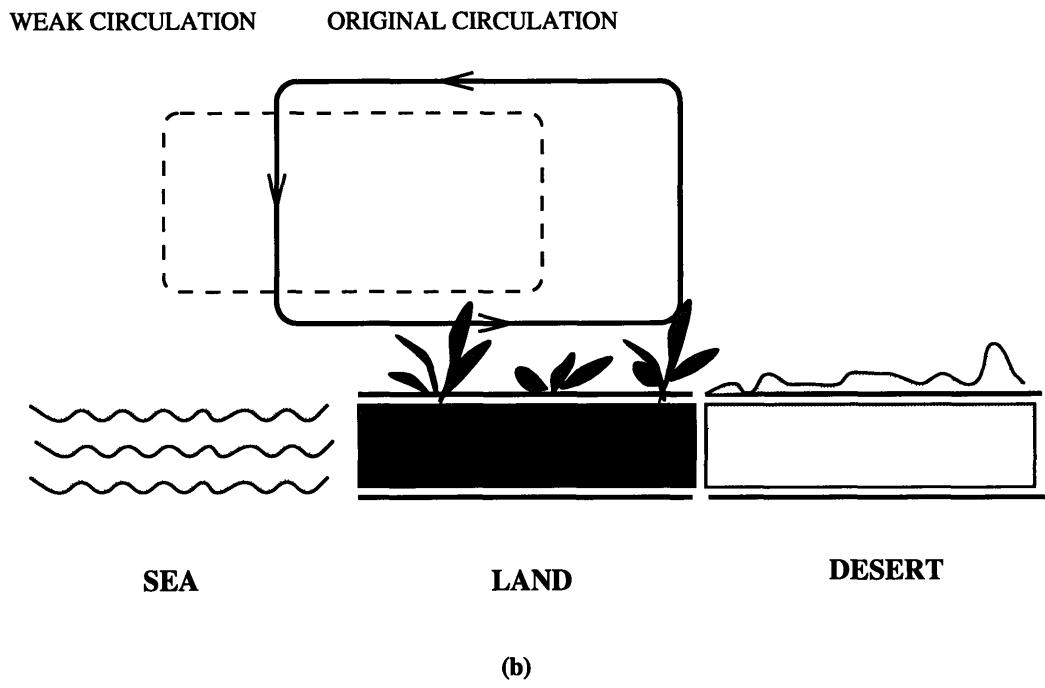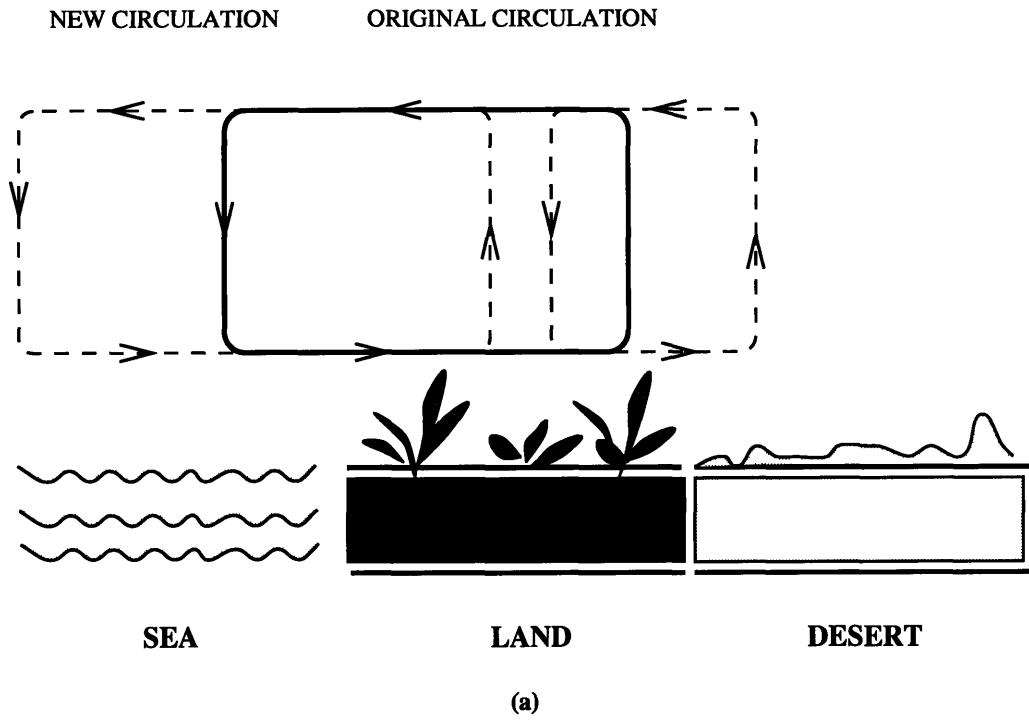
Figure 3-10: Comparison of (a) Charney's mechanism and (b) dynamical monsoon theory

80

As a result, a weak (strong) monsoon circulation and relatively dry (wet) conditions.

3.6 Findings and Discussion

3.6.1 Findings

The proposed theory of land-atmosphere-ocean interactions and monsoon circulations over West Africa is consistent with the observations on both SST and the boundary layer entropy distributions during wet and dry years. Analysis of the observations for 1958 and 1960 over West Africa indicates that rainfall conditions in these two years could have been predicted on the basis of the proposed relation. A healthy monsoon circulation and a large gradient of the boundary layer entropy are observed in the relatively wet year (1958). A relatively weak monsoon circulation and a flat distribution of the boundary layer entropy are observed in the dry year (1960). The proposed relation is also consistent with the observed correlation between the SST and the Sahel rainfall, as reported by lamb (1978) and Lough (1986). Theoretically, cold (warm) SST in the region located south of the West African coast would be likely to produce a large or (small) meridional gradient of entropy in the boundary layer, which would induce a strong (weak) monsoon circulation and results in wet (dry) conditions in West Africa.

The dynamics of monsoons over West Africa are more sensitive to inter-annual fluctuations in the meridional gradient of boundary layer entropy than are those in other regions (Eltahir and Gong, 1996). Because West Africa is located close to the equator, the planetary vorticity is relatively small, and a small magnitude of relative vorticity could result in the cancellation of the planetary vorticity. As a result, monsoon circulations in West Africa develop more easily and is more sensitive to changes in sea surface temperature and in land conditions, as compared to other tropical regions where monsoon circulations are observed.

Figure 3-11: Sea Surface Anomalies in the Tropical Atlantic (a) Dry year (b) wet years in the Sahel region from Lamb (1978)

HIGH SST

NORMAL

LOW SST

SEA   LAND   DESERT

(a)

HIGH ENTROPY OVER LAND

NORMAL

LOW ENTROPY OVER LAND

SST

SEA   LAND   DESERT
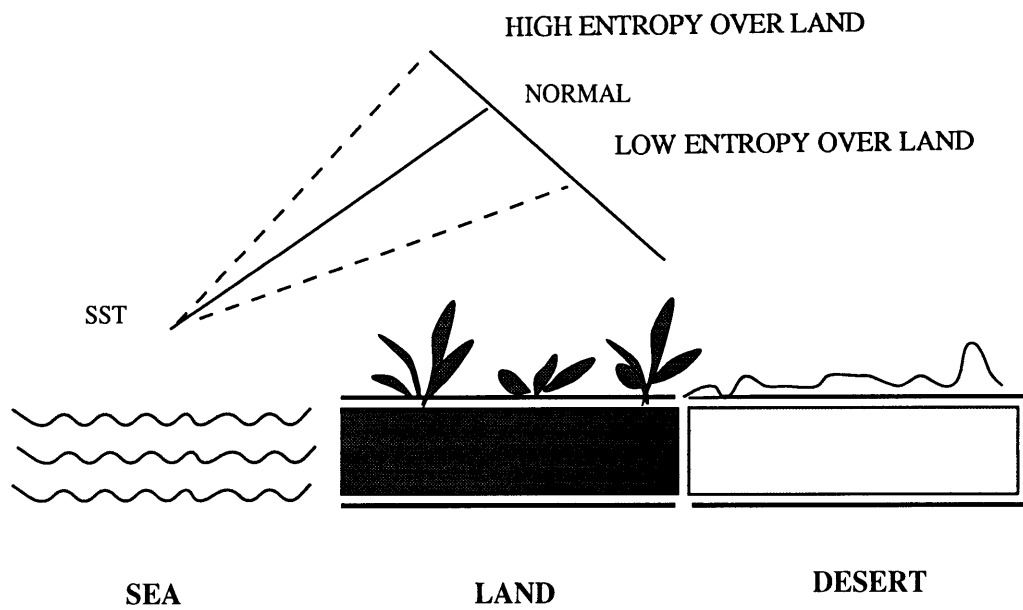
(b)

Figure 3-12: The implications of the dynamical theory of monsoon circulations

83

3.6.2 Implications of the study results

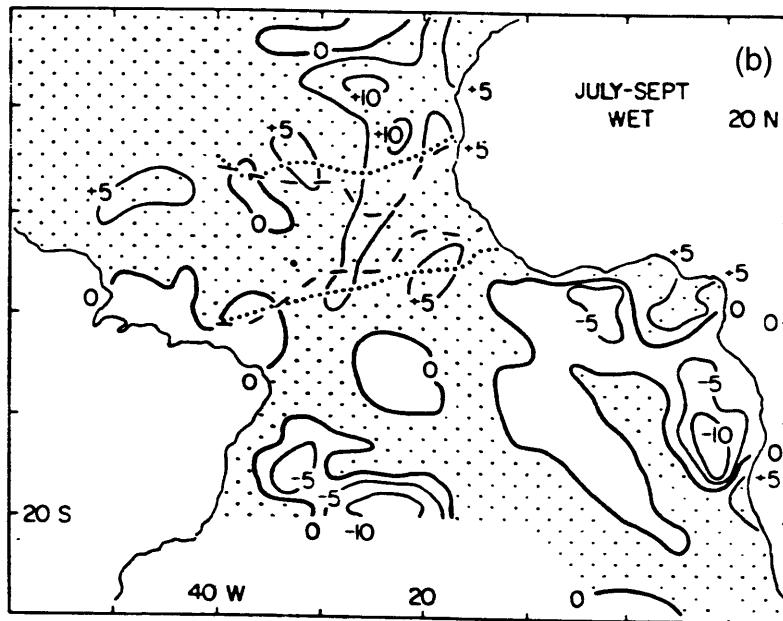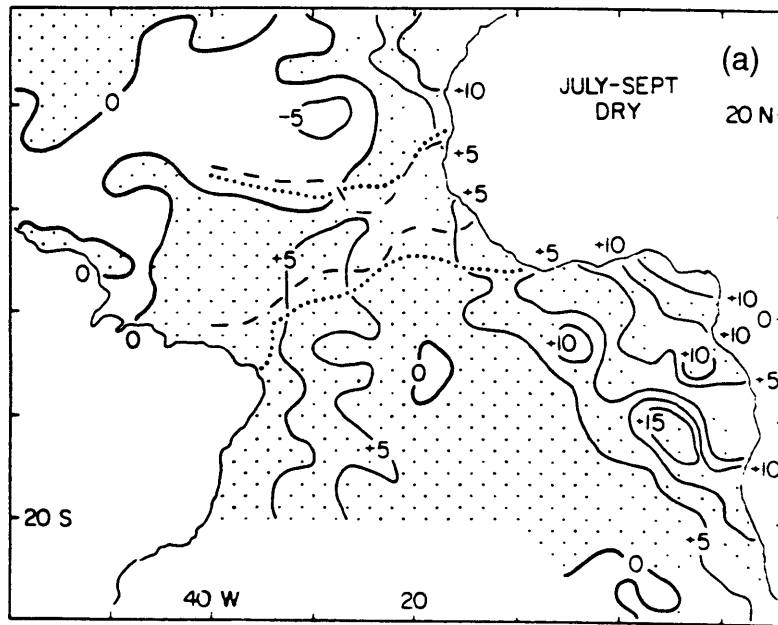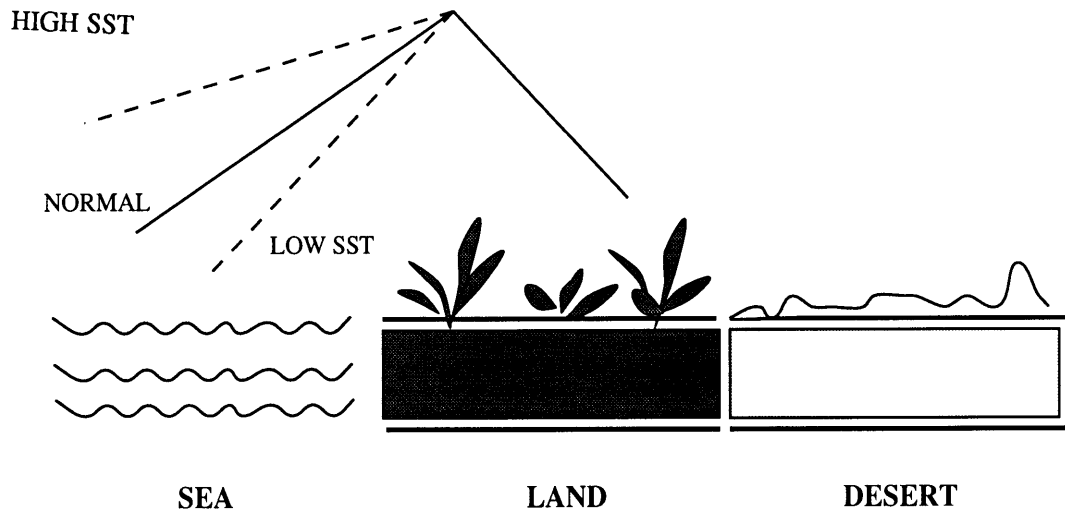The proposed theory of land-atmosphere-ocean interactions bridges the gap between the studies of land-atmosphere interactions and ocean-atmosphere interactions. From our analysis of the observed atmospheric variables in wet and dry years prior to the onset of the current drought in West Africa, we find that the natural variability of the dynamics of the atmosphere in West Africa are dominated by either a radiative-convective-equilibrium regime or an angular-momentum-conserving regime. When the former mechanism dominates the dynamics of the atmosphere, a dry year is expected, and when the angular-momentum-conserving regime dominates, a wet year is expected. The finding that the dynamics of monsoon circulation over West Africa are controlled by the gradient of the boundary layer entropy, which, in turn, is regulated by the interactions of land-atmosphere-ocean, has important implications: both SST and land conditions could regulate the monsoon circulation over West Africa. The distribution of entropy between land and ocean during summer, the southern end is controlled by the ocean and the northern end is determined by the land conditions.

If the land condition remains the same, the SST will control the gradient of the boundary layer entropy. A higher SST will result in a flatter distribution of entropy and a lower SST will favor a larger gradient of entropy. Figure 3-12(a) illustrates the impact of the SST on the gradient of entropy distribution. This circumstance is consistent with the results of Lamb (1978), shown in Figure 3-11. Lamb investigated the relation between the SST in the Tropical Atlantic Ocean and the Sahel rainfall and found that there is a negative correlation between them. Warm SST anomalies in the Atlantic Ocean correspond to dry years, and cold SST anomalies correspond to wet years in Sahel.

If, on the other hand, the SST is kept fixed, the land condition will determine the gradient of the boundary layer entropy. The role of land conditions throughout West Africa in regulating the monsoon circulation is illustrated in Figure 3-12(b). The boundary layer entropy over land is primarily sustained by local fluxes of sensible and latent heat and energy fluxes through the top of the boundary layer, and from

the surrounding regions. Any change in land conditions that modifies the boundary layer entropy, could affect the gradient of the meridional distribution of entropy, the monsoon circulation and cause changes in regional rainfall.

Chapter 4

The Role of Land Surface Conditions in Rainfall Variability over West Africa

4.1 Introduction

In this chapter, we will apply the theory of land-atmosphere-ocean interactions described in Chapter 3 to study the role of land surface conditions in rainfall variability over West Africa. The focus is on a recent hydrologic event: the extremely wet 1994 rainy season. After successfully explaining the wet conditions in 1994 over West Africa based on our theory as due to the large gradient of boundary layer entropy (BLE), we carry out the research further and try to identify the main processes that are responsible for the large gradient of BLE in that year. We study both the SST and land conditions over West Africa. Interestingly, we find that the SST in the Tropical Atlantic in 1994 is not the lowest in the 1990s, and the SST is even lower in 1992. But 1992 was significantly drier compared to 1994. Therefore the extremely wet condition in 1994 must result from other processes other than the SST distribution. Comparing the distributions of BLE between the the land and the ocean in 1992 and 1994, we find that entropy over the land region is much higher in 1994 than that in 1992, which

results in a large gradient of BLE in 1994. Hence we focus on those processes that may affect BLE over land. In particular, we compare the moist static energy budget over the land region in 1992 and 1994.

This chapter is organized as follows. In section 4.2 we apply the theory of land-atmosphere-ocean interactions and analyze the observations for 1992 and 1994. The moist static energy budget and other possible processes that may be responsible for the changes of BLE over land are investigated in section 4.3. Section 4.4 includes a discussion and summarizes the findings of this study.

4.2 Application of the Land-Atmosphere-Ocean Interactions Theory to the 1994 Rainy Season

4.2.1 Rainfall in 1994

According to the report of the Climate Prediction Center of NOAA (1995), the 1994 rainy season was the wettest since 1964 across the Sahel. This conclusion was based on preliminary May through September data using the 1951-80 period as the baseline, "normal conditions." Figure 4-1 shows the standardized departures of rainfall from the long-term mean in Sahel from 1921 to 1994. 1994 is only the second year since 1967 to record above-normal rainfall for the season.

Rainfall over West Africa in 1994 is quite unusual. June brought near- or above-normal rains to much of the Sahel as most areas south of 12N recorded over 200 mm of rain, with the exception of the Gulf of Guinea coastline from extreme eastern Guinea eastward to Benin. Less than half of normal rain fell on these areas. In July, abundant rain fell on much of the Sahel and sub-Saharan Africa, with significant showers reaching exceptionally far north (past 20N) in both Mali and Sudan. Well above-normal July rain also soaked southeastern Niger and parts of central and northern Chad. Further south, less than 25 mm fell on most areas from eastern Liberia to southwestern Ghana.

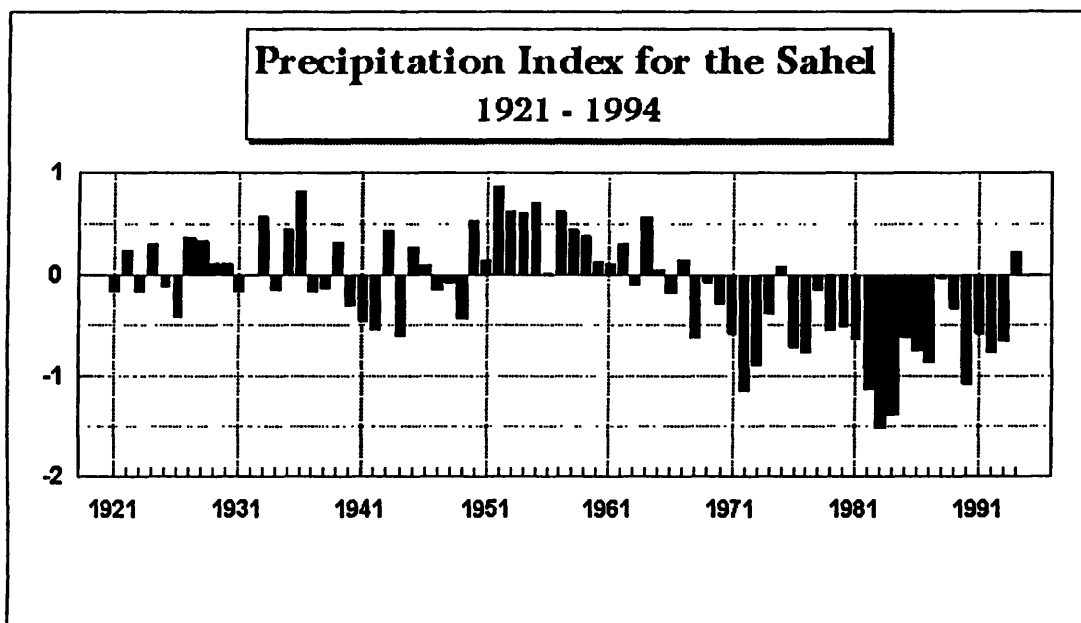August was also unusually wet, with heavy rain (100-400 mm) drenching most

Figure 4-1: May-Sep standardized departures from 1951-1980 mean rainfall for stations 20W-20E and 8N-18N (Climate Analysis Center, NOAA)

areas from Senegal and southern Mali eastward to western Sudan. Totals were well above normal ($>$ 150%) in a swath from north-central Mauritania southeastward to central Chad. The widespread wetness continued through September, with exceptionally heavy rains (100-400 mm) falling from central Senegal southward through Liberia and eastward to central Ethiopia. Convective complexes continued to track unusually far north into typically dry areas of Mali and Niger. October saw drier conditions finally beginning to cover the Sahel, but occasional heavy rains still fell unseasonably far north, with new October records established in southeastern Mauritania.

4.2.2   The 1994 Monsoon

The monsoon is much stronger in 1994 compared to those in 1992 and 1993. Several observations support this argument. First, the location of the ITCZ that occurred further north in 1994, as compared to the normal location shown in Figure 4-2, corresponds to a deep inland strong monsoon circulation. Second, the abundant unusual rainfall received in Sahel in October 1994 also reflects a deep inland strong monsoon. Since as monsoons penetrate further north it will take more time for them to retreat to the south; as a result, more rainfall is seen in October. Third, more rainfall was observed during the monsoon months, which indicates a strong monsoon circulation in 1994.

4.2.3   Application of the Theory

We will apply the theory of land-atmosphere-ocean interactions to the wet 1994 rainy season. To get a better understanding through comparison, we choose a dry rainy season, 1992, as the reference. According to the theory, we expect a large (small) gradient of BLE between the ocean and the land in wet (dry) years in the Sahel.

We estimated BLE in 1992 and 1994 based on temperature and humidity data that are produced by ECMWF. The observed distributions of BLE in July 1992 and 1994 are plotted in Figure 4-3(a) and (b). Obviously, the gradient of BLE is much larger in 1994 than that in 1992. The larger gradient of entropy in 1994 is consistent
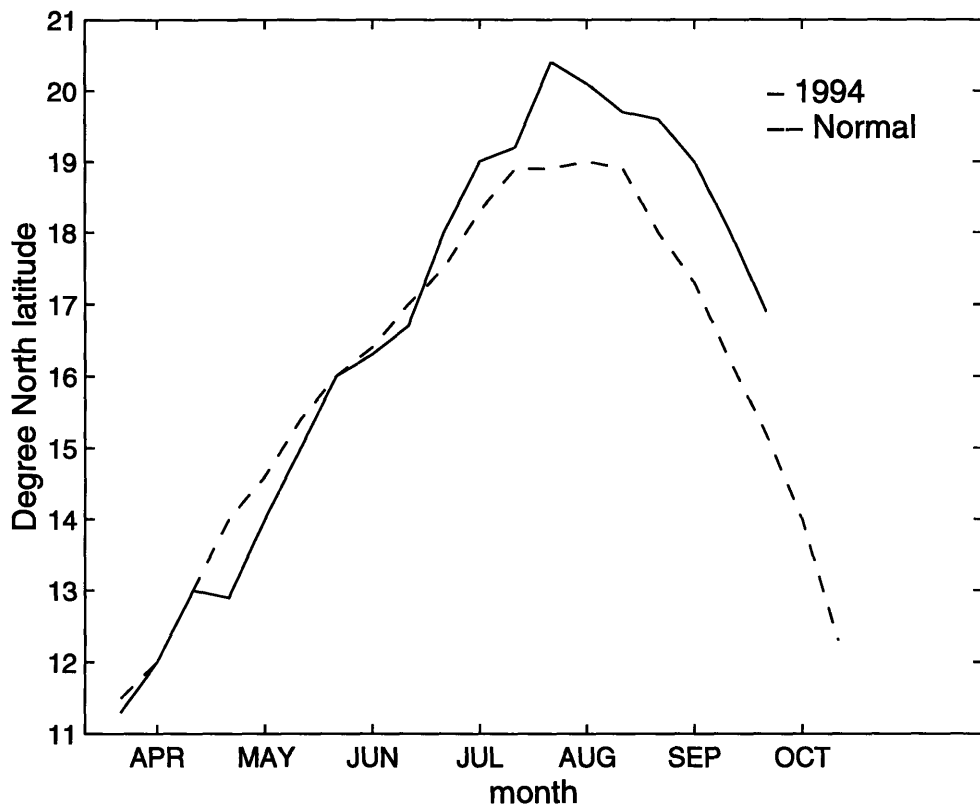
Figure 4-2: West African Seasonal ITCZ Progress: 1994 vs Normal (Climate Analysis Center, NOAA)

with a strong monsoon circulation in that year.

We also examine and compare the wind fields in 1992 and 1994. Figure 4-4 shows the zonal wind contours at the 0 longitude in August 1992 and 1994. The easterlies in the upper atmosphere are much stronger in 1994, which is consistent with a strong monsoon circulation. Similarly, Figure 4-5 shows the meridional wind contours in the same region and same time. The northerly is stronger in the upper atmosphere in 1994. The distributions of relative vorticity for July and August are not very different. However in September, the contrast of the relative vorticity in the tropopause becomes clear, which is consistent with the long-lasting monsoon season in 1994. Figure 4-6 shows the comparison of relative vorticity at 2.5W in September 1992 and 1994. The magnitude of the negative relative vorticity at the tropopause in the northern hemisphere for 1994 is larger than that for 1992, which would bring the absolute vorticity in 1994 closer to zero.

In summary, the theory of land-atmosphere-ocean interactions provides a reasonable explanation of the 1994 wet condition in the Sahel. The large gradient of BLE between the Tropical Atlantic and the West African land region should result in a strong monsoon circulation, which is exactly what was observed in the wind, rainfall, and vorticity fields for 1994. However, to carry out the research one step further, we need to investigate the factors that determine the gradient of BLE over both the ocean and the land.

4.3 Investigation of the Factors that Determine the Distribution of Boundary Layer Entropy

As mentioned in the previous chapter, the gradient of BLE is determined by the magnitudes of entropy over the ocean and the land. The entropy over the ocean is mainly controlled by the SST. We will inspect both SST in the Tropical Atlantic and land conditions in 1992 and 1994 and try to understand the roles of the land and the ocean in determining the gradient of BLE in the 1994 rainy season.
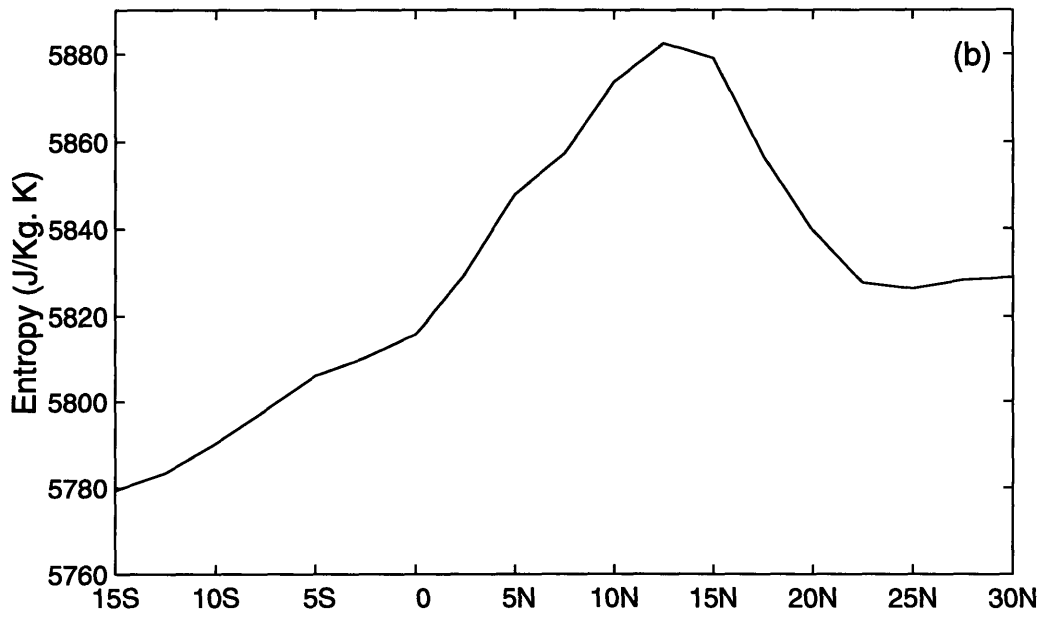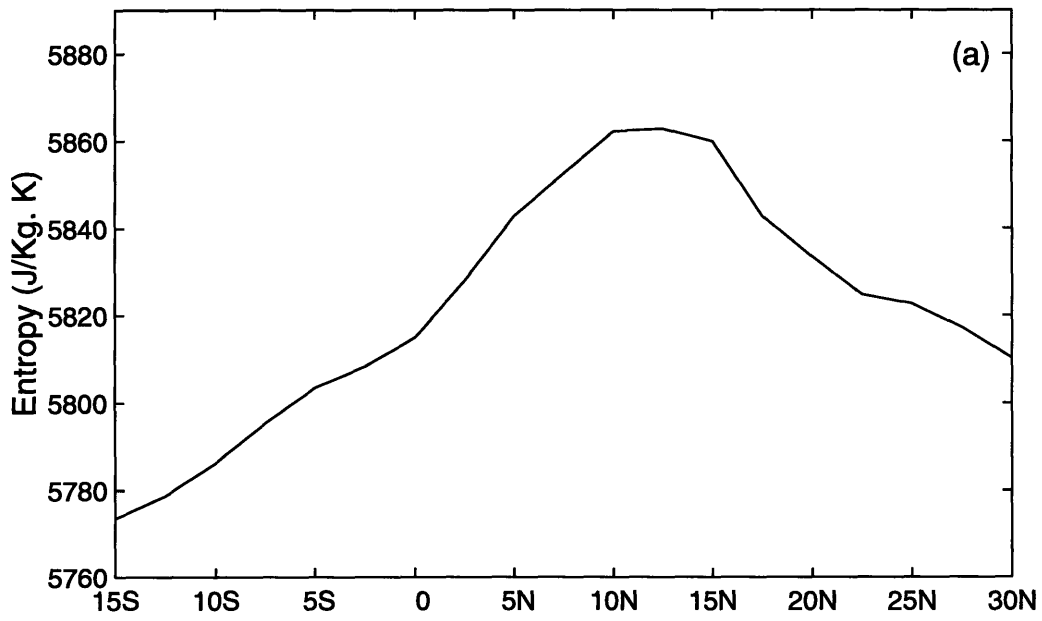
Figure 4-3: The distributions of boundary layer entropy in July   (a) 1992   (b) 1994
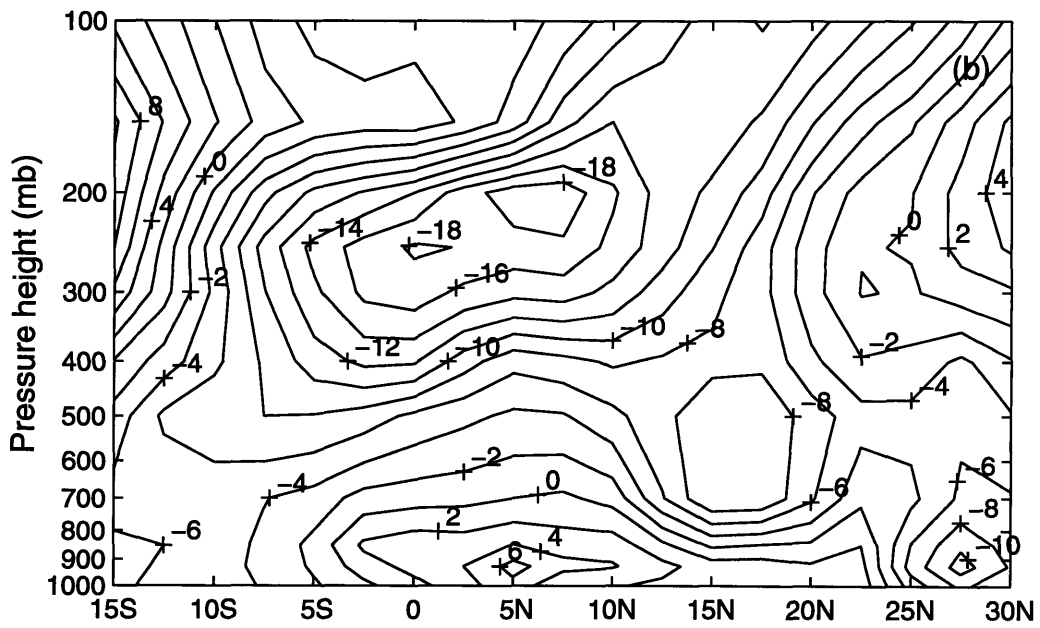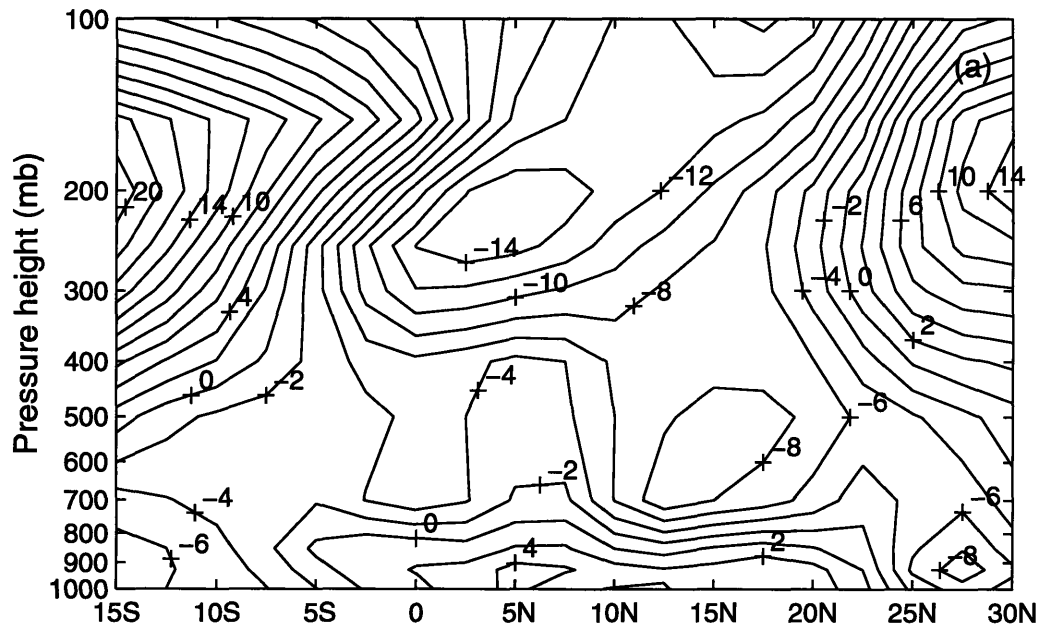
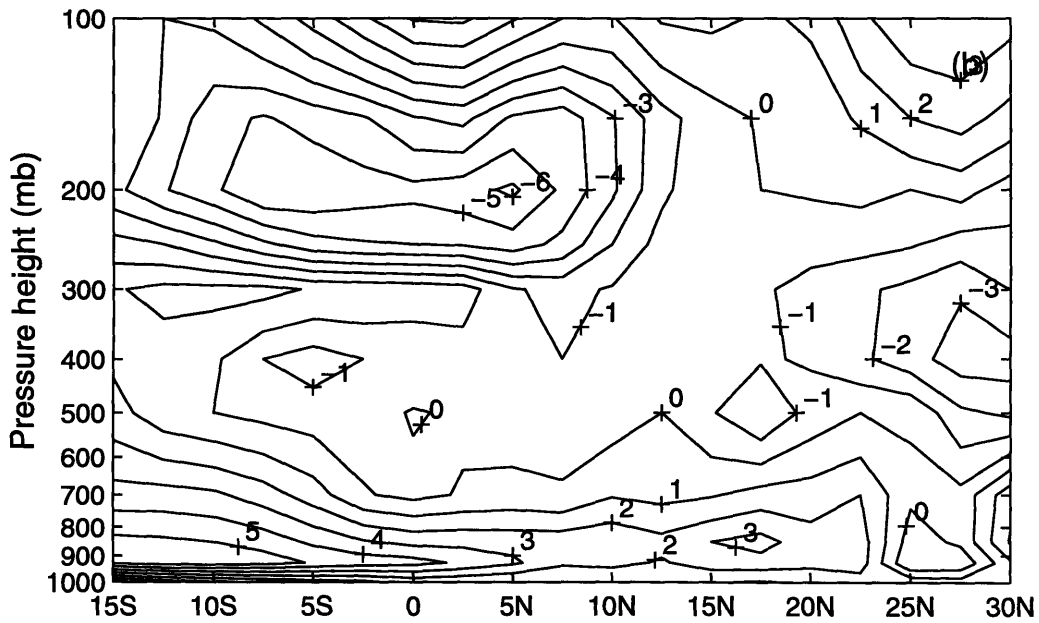Figure 4-4: Zonal wind at the 0 longitude in August   (a) 1992   (b) 1994
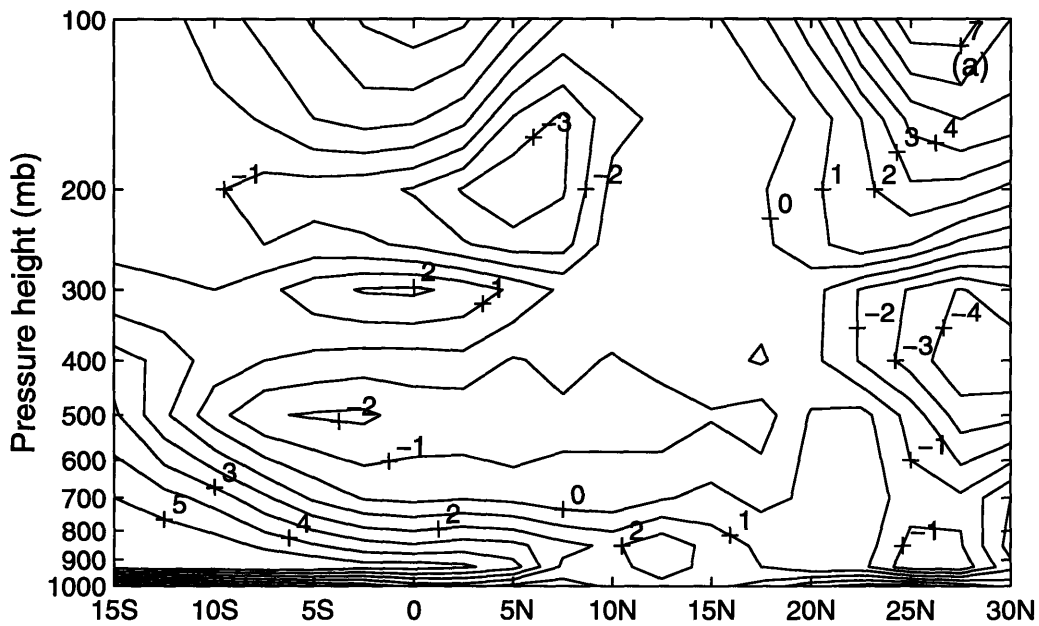
Figure 4-5: Meridional wind at the 0 longitude in August   (a) 1992   (b) 1994

94
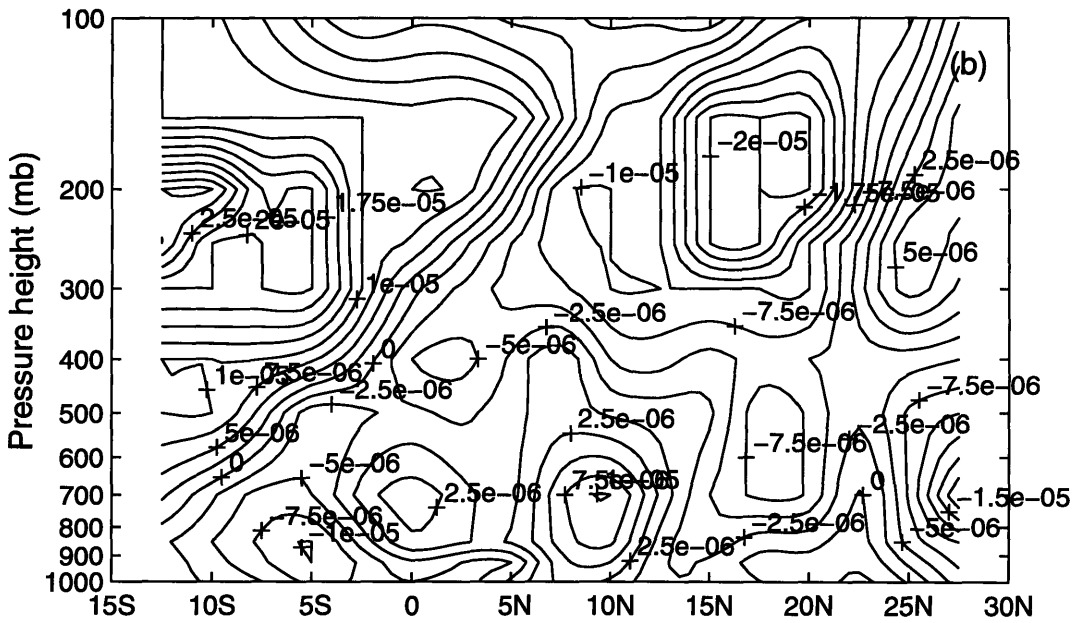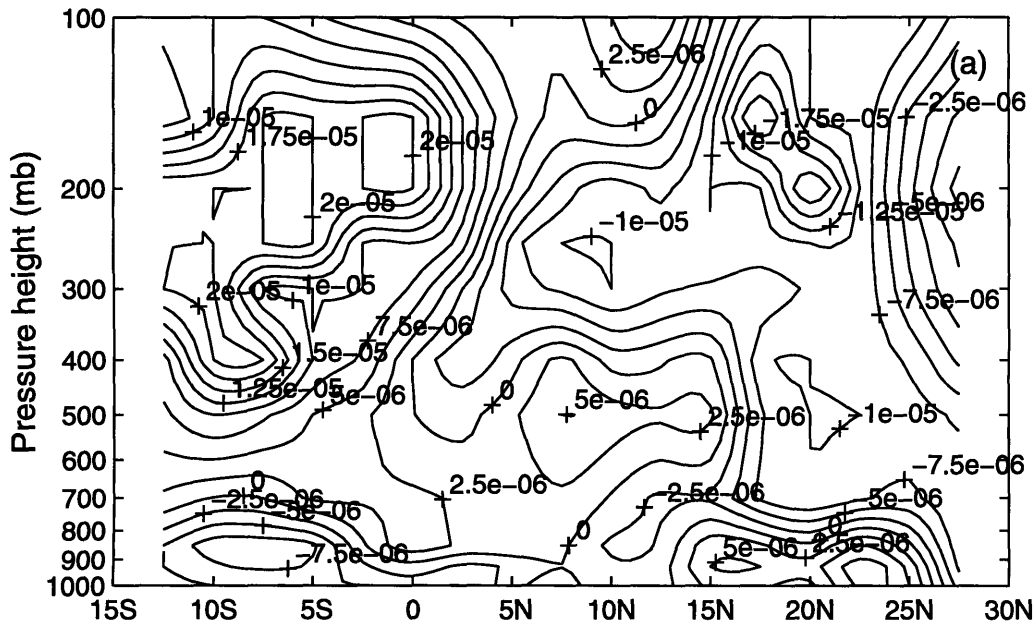
Figure 4-6: Relative vorticity at 2.5W in September   (a) 1992   (b) 1994

4.3.1 Comparison of the SST in 1992 and 1994

The time series of the SST departures from the long-term mean is plotted in Figure 4-7. The SST plotted here is first averaged over July, August and September, and then averaged over the region which extends between 20S and 5N and from 15W to 10E. The monthly average SST is taken from the Comprehensive Ocean-Atmosphere Data Set (COADS, 1985). All observations in this data set are given in 2 degrees latitude by 2 degrees longitude boxes. Within each box, air and sea surface temperatures, wind pressure, humidity, and cloudiness are provided and the SST data coverage starts from 1854 and continues to the current year. From this time series, we can see that the SST in 1994 is lower than other years from 1980 to 1993 except 1992.

The difference of the SST between 1992 and 1994 also appears from the satellite observations of the SST. The SST used here is taken from the monthly optimum interpolation (OI) SST analysis, which uses *in situ* and satellite SSTs plus SSTs simulated by sea-ice cover. The *in situ* data were obtained from radio messages carried on the Global Telecommunication System. The satellite observations were obtained from operational data produced by the National Environmental Satellite Data and Information Service (NESDIS). The data covers the whole globe and has a spatial resolution of 1 degree latitude by 1 degree longitude. The time coverage is from 1982 to the current year. The spatial distributions of the SST averaged over July, August and September in 1992 and 1994 are plotted in Figure 4-8(a) and 4-8(b). The difference of the SST between 1992 and 1994 (1994 minus 1992) is plotted in Figure 4-9. The positive numbers spread over most of the areas in the Tropical Atlantic, which confirms that the SST is warmer in 1994 than that in 1992.

If the land conditions were the same in 1992 and 1994, the lower SST in 1992 would result in a larger gradient of BLE and a wet year. But in fact, the gradient of BLE is smaller in 1992 than that in 1994. Therefore we suggest that the land conditions are responsible for the difference in the gradient of BLE between 1992 and 1994. Actually entropy in the land region, 10N-20N and 10W-15E (called region S later), in 1994, is much higher than that in 1992 in the same region as shown in

Figure 4-3. In the following, we will analyze those processes that affect the land conditions. In particular, we focus on the moist static energy budget for region S.

4.3.2 Moist Static Energy Budget

Since BLE is sustained by energy within the boundary layer, changes in entropy of a region must result from the changes in energy within the boundary layer. The budget of moist static energy within the boundary layer is affected by the energies supplied from all possible sources. We first look at the moist static energy, which is defined as the summation of the sensible heat content, the gravitational potential energy, and the latent heat content. The corresponding mathematical expression is

$$\phi = C_p T + \Phi + Lq \tag{4.1}$$

where ϕ is the moist static energy, C_p is the specific heat at constant pressure, Φ is the gravitational potential energy, which is the work that must be done against the earth's gravitational field in order to raise a mass of 1 Kg from the sea level to the point where the geopotential is measured, L is the latent heat of evaporation, q is the mixing ratio, and T is the temperature.

The moist static energy has the convenient property of being unaffected by condensation processes, which merely redistribute energy between the latent and sensible heat content. To estimate the budget of the moist static energy, we need to know the fluxes of energy. In this study, we estimate the zonal and meridional fluxes of the moist static energy using the following formula:

$$F_u = \int_{1000mb}^{925mb} \phi u \rho \, dz L_1 \tag{4.2}$$

$$F_v = \int_{1000mb}^{925mb} \phi v \rho \, dz L_2 \tag{4.3}$$

where u and v are the zonal and meridional velocities, L_1 and L_2 are the distances in the zonal and meridional directions.

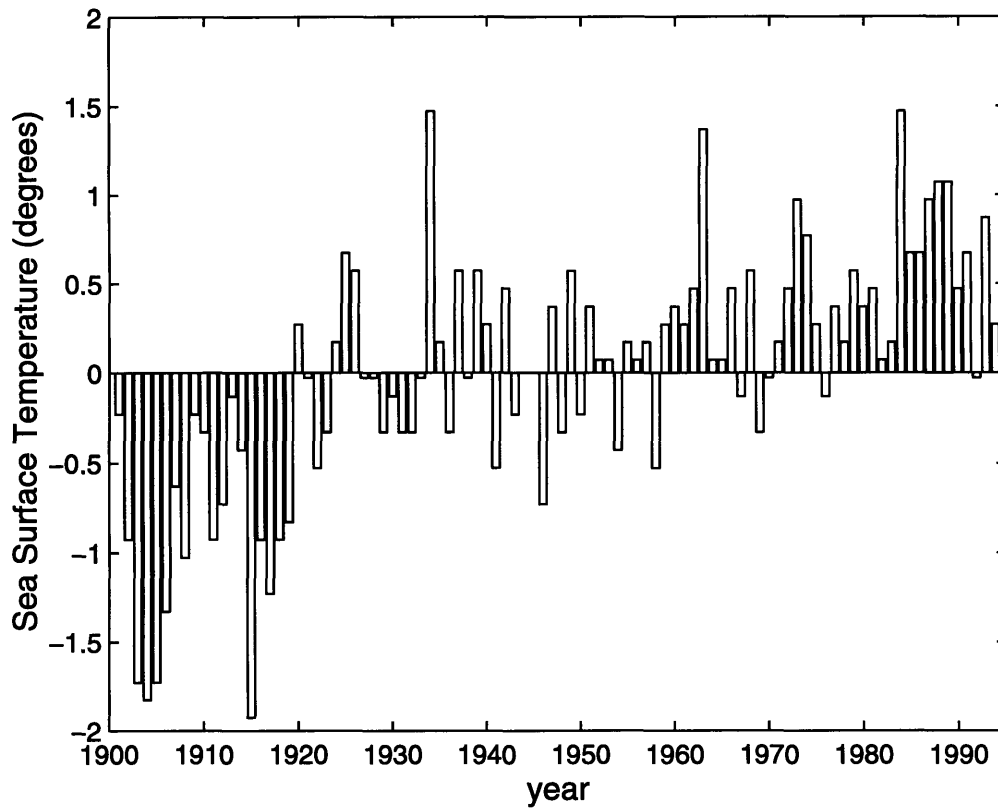Figure 4-10 shows the comparisons of the energy fluxes coming from the northern

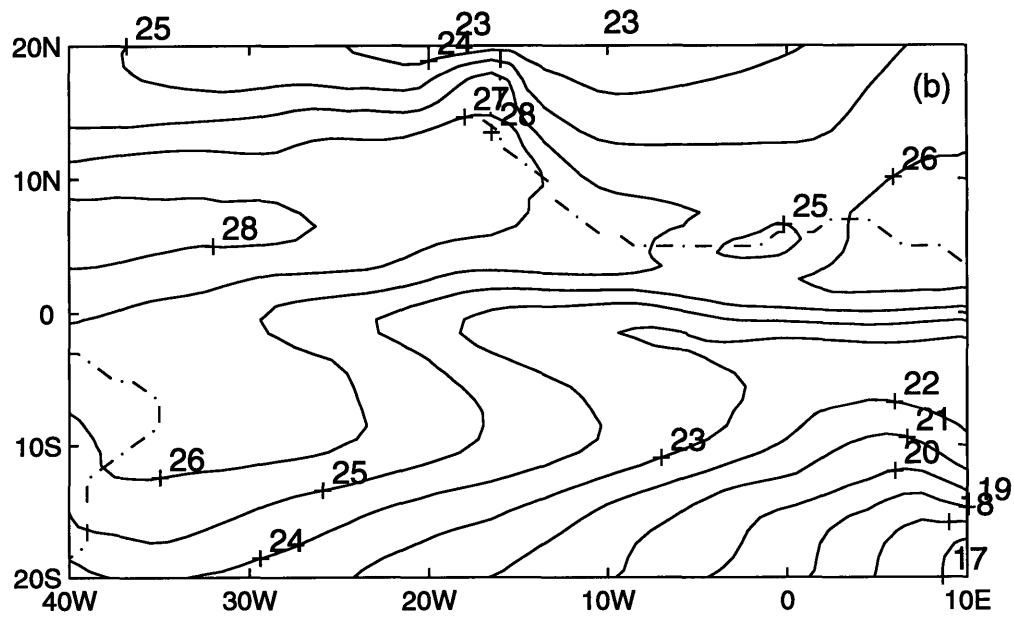Figure 4-7: Departures of the SST from the long-term mean
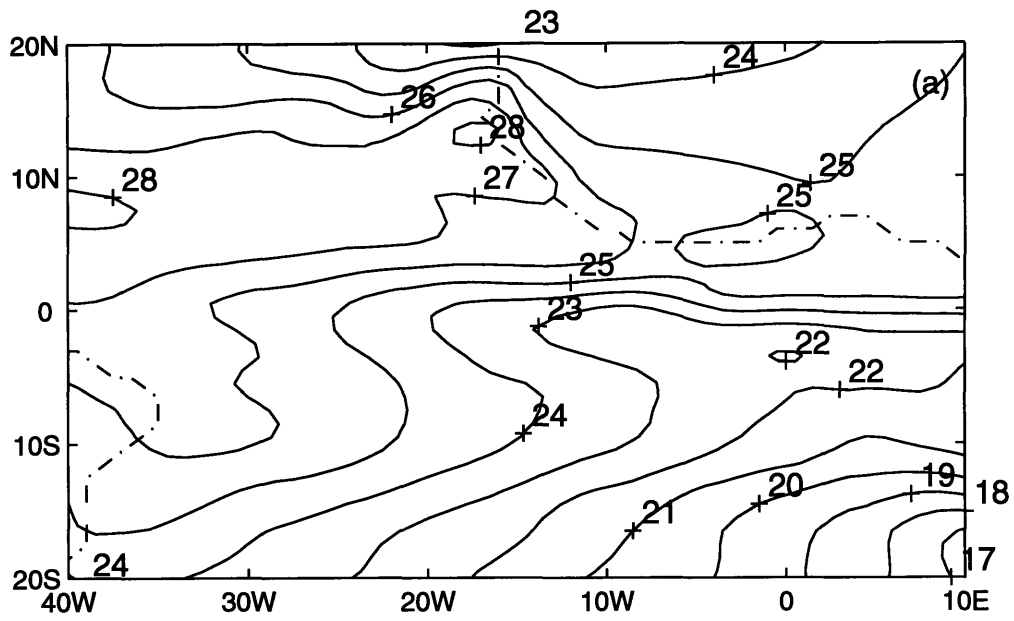
Figure 4-8: The SST distributions in the Tropical Atlantic in   (a) 1992   (b) 1994
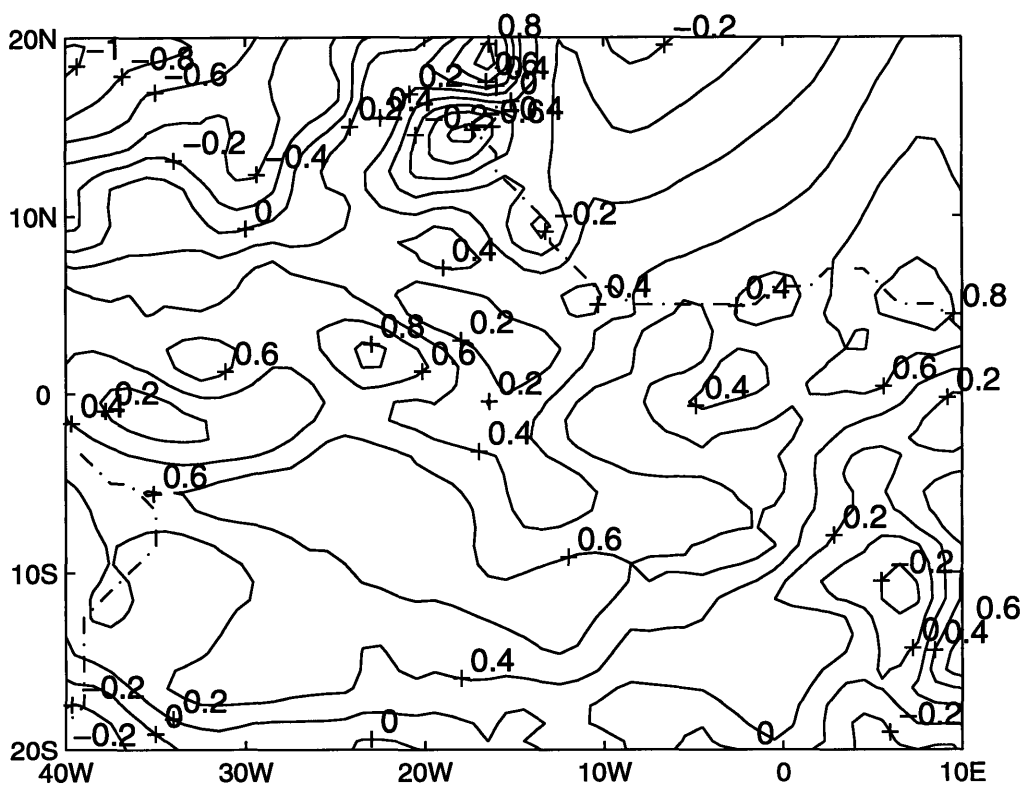
Figure 4-9: The difference of the SST between 1994 and 1992 ($SST_{1994} - SST_{1992}$)

and southern borders of region S in 1992 and 1994. Figure 4-11 shows the energy fluxes coming from the eastern and western borders of the same region. The dash line represents energy fluxes in 1992; the solid line, in 1994. We also estimated the summation of the latent and the sensible heat fluxes from the surface into the entire region S and plotted them in Figure 4-12(a). All the data used for this analysis are extracted from the ECMWF data.

The moist static energy budget in the boundary layer is given by

$$\frac{\partial N}{\partial t} = F_b + (LE + H) + F_{upper} \tag{4.4}$$

where N is defined as

$$N = \int_{1000mb}^{925mb} \phi \rho A dz \tag{4.5}$$

A is the area of the specified region, F_b is the net flux of the moist static energy crossing the borders of the specified region, $LE + H$ is the summation of the latent and sensible heat fluxes from the surface, F_{upper} is the energy flux from the top of the boundary layer, which includes three processes: entrainment, convective downdrafts, and radiative cooling. Energy fluxes from the top of the boundary layer can be estimated based on Equation 4.4 since other terms can be estimated from observations directly. Figure 4-13 shows the storage of the moist static energy in region S. Figure 4-12(b) shows the energy fluxes from the top of the boundary layer.

In general, the differences between the fluxes from the eastern and the western borders during the rainy seasons of 1992 and 1994 are small. The differences of the fluxes from the northern and southern borders are more significant. The energy fluxes off the top of the boundary layer carry energy away and always decrease the boundary layer entropy. The sensible and latent heat release from the surface is one order of magnitude smaller than other energy fluxes. Since in June 1994, more moist static energy comes from these northern border and less from the southern border of region S, the overall contributions from the boundary fluxes differ little between 1992 and 1994. The main contributing factor seems to be the energy flux through the top of

Figure 4-10: Fluxes of the moist static energy   (a) from the northern border   (b) from the southern border
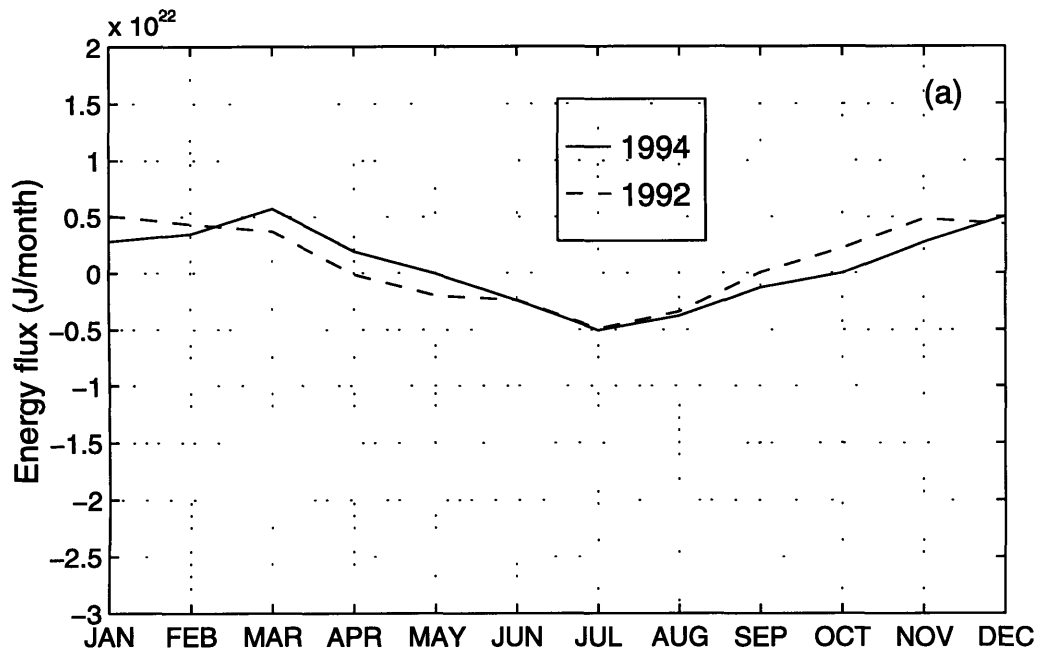
Figure 4-11: Fluxes of the moist static energy (a) from the eastern border (b) from the western border
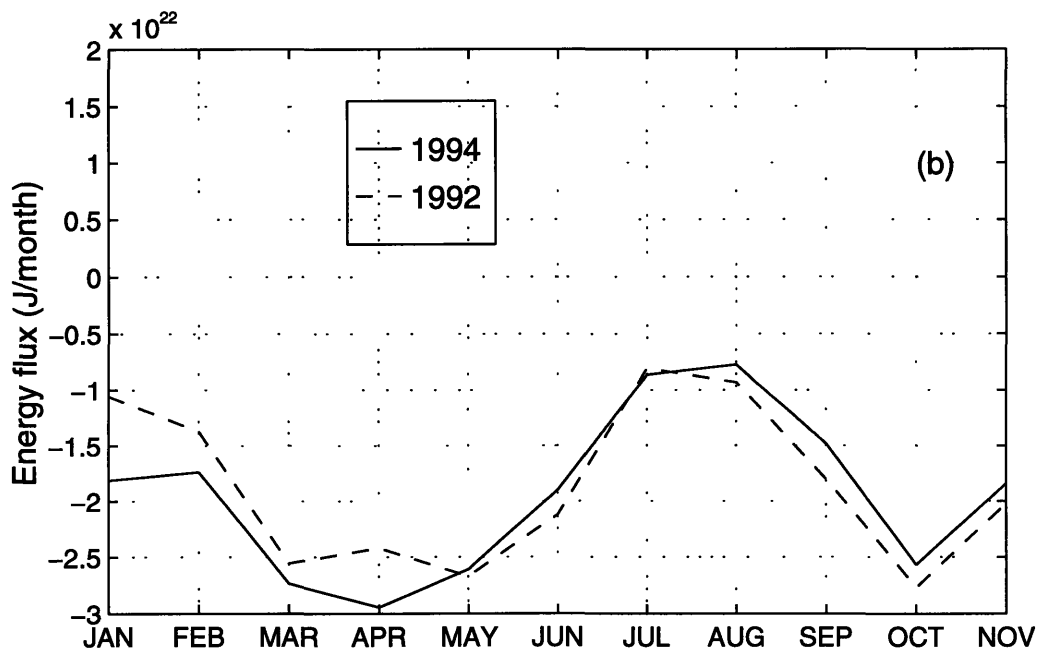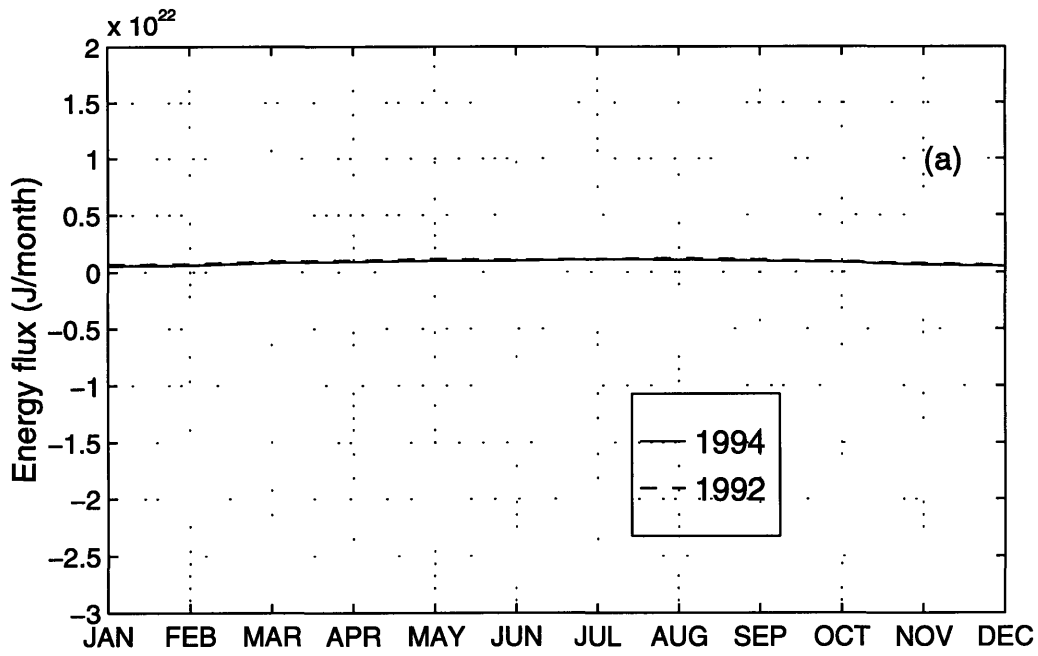
Figure 4-12: Energy fluxes from the surface and from the top of the boundary layer (a) sensible and latent heat fluxes   (b) energy fluxes from the top of the boundary layer
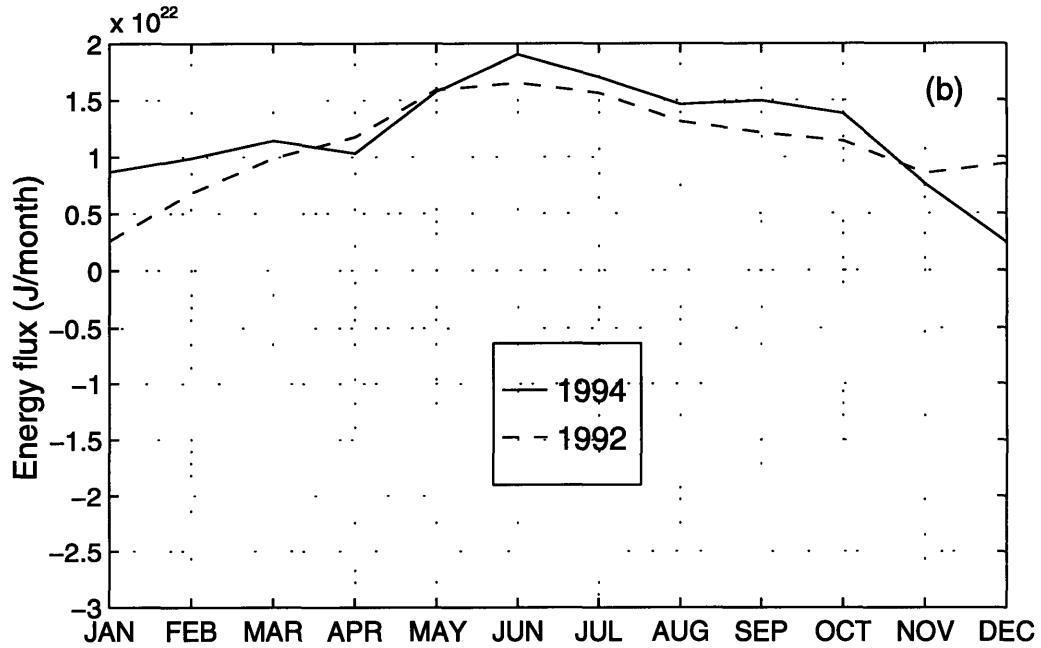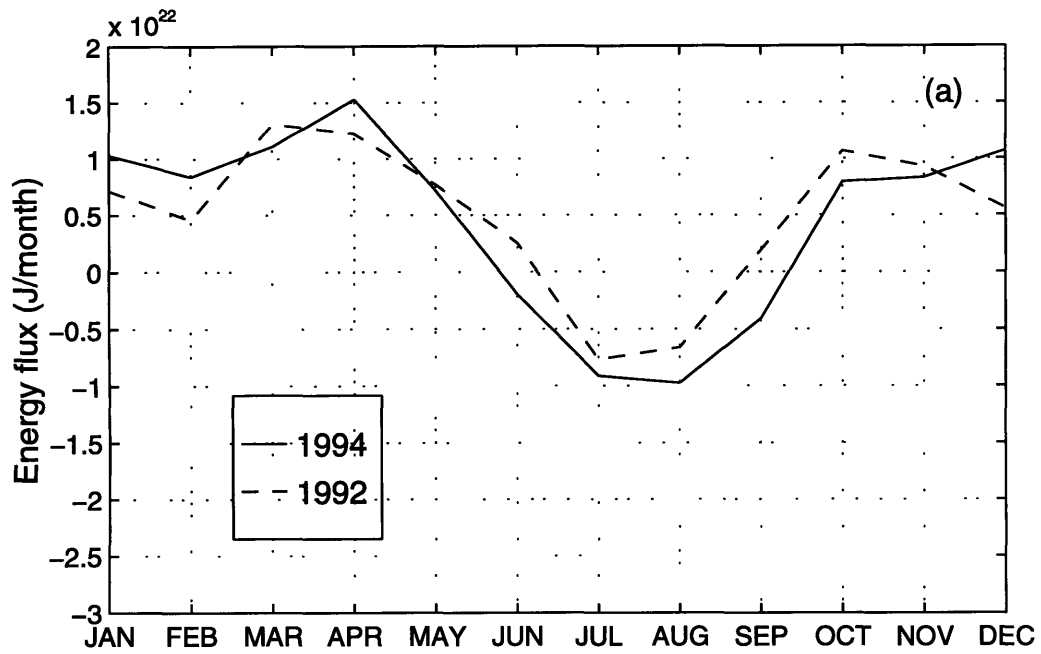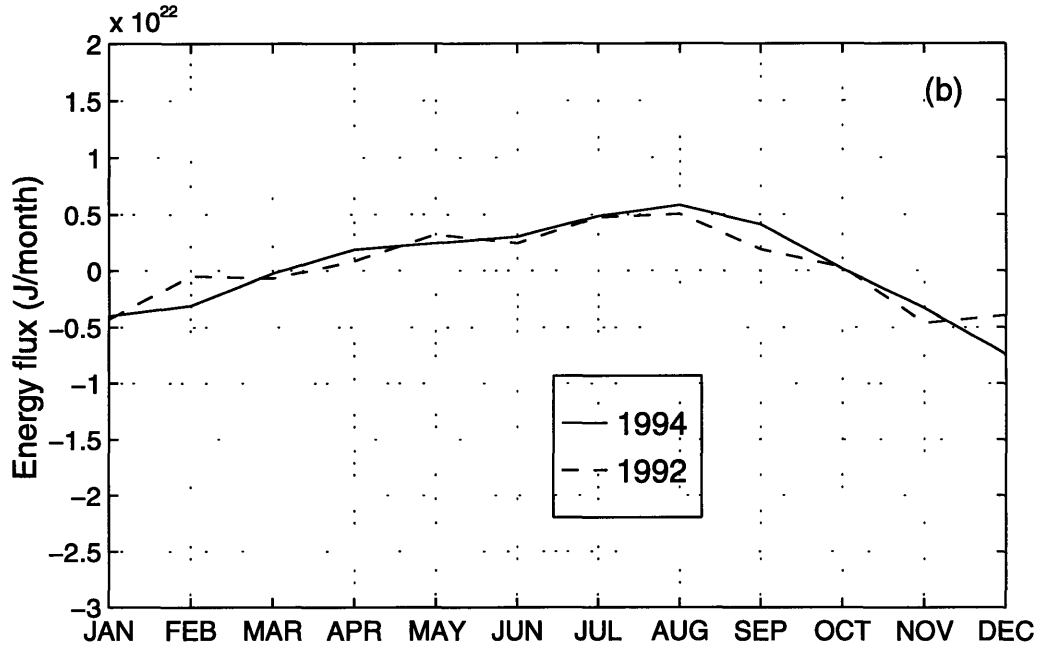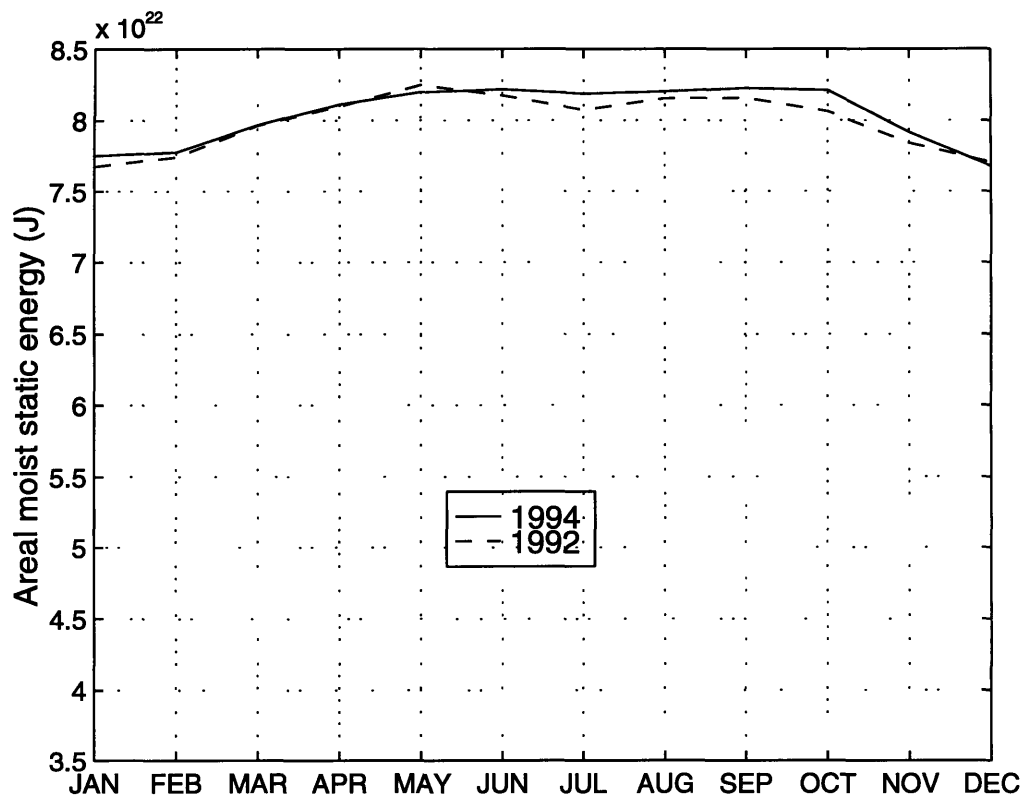
Figure 4-13: Storage of the total moist static energy in the region (10N-20N, 10W-15E)

the boundary layer since less energy fluxes out of the top of the boundary layer were observed in June 1994 as shown in Figure 4-12(b). Notice that the small difference between the energy fluxes through the top of the boundary layer in 1992 and in 1994 results in a big difference in BLE. This may imply that land conditions in West Africa are very sensitive to the energy supplies into the boundary layer.

Temperature and humidity in the boundary layer may affect the energy fluxes from the top of the boundary layer. We analyze the observed sensible and latent heat fluxes from the surface in 1992 and 1994 separately. Figure 4-14 shows the comparison of the monthly sensible and latent heat fluxes. The figure shows that throughout the whole year, sensible heat fluxes are lower in 1994, which reflects the lower surface temperature in 1994. As shown in Figure 4-14(b), the latent heat fluxes increase significantly in July 1994 and remains at a high value until the end of the rainy season.

The comparison of the areal and monthly average of the internal energy and latent heat content shows similar results. Figure 4-15(a) shows the comparison of the internal energy between 1992 and 1994; Figure 4-15(b), the latent heat contents for the same period. The figure shows that in July 1994, the internal heat of the boundary layer is lower and the latent heat content is higher. The lower boundary layer temperature and higher humidity in July 1994 should relate to rainfall in that month. To confirm this, we inspect the monthly rainfall in June and July in both 1992 and 1994. Figure 4-16 shows the rainfall difference between 1992 and 1994 (1994 minus 1992) in June and July. In both months, more rain falls in 1994 than in 1992 in region S. More rainfall in a region makes it possible for more evaporation, and more evaporation increases humidity of the air above the surface and reduces the surface temperature. This is consistent with the observations in the sensible heat fluxes from the surface, which show that the sensible heat fluxes are much lower in 1994 than in 1992 because region S receives more rainfall in 1994. Also the latent heat fluxes in 1994 increase significantly starting from June. Figure 4-15(b) shows that the latent heat content in the boundary layer of the region also increases from June. The lower surface temperature and drier humidity conditions reduce the radiative cooling of the
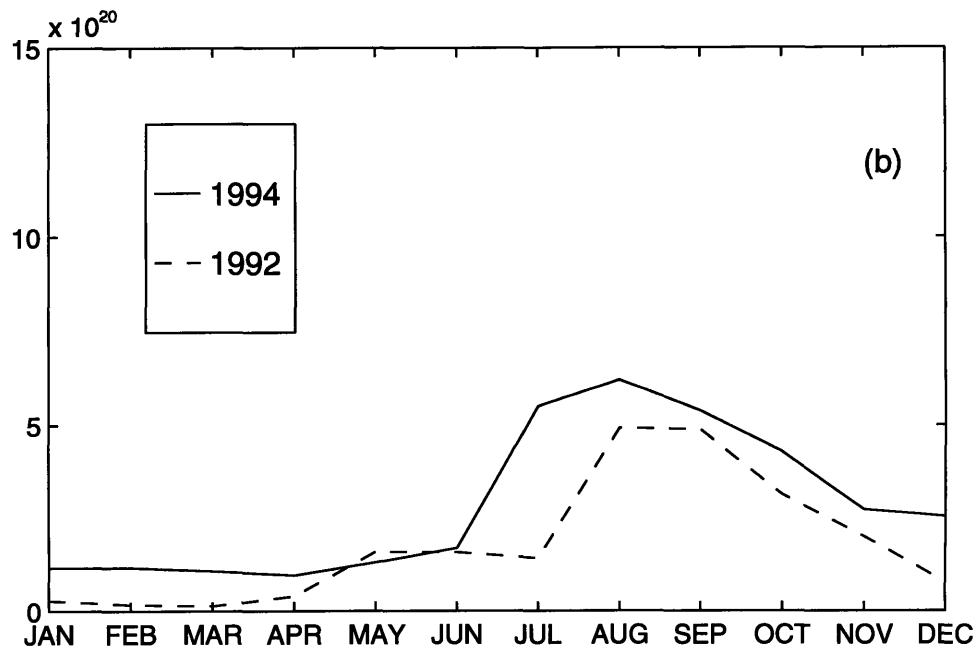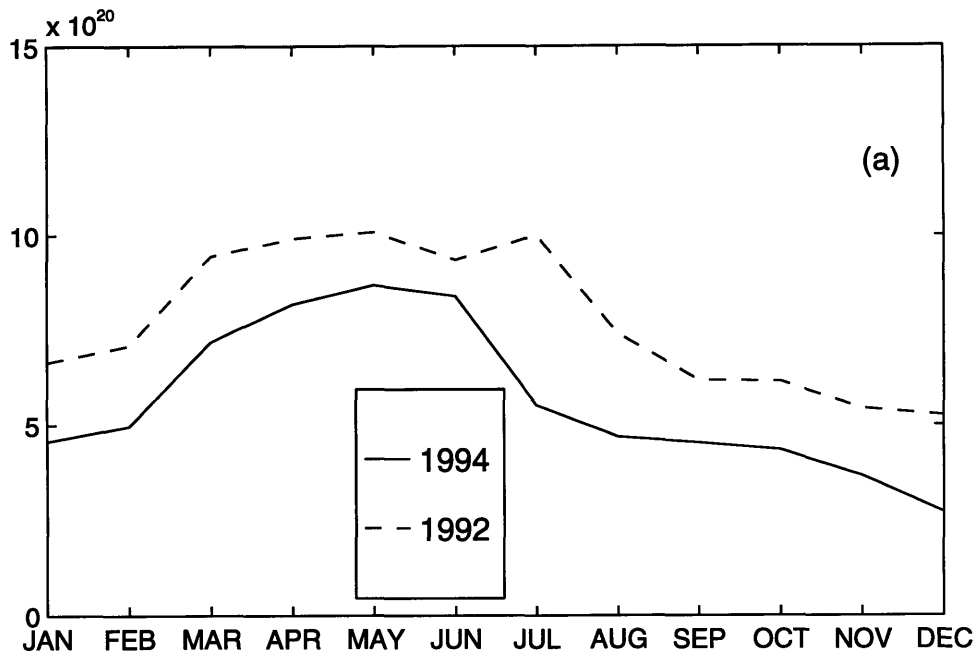
Figure 4-14: (a) monthly sensible heat fluxes   (b)monthly latent heat fluxes from the surface

boundary layer, which results in less energy fluxes from the top of the boundary layer in 1994 than in 1992, as shown in Figure 4-12(b).

4.3.3 Trends in the SST and Rainfall in Sahel

We performed the Kendall Rank test (Kendall, 1962) in both rainfall and the SST within two intervals of the SST (22.1-22.5 and 22.6-23). Rainfall in the Sahel used in this analysis is based on Nicholson's study (Nicholson, 1993) and the SST is based on the observations provided by COADS. Table 4.1 shows the results of trends in rainfall and the SST from 1900 to 1990. Rainfall shows strong descending trends in both intervals of the SST, especially after the 1940s. During the period of 1950-1983, the descending trend is even more significant. The Kendall τ reaches -0.88 while the 10 percent confidence interval is only ± 0.32. However the SST does not have significant ascending or descending trend within each interval of the SST (all Kendall's τs for the SST are within the 10% confidence interval). Since the SST does not vary much and does not have a trend within each interval, the SST should not affect the rainfall variation much. Therefore these statistical results suggest that other processes other than the SST may play important roles in rainfall variability over West Africa.

4.4   Findings and Discussion

We successfully apply the theory of land-atmosphere-ocean interactions to the wet 1994 rainy season and once again the observations support the theory. The large gradient of BLE, which results from the land-atmosphere-ocean interactions, is associated with a strong monsoon circulation and abundant rainfall in West Africa in 1994. The anomalous northward extension of the ITCZ during 1994, as shown in Figure 4-2, is associated with a northward extension of the peak of the entropy in the land region. As a result, a strong monsoon circulation develops further inland. This monsoon circulation, which is likely to have a descending branch around the coast region instead of the ocean, may be responsible for the wet conditions across
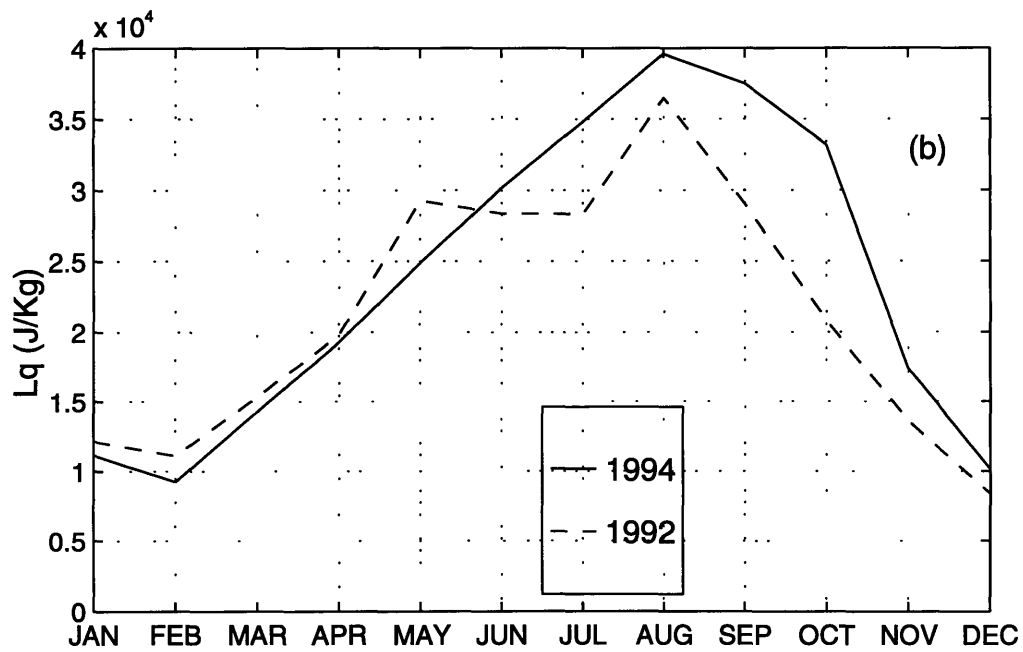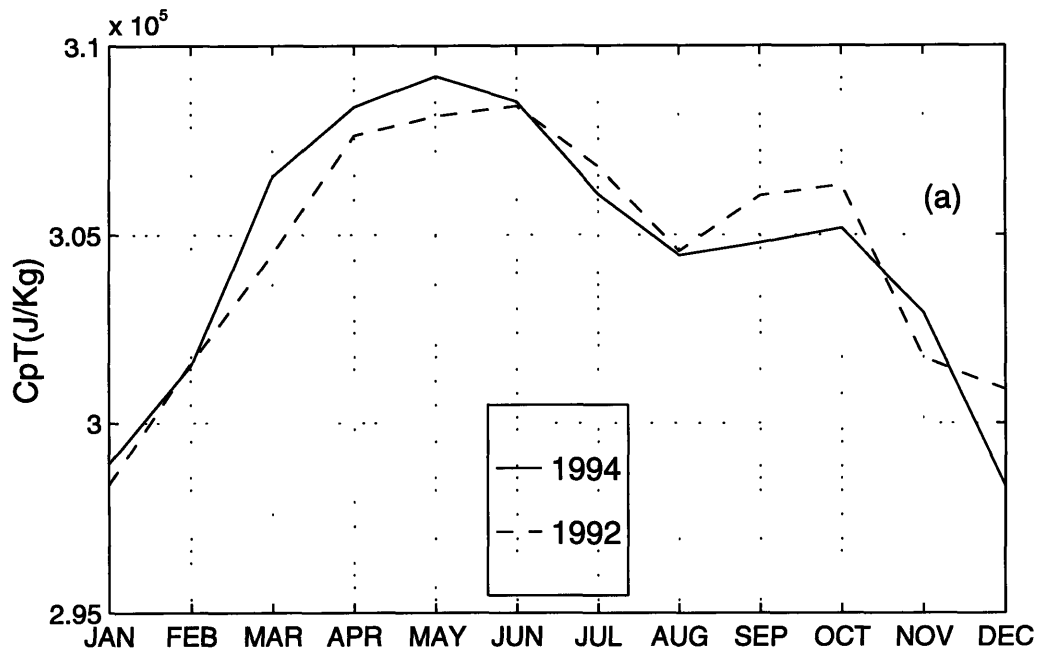
Figure 4-15: (a) Monthly average of the internal energy $C_p T$ in the region (10N-20N, 10W-15E)   (b) Monthly average of the latent heat content Lq in the same region
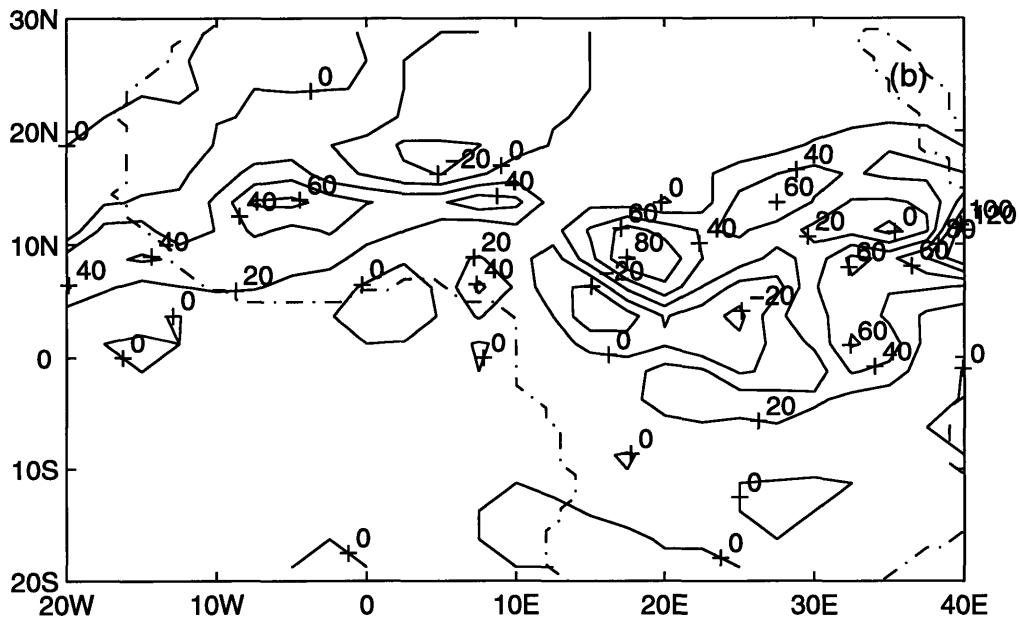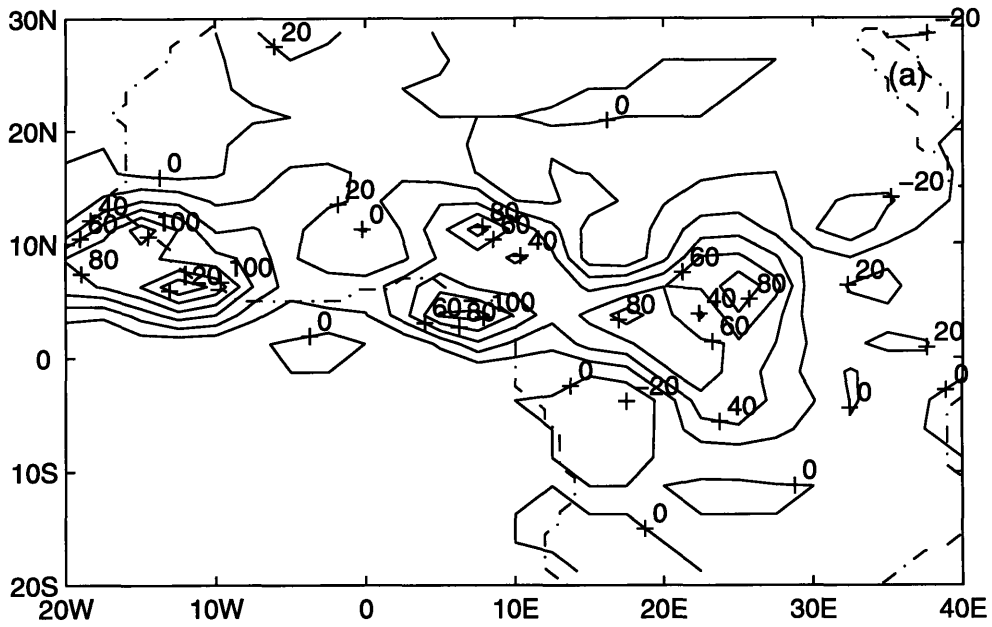
Figure 4-16: Rainfall difference between 1994 and 1992 (1994 minus 1992)   (a) June
(b) July

the Sahel/Sudan zones of Africa and dry conditions that were observed along the Gulf of the Guinea Coast (Climate Analysis Center, NOAA, 1995).

In 1994, land conditions play a more important role in West African rainfall than the SST does. The energy fluxes from the top of the boundary layer of region S may be responsible for the high boundary layer entropy over the region (10N-20N, 10W-15E) in July 1994. Rainfall in that region in the early rainy season of 1994 increases the humidity and decreases the temperature of the boundary layer, which may cause less radiative cooling and hence less energy loss through the top of the boundary layer. The high BLE over the land enhances the gradient of BLE and supports a strong circulation and results in the wet condition in 1994.

a statistical analysis shows that rainfall has a significant descending trend after the 1940s, even when the variation of the SST is small and hence the effect of the SST on rainfall can be ignored. These results suggest that processes other than the SST also play important role in rainfall variability over West Africa.

Table 4.1: Trends for rainfall and the SST within different SST intervals

SST (21.6-22)				
period	τ for rain	τ for SST	10% confidence	total observations
1900 to 1983	-0.25	0.14	±0.22	27
1910 to 1983	-0.29	0.03	±0.23	25
1920 to 1983	-0.38	-0.01	±0.24	24
1930 to 1983	-0.57	0.04	±0.27	20
1940 to 1983	-0.83	0.02	±0.30	16
1950 to 1983	-0.88	-0.1	±0.32	15
SST (22.6-23.0)				
period	τ for rain	τ for SST	10% confidence	total observations
1920 to 1990	-0.35	-0.11	±0.23	25
1930 to 1990	-0.33	-0.04	±0.25	22
1940 to 1990	-0.32	0.13	±0.27	20
1950 to 1990	-0.55	0.23	±0.30	16
1960 to 1990	-0.49	0.16	±0.33	14

Chapter 5

Conclusions

This chapter will summarize the results and conclusions of this study. Some future research is proposed.

5.1   Summary of Results

5.1.1   Sources of Moisture for Rainfall in West Africa

A precipitation recycling model is applied to the West African region. By defining different source regions, we estimated the contributions to rainfall from local evaporation, as well as advection from the surrounding regions. Local evaporation and evaporation in the areas to the east and to the south of the West African region contribute about 70 percent of the total precipitation in West Africa. The local evaporation contributes about 30 percent of the precipitation. The Tropical Atlantic Ocean contributes nearly as much rainfall as local evaporation.

Atmospheric moisture flux and rainfall in West Africa exhibit similar seasonal variations. Evaporation is positively correlated with rainfall. Moisture supply from Central Africa decreases significantly in monsoon months: August and September, while moisture supply from the Tropical Atlantic Ocean, which is almost in phase with the rainfall, increases significantly.

5.1.2 Theory of Land-Atmosphere-Ocean Interactions

A theory of land-atmosphere-ocean interactions is proposed and tested by observations. The gradient of boundary layer entropy between the ocean and the land, which reflects the interactions among land, atmosphere and ocean, regulates the development of monsoon circulations. A healthy monsoon circulation and a large gradient of the boundary layer entropy are observed in the wet years 1958 and 1994. A relatively weak monsoon circulation and a flat distribution of the boundary layer entropy are observed in dry years 1960 and 1992. Also we find that monsoon circulations in West Africa could develop more easily, but in general more sensitive to changes in sea surface temperature and land surface conditions. This feature is attributed to the location of West Africa, being close to the equator.

The observations on wind and vorticity fields show obvious contrast between the wet and dry years in West Africa. The easterly jet at the upper atmosphere of West Africa is much stronger in wet years than that in dry years. Also the meridional circulations are significantly stronger and the absolute vorticity is closer to zero at the tropopause in wet years.

5.1.3 The Impact of Land Surface Conditions on Rainfall in West Africa

We can study the impact of land surface conditions on West African rainfall by studying the effect of changes in land conditions on the distribution of boundary layer entropy. The impact of land surface conditions on the boundary layer entropy in 1994 is investigated and compared to the relatively dry year, 1992. The budget of the moist static energy is investigated. The variations of the fluxes of the moist static energy from the eastern and western borders between 1992 and 1994 are small and variations of the fluxes from the northern and southern borders are more significant. The energy fluxes through the top of the boundary layer tend to reduce the energy content in the boundary layer. However, this reduction is significantly smaller in 1994 than in 1992. The sensible and latent heat fluxes from the surface are one order of

magnitude smaller than the other energy fluxes.

The Kendall test of trends is applied to rainfall and the SST records from 1900 to 1990. The statistical results show that rainfall has a strong descending trends in the intervals of the SST (22.1-22.5) and (22.6-23.0). During the period of 1950-1983, the descending trend is even more significant. The SST has no significant ascending or descending trend in the corresponding intervals of the SST.

5.2   Summary of Conclusions

The precipitation in West Africa is mainly contributed by local evaporation and evaporation in the areas to the east and to the south of the region. Moisture supply and rainfall in West Africa relate to each other closely. Atmospheric moisture provides the source for rainfall and controls the maximum amount of rainfall; rainfall is associated with atmospheric circulations, which control where the moisture fluxes come from. The large scale monsoon circulation enhances southerly flux into the region and induces strong westerlies, which, in turn, shuts off the easterly flux into West Africa. As a result, moisture supply from Central Africa decreases in monsoon months and moisture supply from the Tropical Atlantic Ocean increases significantly.

The observations that have been recorded for both SST and the boundary layer entropy distributions during wet and dry years strongly support the proposed theory of land-atmosphere-ocean interactions and monsoon circulations over West Africa. The land-atmosphere-ocean interactions result in different distributions of boundary layer entropy between the ocean and the land. A large gradient of the boundary layer entropy drives a strong monsoon circulation; a flat distribution of the boundary layer entropy does not drive any circulation. The proposed theory on the dynamics of monsoon circulations over West Africa provides a better approach to explain the natural variability of the rainfall. Changes in either SSTs or land conditions could modify the distribution of boundary layer entropy, which, in turn, affects the monsoon circulation and rainfall in West Africa.

The land conditions play a very important role in West African rainfall since

entropy in the land region controls the northern end of the entropy distribution curve. Surface latent and sensible heat fluxes, and energy fluxes from the surrounding regions and the upper atmosphere are the sources and sinks of energy that maintain the boundary layer entropy. Any change of them would result in changes in the boundary layer entropy. In 1994, the fluxes of energy from the top of the boundary layer seem to play an important role in the anomalously high boundary layer entropy. More rainfall in the early rainy season of 1994 is associated with increases in evaporation and atmospheric humidity and a decrease in the temperature of the boundary layer. These processes favor less radiative cooling in the boundary layer and less energy fluxes away through the top of the boundary layer.

The strong descending trend that has been documented in the rainfall series between 1950 and 1983 while considering only years with similar SST conditions, shows that processes other than the SST play important role on rainfall variability over West Africa. One of those processes could be the large scale deforestation in West Africa. Since vegetation and rainforests help to sustain large scale atmospheric circulations in the tropics, deforestation decreases boundary layer entropy, which would weaken the monsoon circulation and result in a dry condition in West Africa. This issue can be further investigated in future research.

5.3   Future Research

The current study of the sources of moisture for rainfall in West Africa can be applied to other regions since the two assumptions involved in the recycling model are generally valid in other regions. The scaling study can be extended in both time and space domain, for example, the time domain could be extended to months other than August, or the whole rainy season; the space domain can be divided into smaller scales if the resolution of observations increases. Similar recycling studies can be done in the years before and after large scale deforestation took place so that any effect of deforestation may be detected from the difference of recycling ratio between the two periods.

The theory of the land-atmosphere-ocean interactions can be further tested by observations in typical dry and wet years. Since this theory is based on the pre-monsoon conditions, it could be used to predict monsoon circulations and rainfall in West Africa. One possible and interesting topic related to this theory is to study the impact of SST and land conditions on the gradient of entropy between the ocean and the land quantitatively. For example, if we fix the entropy in the land region, how many degrees difference in SST could affect the development of monsoon circulations significantly? Or if we fix the entropy in the ocean, what is the combination of temperature and humidity in the land region that could make the gradient of entropy large enough to drive a strong monsoon circulation?

The factors contributing to entropy changes in the land region are rather complicated. Latent and sensible heat fluxes from the land surface, energy form the top of the boundary layer, and energy fluxes from the surrounding regions can all affect entropy in the land region. More research can be done to investigate this issue further.

Bibliography

[1] T. Beer, G. K. Greenhut, and S. E. Tandoh. Relations between the z criterion for the sub-tropical high, Hadley Cell parameters and rainfall in northern Ghana. *Monthly Weather Review*, 105:849–855, 1977.

[2] A. ben Mohamed and J. P. Frangi. Humidity and turbidity parameters in Sahel: A case study for Niamey (Niger). *Journal of Climate and Applied Meteorlogy*, 22:1820–1823, 1983.

[3] A. ben Mohamed and J. P. Frangi. Results from ground-based monitoring of spectral aerosol optical thickness and horizontal extinction: some specific characteristics of dusty sahelian atmopheres. *Journal of Climate and Applied Meteorlogy*, 25:1807–1815, 1986.

[4] G. S. Benton and M. A. Estoque. Water vapor transfer over the North American Continent. *Journal of Meteorology*, 11:462–477, 1954.

[5] Fontaine BERNARD and Janicot SERGE. Wind-field coherence and its variations over West Africa. *Journal of the Atmospheric Sciences*, 5:512–524, 1992.

[6] D. Bolton. The computation of equivalent potential temperature. *Monthly Weather Review*, 108:1046–1053, 1980.

[7] E. Eltahirand R. Bras. Precipitation recycling in the Amazon basin. *Quarterly Journal of the Royal Meteorological Society*, 120:861–880, 1994.

[8] V. S. Brezgunov. Character of atmospheric moisture exchange of the issyuk-kul basin with the surrounding territory on the basis of the distribution of stable oxygen isotopes in natural waters. *Water Resources*, 17:616–624, 1991.

[9] K. L. Brubaker, D. Entekhabi, and P. S. Eagleson. Estimation of continental precipitation recycling. *Journal of Climate*, 6:1077–1089, 1993.

[10] M. I. Budyko. *Climate and Life*. Academic Press, 1974.

[11] T. N. Carlson and S. G. Benjamin. Radiative heating rates for Saharan dust. *Journal of the Atmospheric Sciences*, 37:193–213, 1980.

[12] Climate Analysis Center. The 1994 Sahelian rainy season – the wettest since 1964. Technical report, NOAA, 1995.

[13] J. G. Charney. Dynamics of deserts and drought in the Sahel. *Quarterly Journal of the Royal Meteorological Society*, 101:193–202, 1975.

[14] J. G. Charney, P. H. Stone, and W. J. Quirk. Drought in the Sahara: insufficient biogeophysical feedback mechanism. *Science*, 187:434–435, 1975.

[15] CIRES, ERL, NCAR, and NCDC. Comprehensive ocean-atmosphere data set, release 1. Technical report, Boulder, Colorado, 1985.

[16] T. D. Crum and R. B. Stull. Field measurements of the amount of surface layer air versus height in the entrainment zone. *Journal of the Atmospheric Sciences*, 44:2473–2753, 1987.

[17] C. Cunningto and P. R. Rowntree. Simulations of the Saharan atmosphere-dependence on moisture and albedo. *Quarterly Journal of the Royal Meteorological Society*, 112:971–999, 1986.

[18] P. K. Das. *The monsoons*. National Book Trust, India, 1968.

[19] M. D. Dennett, J. Elston, and J. A. Rodgers. A reappraisal of rainfall trends in the Sahel. *Journal of Climatology*, 5:353–362, 1985.

[20] E. A. B. Eltahir. *Interactions of Hydrology and Climate in the Amazon Basin.* PhD thesis, MIT, 1993.

[21] E. A. B. Eltahir and R. L. Bras. On the response of the tropical atmosphere to large-scale deforestation. *Quarterly Journal of the Royal Meteorological Society,* 119:779–793, 1993.

[22] E. A. B. Eltahir and C. Gong. Dynamics of wet and dry years in West Africa. To be published in Journal of Climate.

[23] K. A. Emanuel. On thermally direct circulations in moist atmospheres. *Journal of the Atmospheric Sciences,* 52:1529–34, 1995.

[24] K. A. Emanuel, J. D. Neelin, and C. S. Bretherton. On large scale circulations in convecting atmospheres. *Quarterly Journal of the Royal Meteorological Society,* 120:1111–1143, 1994.

[25] G. Farmer and T. M. L. Wigley. Climatic trends for tropical africa, a research report for the overseas development administration. Technical report, University of East Anglia, 1985.

[26] C. K. Folland, T. N. Palmer, and D. E. Parker. Sahel rainfall and worldwide sea temperatures, 1901-85. *Nature,* 320:602–607, 1986.

[27] A. E. Gill. Some simple solutions for heat-induced tropical circulation. *Qauarterly Journal of the Royal Meteorological Society,* 106:447–462, 1980.

[28] G. K. Greenhut. A new criterion for locating the subtropical high in West Africa. *Journal of Applied Meteorlogy,* 16:727–734, 1977.

[29] D. M. Helgren and J. M. Prospero. Wind velocities associated with dust deflation events in the western Sahara. *Journal of Climate and Applied Meteorlogy,* 26:1147–1151, 1987.

[30] A. Y. Hou. The influence of tropical displacement on the extratropical climate. *Journal of the Atmospheric Sciences,* 50:3553–70, 1993.

[31] A. Y. Hou and R. S. Lindzen. Hadley circulations for zonally averaged heating centered off the equator. *Journal of the Atmospheric Sciences*, 45:2416–27, 1988.

[32] A. Y. Hou and R. S. Lindzen. The influence of concentrated heating on the Hadley circulation. *Journal of the Atmospheric Sciences*, 49:1233–41, 1992.

[33] A. Y. Hou and A. Molod. Modulation of dynamic heating in the winter extra-tropics associated with the cross-equatorial Hadley circulation. *Journal of the Atmospheric Sciences*, 52:2609–26, 1995.

[34] J. Hsiung and R. Newell. The principal non-seasonal modes of variation of global sea-surface temperature. *Journal of Physical Oceanography*, 13:1952–1967, 1983.

[35] M. Kanamitsu and T. N. Krishnamurti. Northern summer tropical circulations during drought and normal rainfall months. *Monthly Weather Review*, 106:331–347, 1978.

[36] M. G. Kendall. *Rank correlation methods*. New York, Hafner Pub. Co., 1962.

[37] J. W. Kidson. African rainfall and its relation to the upper air circulation. *Quarterly Journal of the Royal Meteorological Society*, 103:441–456, 1977.

[38] A. Kitoh, K. Yamzaki, and T. Takiota. Influence of soil moisture and surface albedo changes over African tropical rainforest on summer climate investigated with mri-gcm-i. *Journal of the Meteorological Society of Japan*, 66:65–85, 1988.

[39] R. Koster, J. Jouzel, R. Suozzo, G. Russell, W. Broecker, D. Rind, and P. Eagleson. Global souces of local precipitation as determined by the NASA/GISS GCM. *Geophysical Research Letters*, 13:121–124, 1986.

[40] E. B. Kraus. The seasonal excursion of the intertropical convergence zone. *Monthly Weather Review*, 105:1009–1018, 1977.

[41] P. J. Lamb. Large-scale Tropical Atlantic surface circulations patterns associated with Subsaharan weather anomalies. *Tellus*, 30:240–251, 1978.

[42] P. J. Lamb. West African water vapor variations between recent contrasting Subsaharan rainy seasons. *Tellus*, 35:198–212, 1983.

[43] P. J. Lamb and R. A. Peppler. Further case studies of Tropical Atlantic surface atmospheric and oceanic patterns associated with Sub-Saharan drought. *Journal of Climate*, 5:476–488, 1992.

[44] H. Lettau, K. Lettau, and L. C. B. Molion. Amazonia's hydrologic cycle and the role of atmospheric recycling in assessing deforestation effects. *Monthly Weather Review*, 107:227–238, 1979.

[45] R. S. Lindzen and A. Y. Hou. Hadley circulations for zonally averaged heating centered off the equator. *Journal of the Atmospheric Sciences*, 45:2416–2427, 1988.

[46] R. S. Lindzen and S. Nigam. On the role of sea surface temperature gradients in forcing low-level winds and convergence in the tropics. *Journal of the Atmospheric Sciences*, 44:2418–36, 1987.

[47] J. G. Lockwood. *Causes of climate*. John Wiley and Sons, 1979.

[48] J. M. Lough. Tropical sea surface temperature and rainfall variation in Sub-Saharan Africa. *Monthly Weather Review*, 114:561–570, 1986.

[49] R. E. Newell and J. W. Kidson. *The tropospheric circulation over Africa. Saharan Dust (Scope Report 14)*. Wiley and Sons, 1979.

[50] R. E. Newell and J. W. Kidson. African mean wind changes in sahelian wet and dry periods. *Journal of Climatology*, 4:1–7, 1984.

[51] S. E. Nicholson. African drought: characteristics, causal theories, and global telconnections. *American Geophysical Union*, pages 79–100, 1989.

[52] S. E. Nicholson. An overview of African rainfall fluctuations of the last decade. *Journal of Climate*, 6:1463–1466, 1993.

[53] S. E. Nicholson and D. Entekhabi. The quasi-periodic behavior of rainfall variability in africa and its relationship to the Southern Oscillation. *Archives for Meterorology, Geophysics and Bioclimatology, Ser. A*, 34:311–348, 1986.

[54] S. E. Nicholson and D. Entekhabi. Rainfall variability in equatorial and southern Africa: relationships with sea-surface temperatures along the southwestern coast of Africa. *Journal of Climate and Applied Meteorlogy*, 26:561–578, 1987.

[55] A. H. Oort. *Global atmospheric circulation statistics, 1958-1973*. Rockville, Md : Washington, D.C. : U.S. Dept. of Commerce, National Oceanic and Atmospheric Administration, 1983.

[56] A. H. Oort. GFDL atmospheric circulation tape library, 1958-1989. Technical report, Geophysical Fluid Dynamics Laboratory/NOAA, Princeton University, 1994.

[57] J. A. Owen and M. N. Ward. Forecasting Sahel rainfall. *Weather*, 44:57–64, 1989.

[58] T. N. Palmer. The influence of the Atlantic, Pacific, and Indian oceans on Sahel rainfall. *Nature*, 322:251–253, 1986.

[59] J. P. Peixoto. *Physics of climate*. New York : American Institute of Physics, 1992.

[60] R. A. Plumb and A. Y. Hou. The response of a zonally symmetric atmosphere to subtropical thermal forcing: threshold behaviour. *Journal of the Atmospheric Sciences*, 49:1790–1799, 1992.

[61] C. F. Popelewski and M. S. Halpert. Global and regional scale precipitation and temperature patterns associated with El Nino/Southern Oscillation. *Monthly Weather Review*, 115:1606–1626, 1987.

[62] D. P. Powell and C. Blondin. The influence of soil wetness distribution on short range rainfall forecasting in the West African Sahel. *Quarterly Journal of the Royal Meteorological Society*, 116:1471–1485, 1990.

[63] J. M. Prospero and R. T. Nees. Dust concentrations in the atmosphere of the of the equatorial North Atlantic: possible relationship to the Sahelian drought. *Science*, 196:1196–1198, 1977.

[64] J. M. Prospero and R. T. Nees. Impact of theNorth African drought and el nino on mineral dust in the Barbados trade winds. *Nature*, 320:735–738, 1986.

[65] I. Rodriguez-Iturbe. Exploring complexity in the structure of rainfall. *Advances in water resources*, 14:162–167, 1991.

[66] R. R. Rogers and M. K. Yau. *A short course in cloud physics*. Pergamon, 1989.

[67] C. F. Ropelewski, P. J. Lamb, and D. H. Portis. The global climate for june to august 1990: Drought returns to Sub-Saharan West Africa and warm Southern Oscillatione pisode conditions develop in the Central Pacific. *Journal of the Atmospheric Sciences*, 6:2188–2212, 1993.

[68] G. L. Russell and J. A. Lerner. A new finite-differencing scheme fro the tracer transport equation. *Journal of Applied Meteorlogy*, 20:1483–1498, 1981.

[69] E. Salati, A. Dall'Olio, E. Matsui, and J. R. Gat. Recycling of water in the Amazon basin: an isotopic study. *Water Resources Research*, 15:1250–1258, 1979.

[70] H. H. G. Savenije. New definitions for moisture recycling and the relationship with land-use changes in the Sahel. *Journal of Hydrology*, 167:57–78, 1995.

[71] F. H. M. Semazzi, V. Mehta, and Y. C. Sud. An investigation of the relationship between sub-saharan rainfall and global sea surface temperatures. *Atmosphere-Ocean*, 26:118–138, 1988.

[72] D. J. Shea. Climatological Atals: 1950-1979, surface air temperature, precipitation, sea-level pressure, and sea-surface temperature (45s-90n). Technical report, National Center for Atmospheric Research, Boulder, Colorado, 1986.

[73] Y. C. Sud and M. J. Fennessy. Influence of evaporation in semi-arid regions on the july circulation: A numerical study. *Journal of Climatology*, 4:383–398, 1984.

[74] Y. C. Sud and A. Molod. A gcm simulation study of the influence of Saharan evapotranspiration and surface albedo anomalies on july circulation and rainfall. *Monthly Weather Review*, 116:2388–2400, 1988.

[75] Graham Sumner. *Precipitation progress and analysis*. John Wiley and Sons, 1988.

[76] M. Tanaka, B. C. Weare, A. R. Navato, and R. E. Newell. Recent African rainfall patterns. *Nature*, 255:201–203, 1975.

[77] K. E. Trenberth and J. G. Olson. ECMWF global analyses 1979-1986: circulation statistics and data evaluation. Technical report, NCAR Technical Note NCAR/TN300+STR, 1988.

[78] J. Walker and P. R. Rowntree. The effect of soil moisture on circulation and rainfall in a tropical model. *Quarterly Journal of the Royal Meteorological Society*, 103:29–46, 1977.

[79] J. M. Wallace. *Atmospheric science : an introductory survey*. New York : Academic Press, 1977.

[80] D. Winstanley. The impact of regional climatic fluctuations on man: some global implications. *Proceedings of the WMO/IAMAP symposuim on long term climatic fluctuations, Geneva: WMO*, pages 479–91, 1975.

[81] T. C. Yeh and R. T. Wetheraldand S. Manabe. The effect of soil moisture on the short-term climate and hydrology change- a numerical experiment. *Monthly Weather Review*, 112:474–490, 1984.

[82] X. Zheng and R. A. Plumb. Threshold behavior in a moist zonally-symmetric model-application to the monsoon onset. manuscript, 1994.